Inorganic and organic carbon in ocean sediments

Alberto Malinverno

Lamont-Doherty Earth Observatory
of Columbia University
Palisades, NY
alberto@ldeo.columbia.edu

2015 CIDER workshop

Outline

- Long-term C burial in ocean sediments within the global C cycle
- Where is C? How does it get there?
- Inorganic (calcium carbonate)
  - Calcite compensation depth and its history
- Particulate organic carbon (POC)
  - POC degradation fuels the deep subseafloor biosphere
  - Methane hydrates in the world continental margins
- Subduction of inorganic and organic sedimentary C

Kinds of carbon

- **Organic carbon**
  - In compounds usually formed by living organisms
  - Contains C-C and C-H bonds
- **Inorganic carbon**
  - Not organic, e.g., CO_2, $CaCO_3$

- **Reduced carbon**
  - Low oxidation state, e.g., methane CH_4
- **Oxidized carbon**
  - High oxidation state, e.g., CO_2

Photosynthesis and respiration

- Schematic photosynthesis reaction

$$CO_2 + H_2O + \textit{energy} \rightarrow CH_2O + O_2$$

Inorganic C

Organic C

- Aerobic respiration / organic matter oxidation

$$CH_2O + O_2 \rightarrow CO_2 + H_2O + \textit{energy}$$

Organic C

Inorganic C

The short-term C cycle

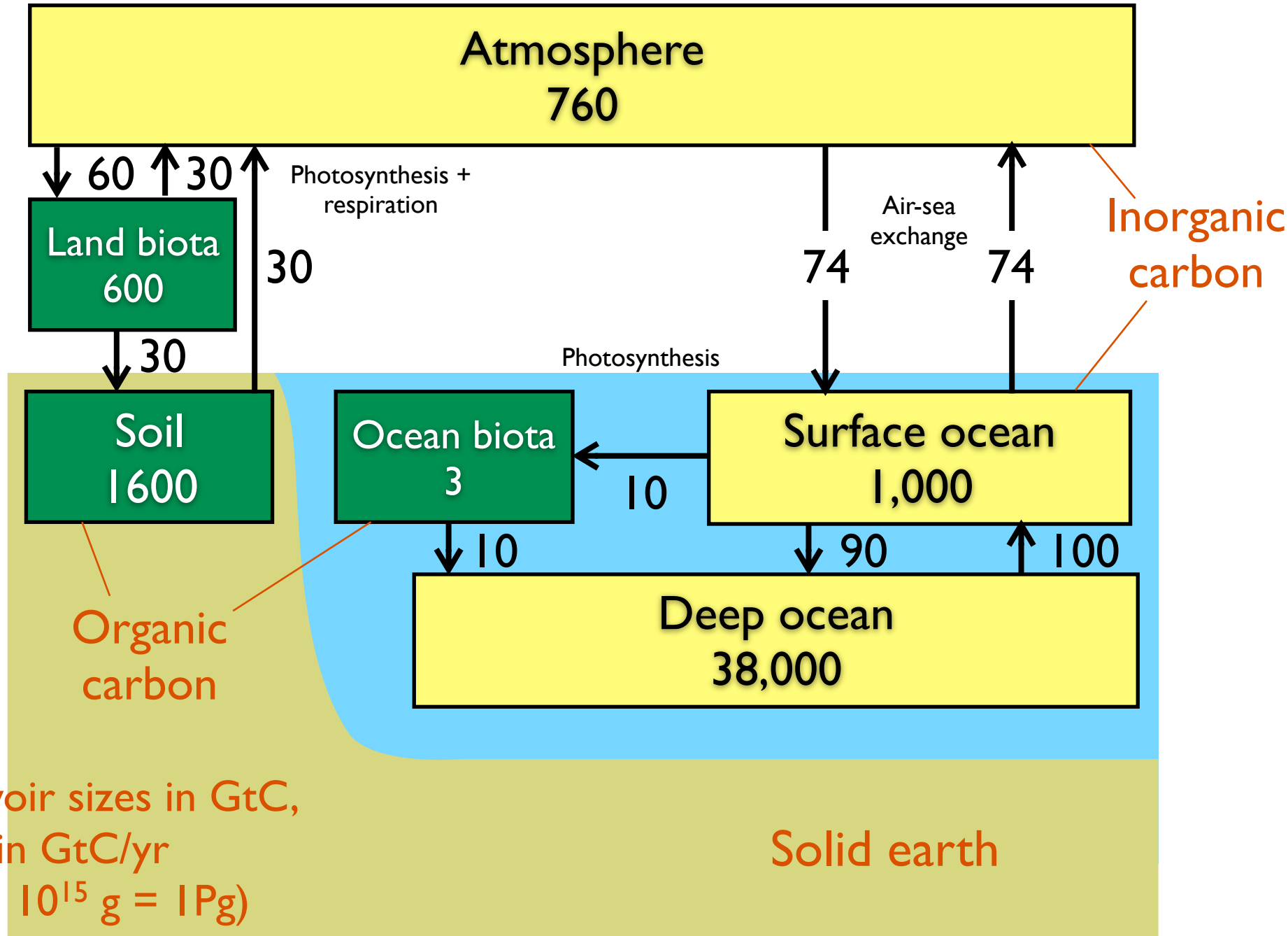

The short- and long-term C cycle

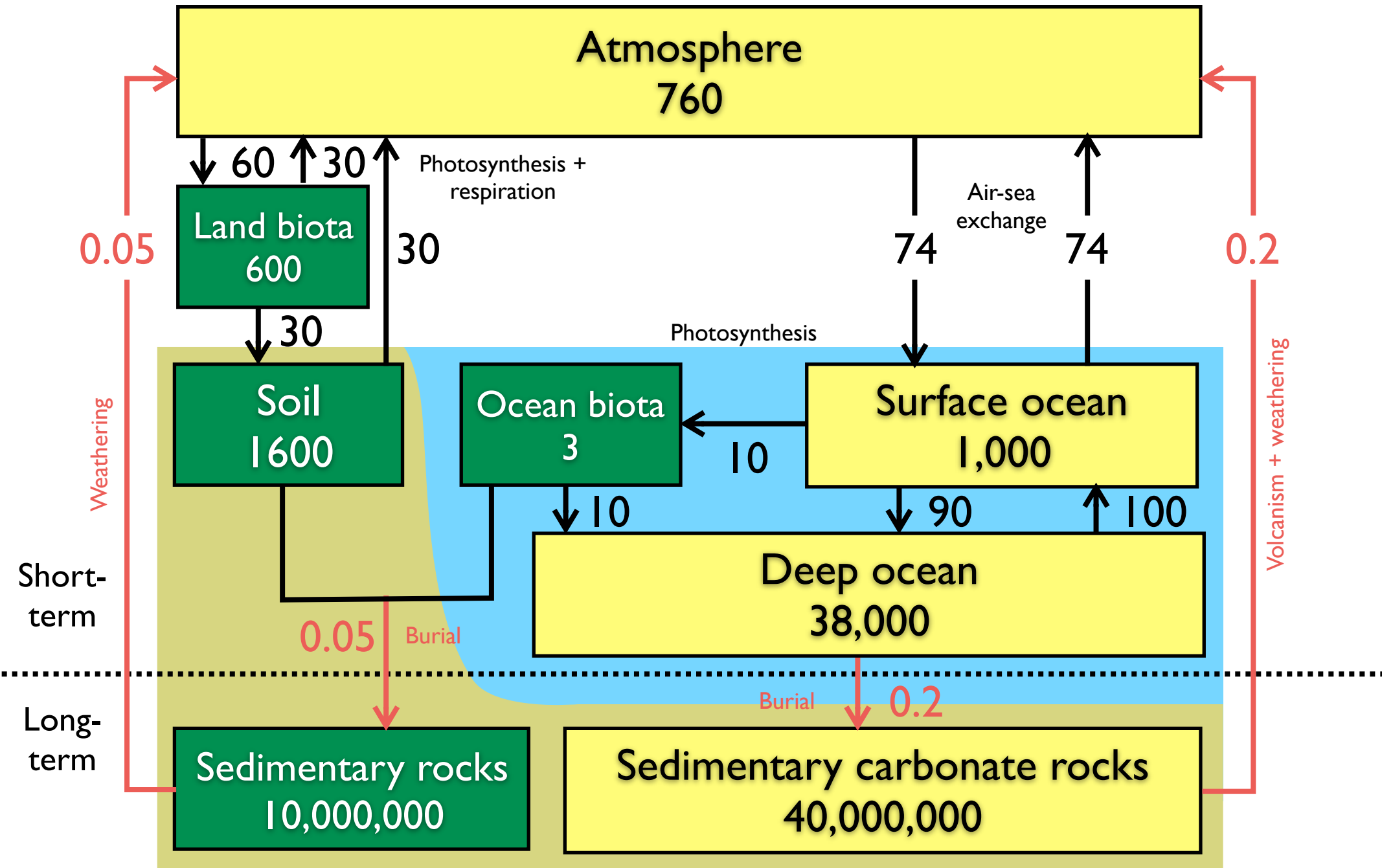

Reservoir sizes

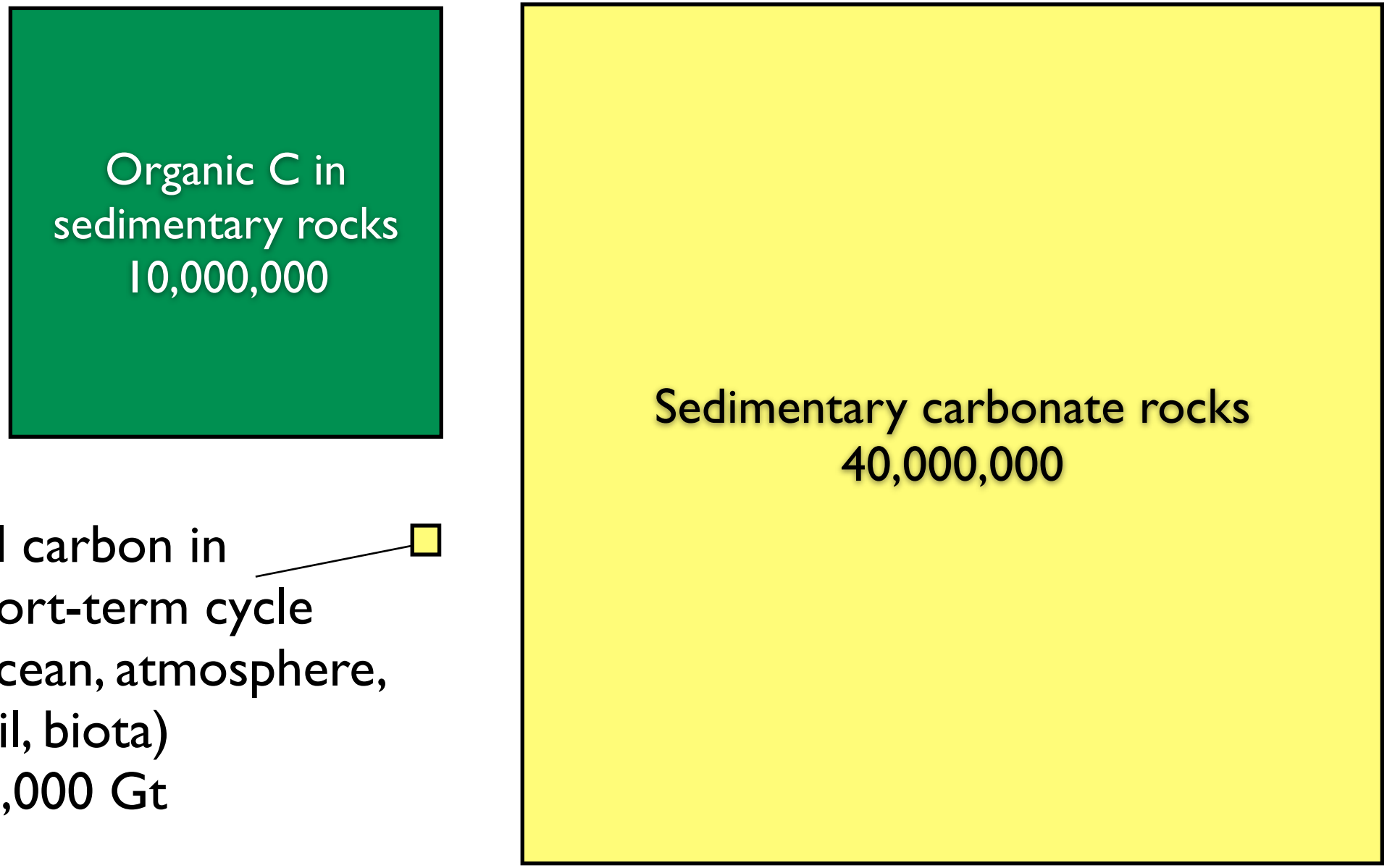

Residence times

- Total short-term C cycle:

  ~42,000 Gt / 0.25 Gt/yr = 160 kyr

- Total long-term C cycle:

  ~50,000,000 Gt / 0.25 Gt/yr = 200 Myr

Ocean sediment types

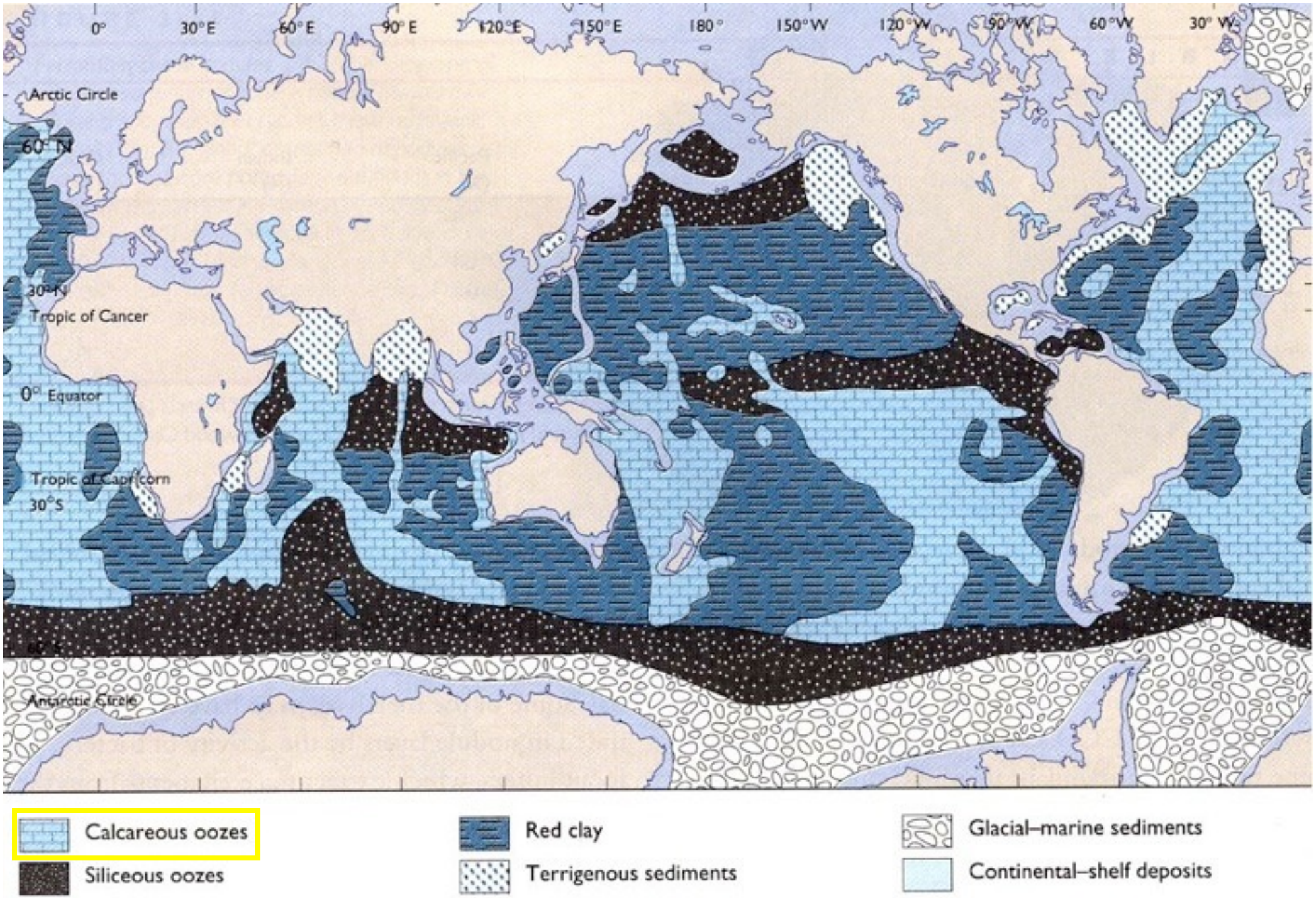

Foraminifera: Small animals with calcite shells ($CaCO_3$)

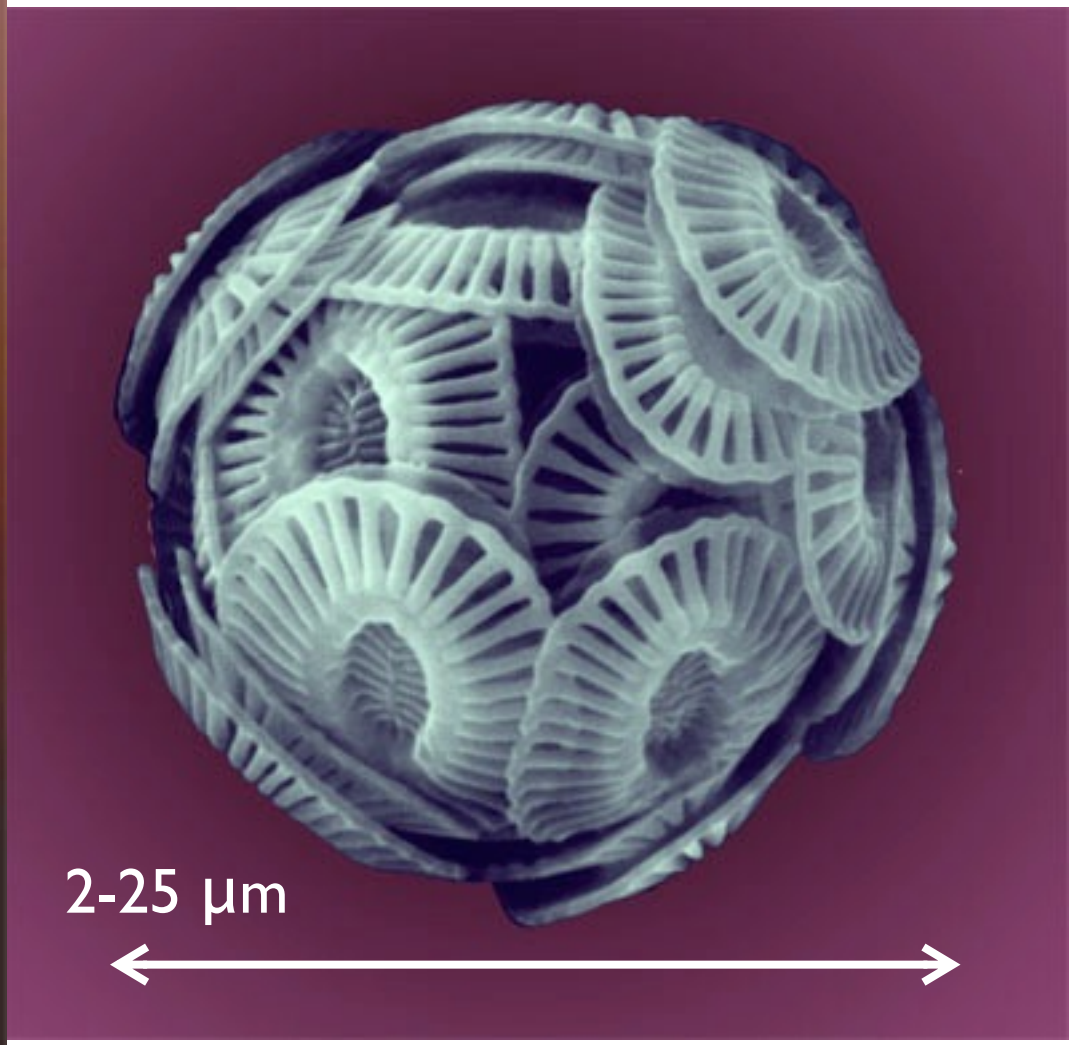

Coccoliths: Tiny plants with a calcite skeleton ($CaCO_3$)

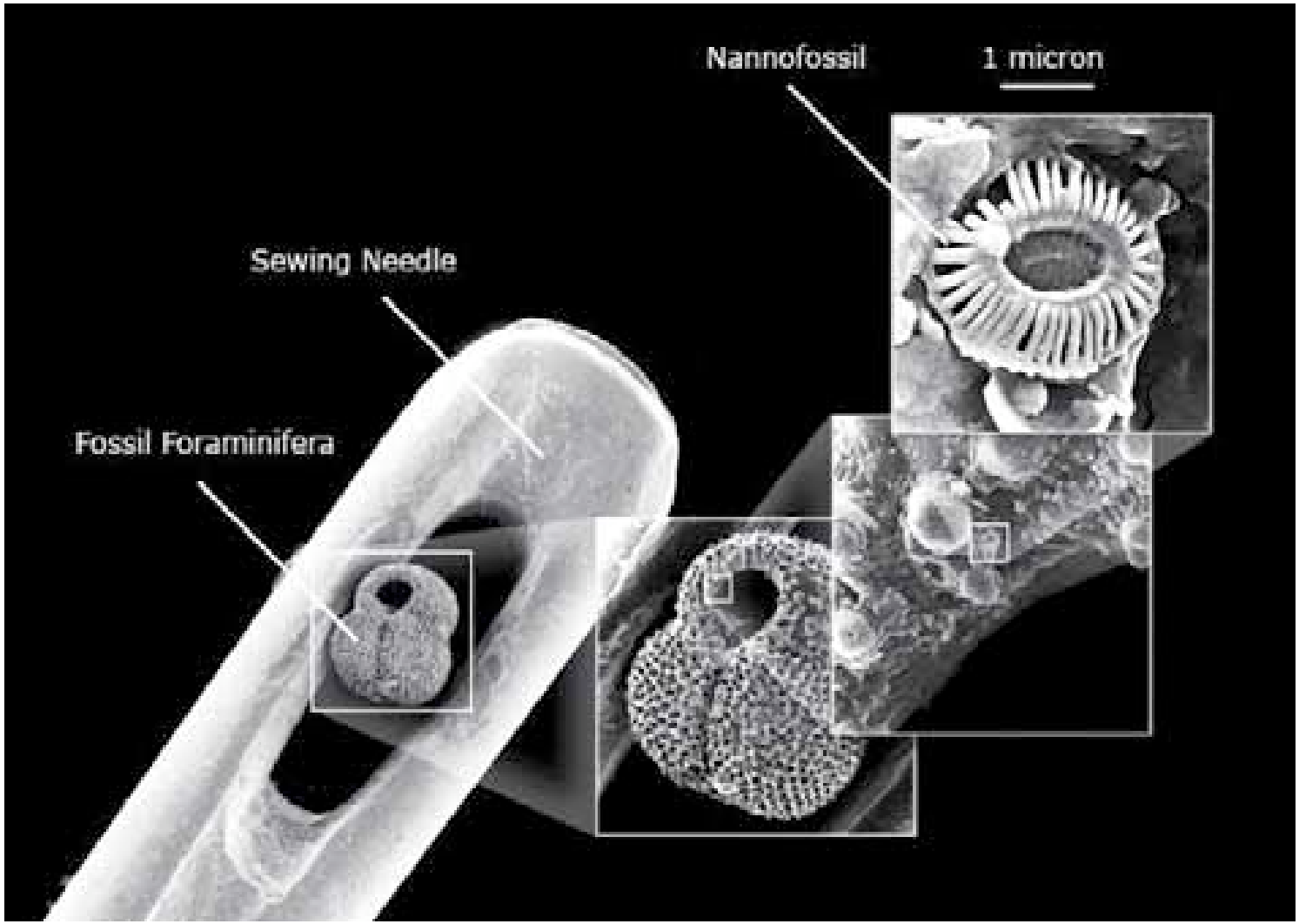

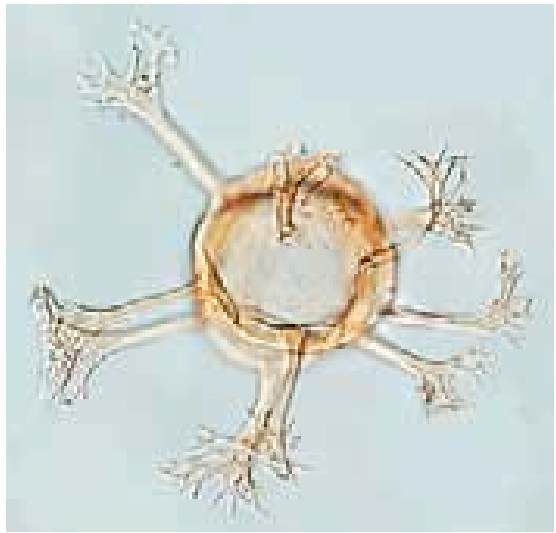

Upper cluster: Foraminifera *(Globigerinoides ruber)*, pictured for scale in the eye of a needle. With additional magnification, shown in increasing stages from left, the nannofossil *(Emiliania huxleyi)* is visible. **Top right:** Dinoflagellate microfossil *(Oligosphaeridium pulcherimum)* from Early Cretaceous rocks (about 100 million years old). **Lower right:** Plant spore microfossil *(Leschikisporites sp.)* from Triassic rocks (about 200 million years old).

Ocean surface productivity

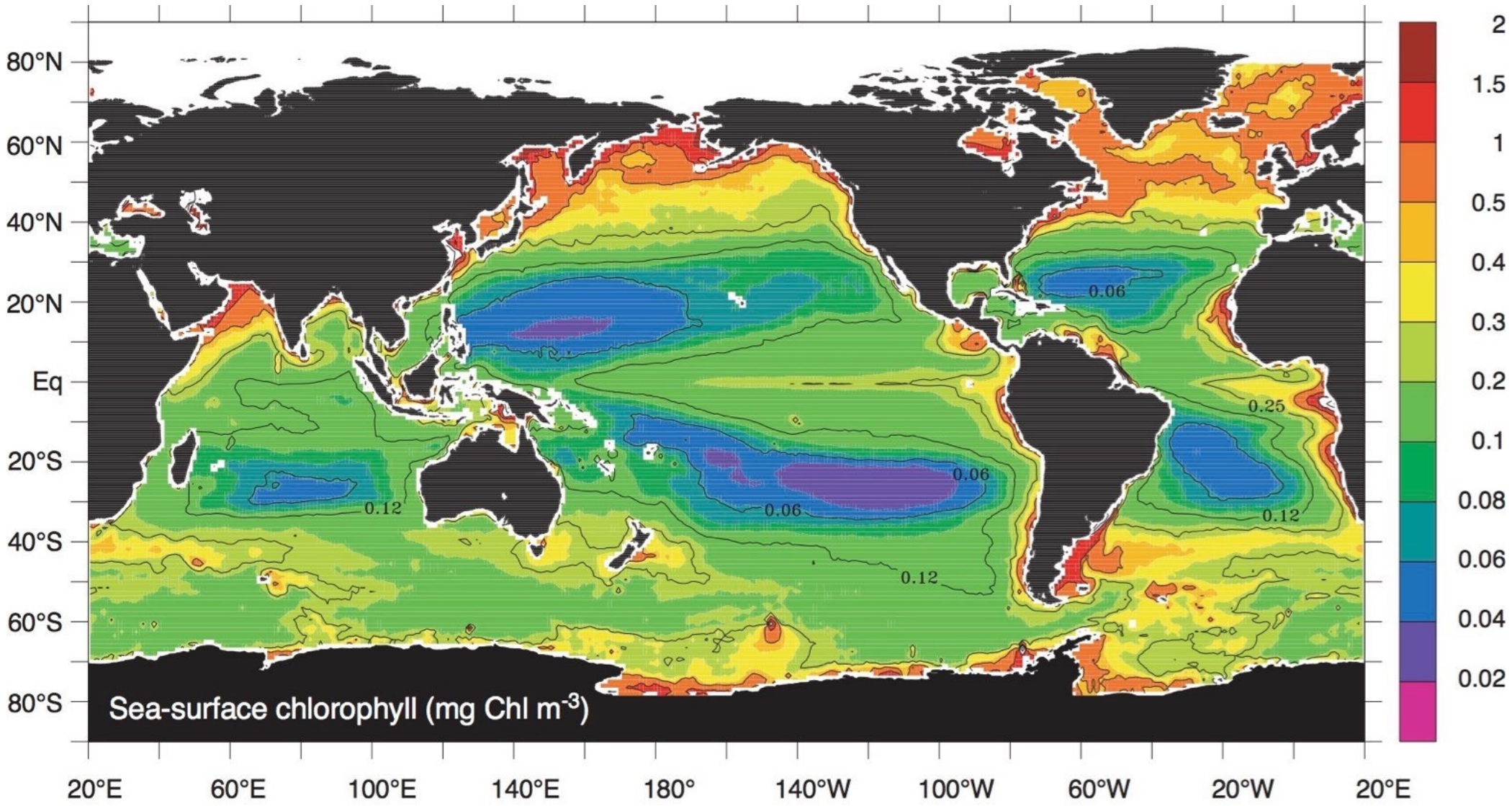

$CaCO_3$ in seafloor sediments

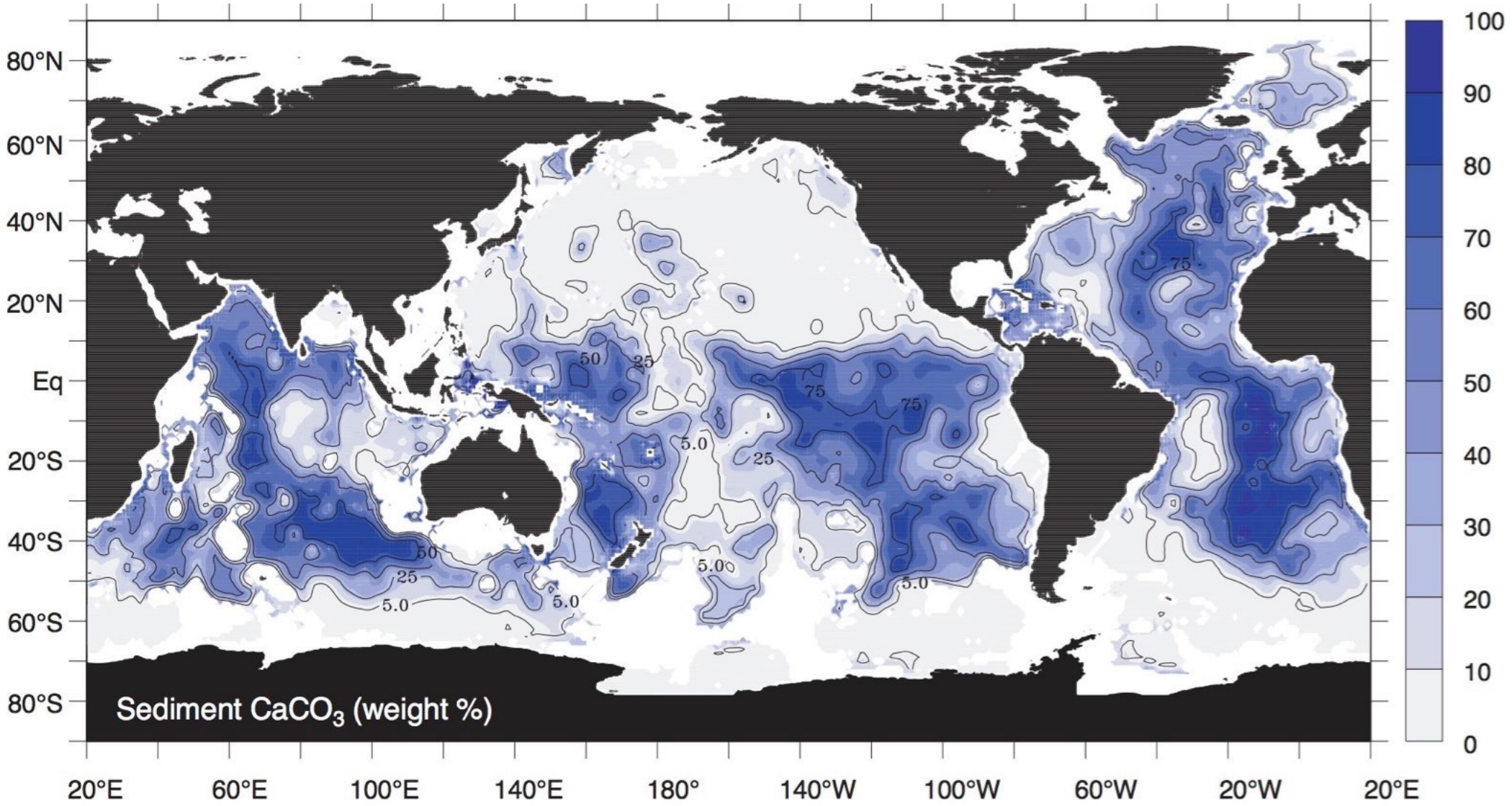

Archer, 1996

Ocean floor topography

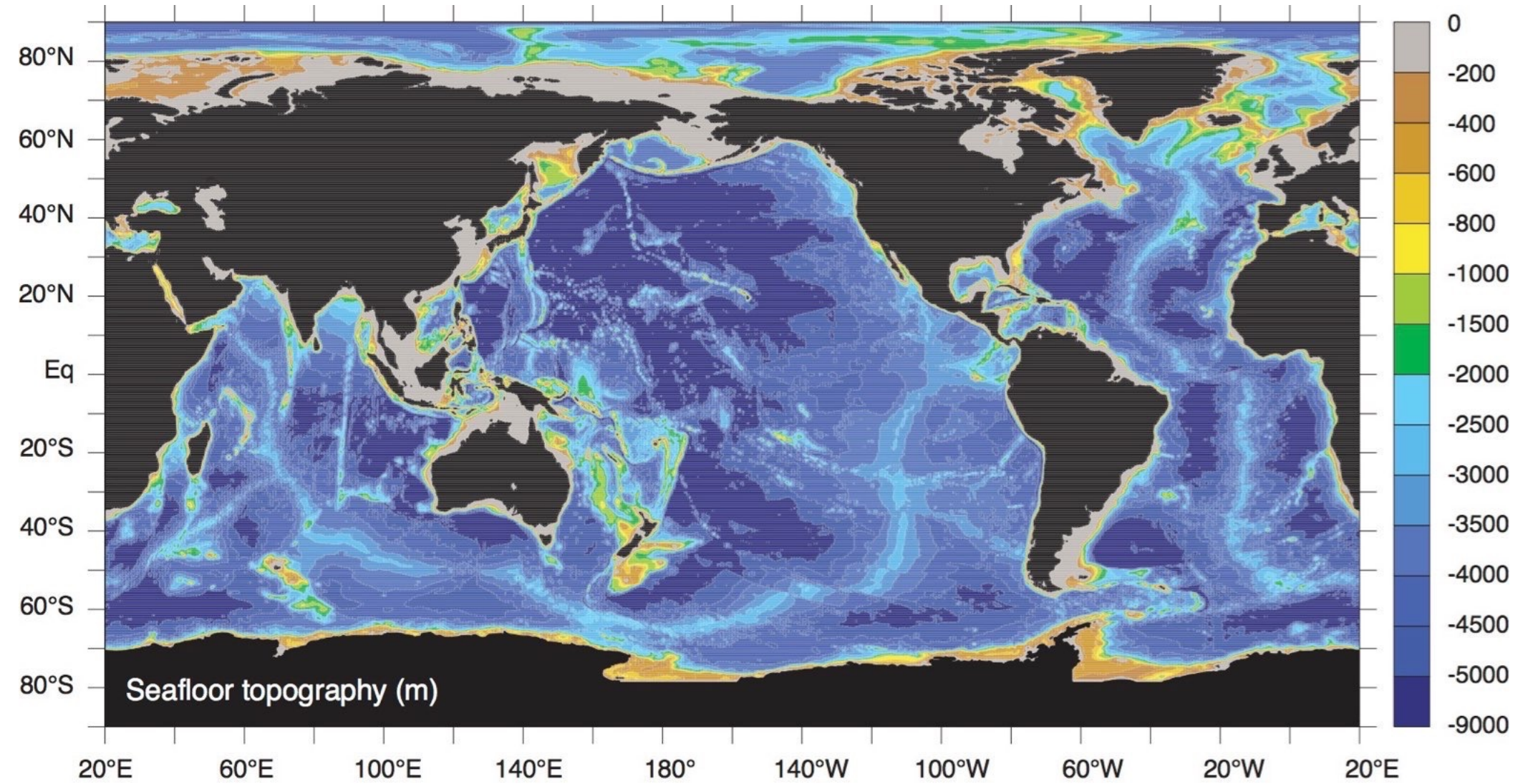

Calcite compensation depth (CCD)

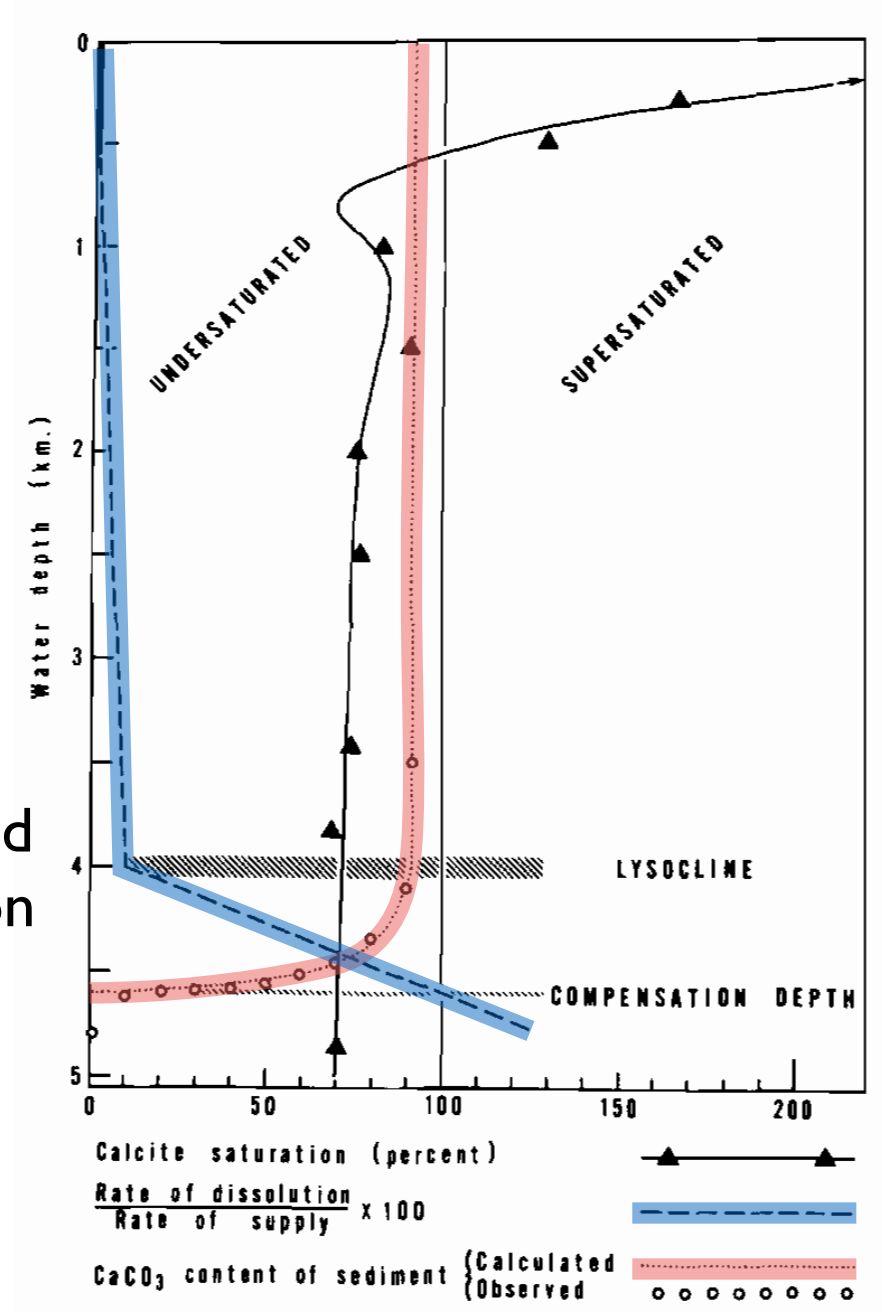

Heath and Culberson 1970

- Calcite is more soluble in sea water as
  - T decreases
  - P and CO_2 content increase
- Deep ocean waters are corrosive for calcite
- CCD is the depth where calcite dissolution rate = supply rate
- Below the CCD, no calcite is preserved in sediment

CCD as a snow line

Calcite compensation depth (CCD)

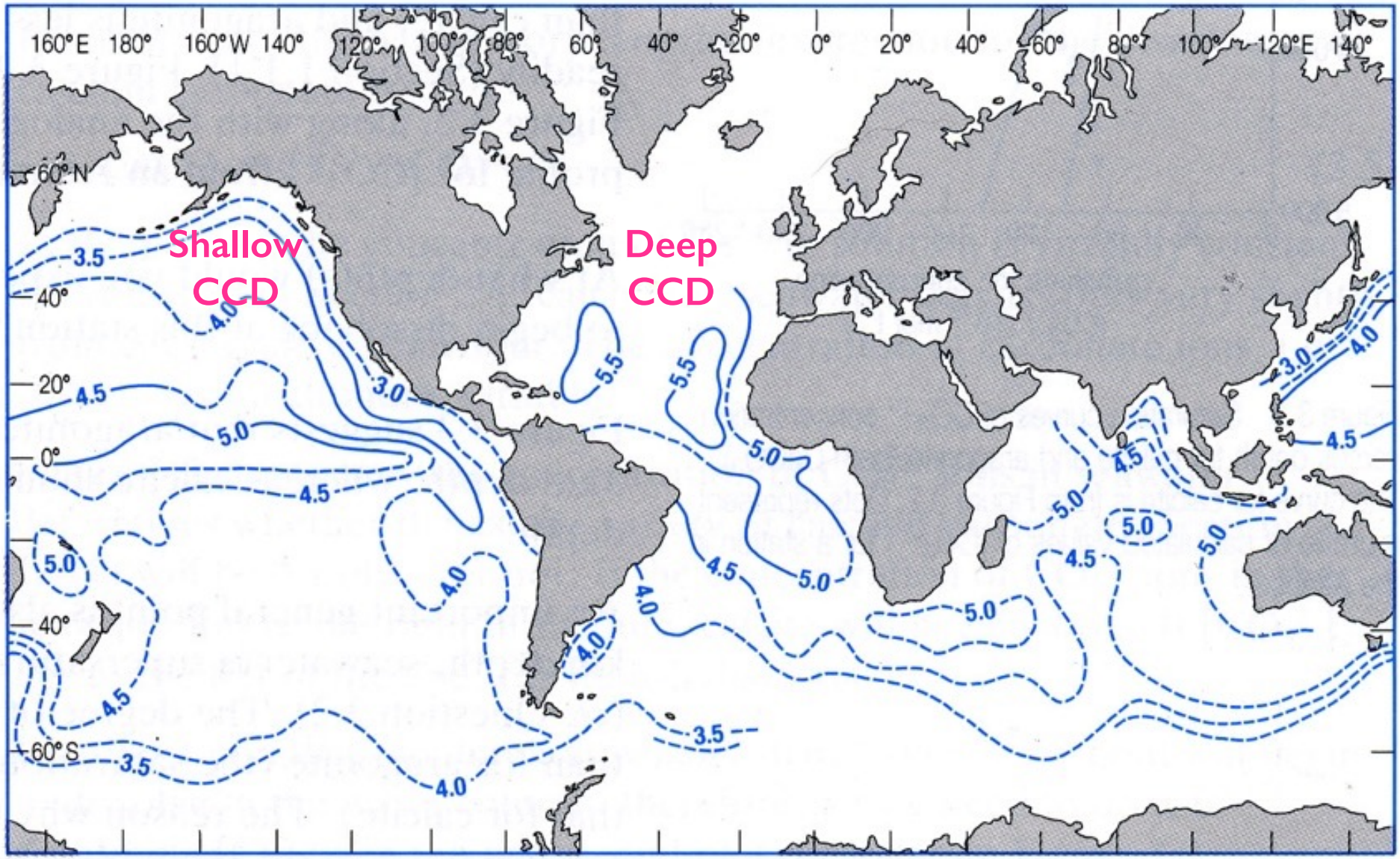

Present-day CCD varies between ~5.5 and 3.5 km

Deep ocean circulation

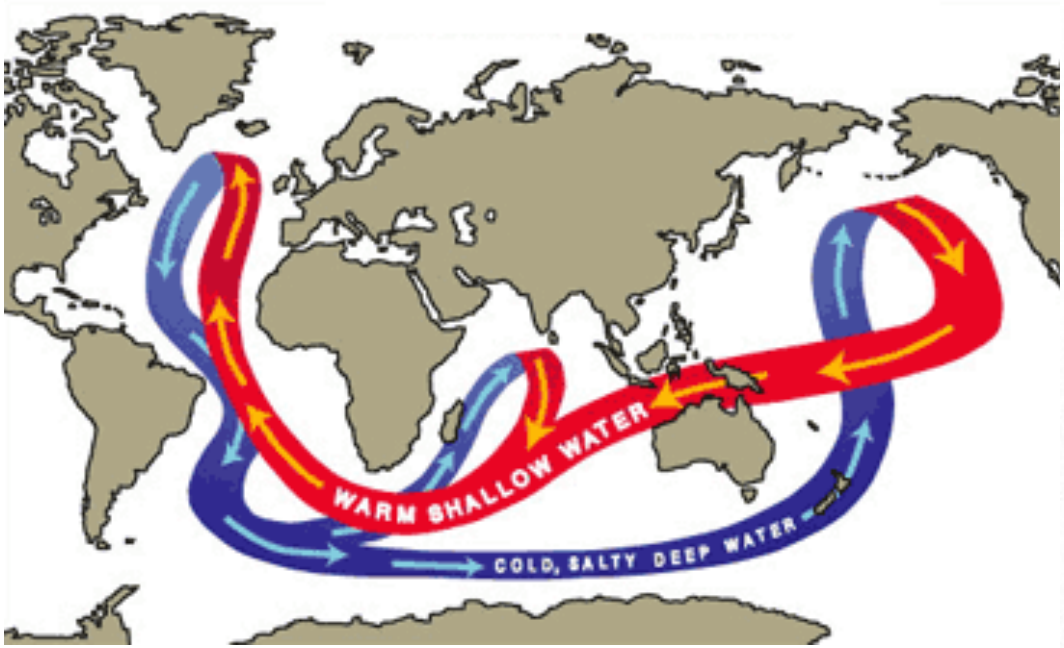

The ocean conveyor belt

Broecker 1974

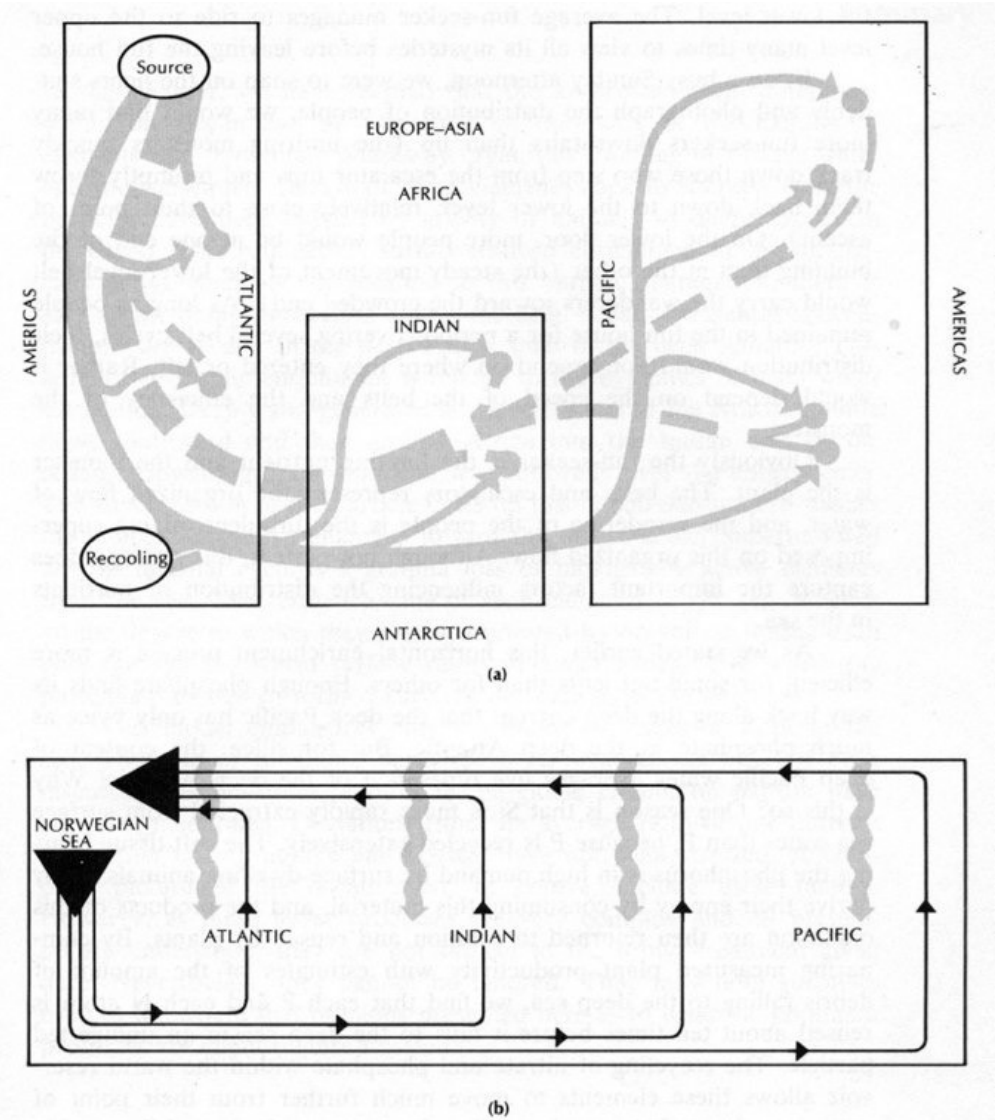

Figure 1-6 (a) is an idealized map of the patterns of deep water flow (solid lines) and surface water flow (dashed lines). The large circles designate the sinking of NADW in the Norwegian Sea and the recooling of water along the perimeter of the Antarctic Continent; the shaded circles indicate the distributed upwelling which balances this deep water generation. (b) is an idealized vertical section running from the North Atlantic to the North Pacific showing the major advective flow pattern (solid lines) and the rain of particles (wavy lines). The combination of these two cycles leads to the observed distribution of nutrients.

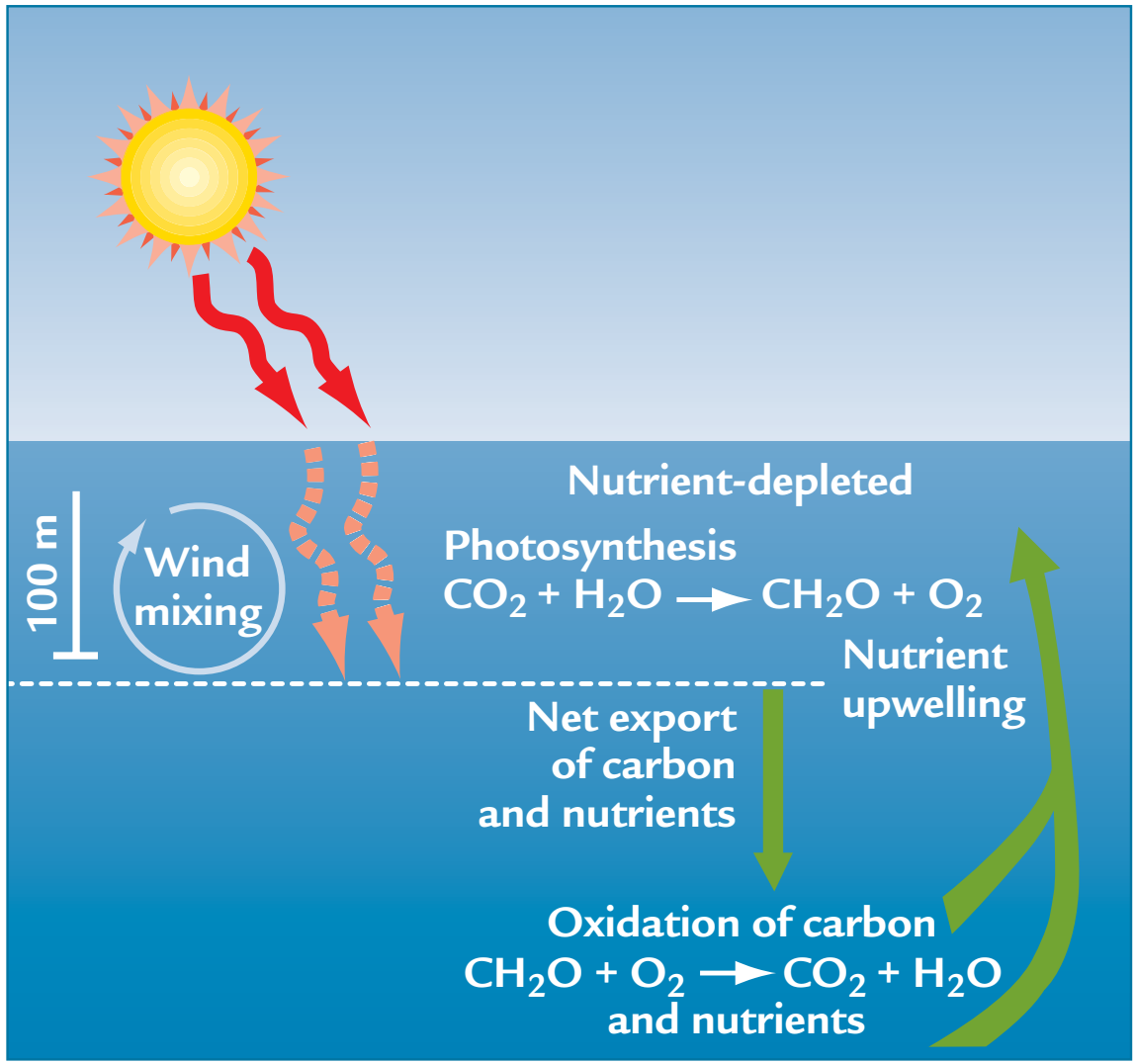

FIGURE 2-35 **Photosynthesis in the ocean** Sunlight penetrating the surface ocean causes photosynthesis by microscopic plants. As they die, their nutrient-bearing organic tissue descends to the seafloor. Oxidation of this tissue at depth returns nutrients and inorganic carbon to the surface ocean in regions of upwelling.

Biological pump

- As deep water moves along the conveyor belt, oxidation of sinking organic matter releases CO_2 and nutrients
- More CO_2 means a shallower CCD
- Nutrients can be returned to surface waters by upwelling driven by wind and surface currents

Ruddiman 2000

Plate stratigraphy

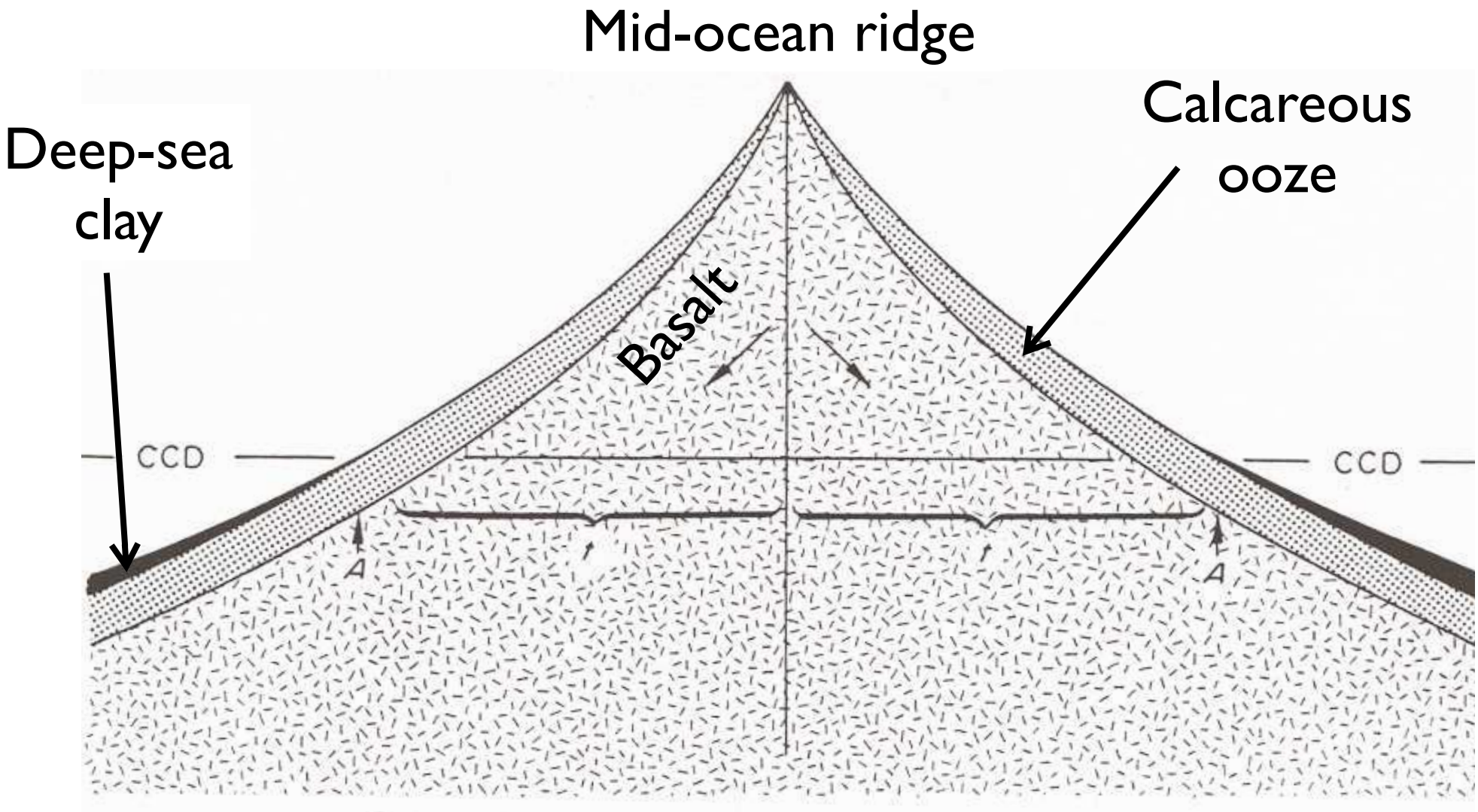

Berger and Winterer 1974

Scientific Ocean Drilling History

- Project Mohole (1958 -1966)
- Deep Sea Drilling Project (1968 -1983)
- Ocean Drilling Program (1985 - 2003)
- Integrated Ocean Drilling Program (2003 - 2013)
- International Ocean Discovery Program (2013 - ...)

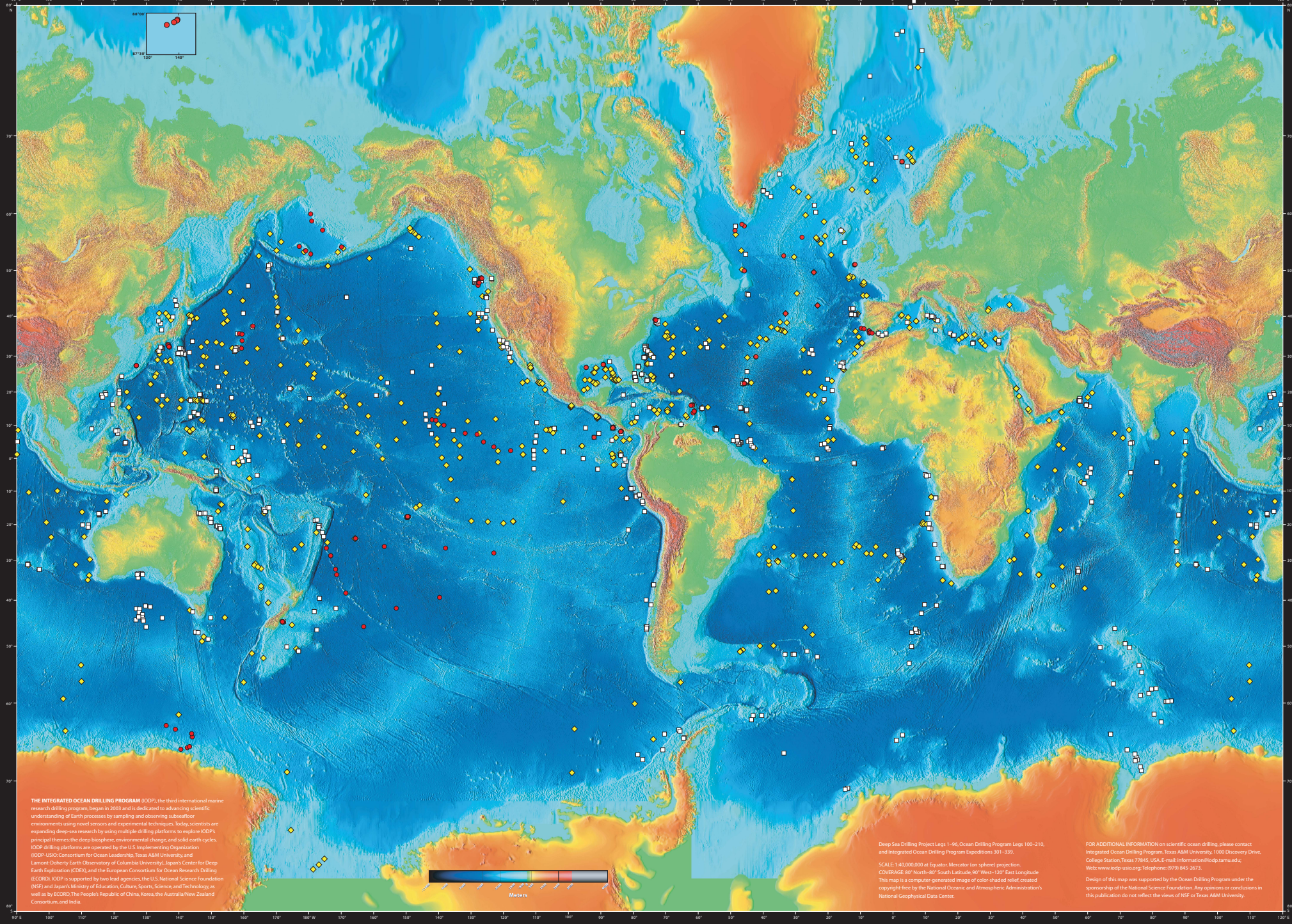

THE INTEGRATED OCEAN DRILLING PROGRAM (IODP), the third international marine research drilling program, began in 2003 and is dedicated to advancing scientific understanding of Earth processes by sampling and observing subseafloor environments using novel sensors and experimental techniques. Today, scientists are expanding deep-sea research by using multiple drilling platforms to explore IODP's principal themes: the deep biosphere, environmental change, and solid earth cycles. IODP drilling platforms are operated by the U.S. Implementing Organization (IODP-USIO: Consortium for Ocean Leadership, Texas A&M University, and Lamont-Doherty Earth Observatory of Columbia University), Japan's Center for Deep Earth Exploration (CDEX), and the European Consortium for Ocean Research Drilling (ECORD). IODP is supported by two lead agencies, the U.S. National Science Foundation (NSF) and Japan's Ministry of Education, Culture, Sports, Science, and Technology, as well as by ECORD, The People's Republic of China, Korea, the Australia/New Zealand Consortium, and India.

Deep Sea Drilling Project Legs 1–96, Ocean Drilling Program Legs 100–210, and Integrated Ocean Drilling Program Expeditions 301–339.

SCALE: 1:40,000,000 at Equator. Mercator (on sphere) projection.
COVERAGE: 80° North–80° South Latitude, 90° West–120° East Longitude
This map is a computer-generated image of color-shaded relief, created copyright-free by the National Oceanic and Atmospheric Administration's National Geophysical Data Center.

FOR ADDITIONAL INFORMATION on scientific ocean drilling, please contact Integrated Ocean Drilling Program, Texas A&M University, 1000 Discovery Drive, College Station, Texas 77845, USA. E-mail: information@iodp.tamu.edu; Web: www.iodp-usio.org; Telephone: (979) 845-2673.

Design of this map was supported by the Ocean Drilling Program under the sponsorship of the National Science Foundation. Any opinions or conclusions in this publication do not reflect the views of NSF or Texas A&M University.

◆ Deep Sea Drilling Project ▪ Ocean Drilling Program ● Integrated Ocean Drilling Program

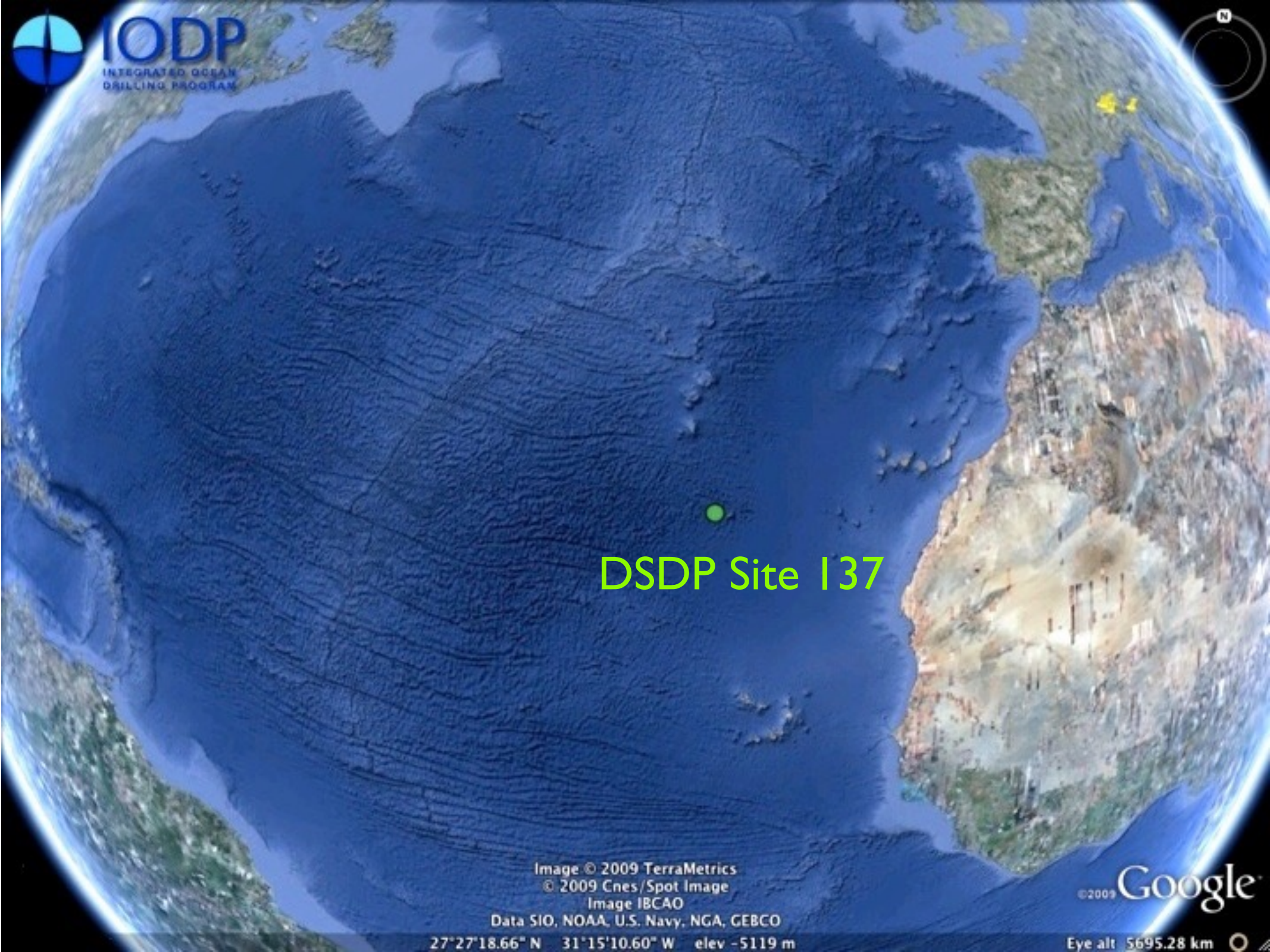
IODP
INTEGRATED OCEAN DRILLING PROGRAM
DSDP Site 137
Image © 2009 TerraMetrics
© 2009 Cnes/Spot Image
Image IBCAO
Data SIO, NOAA, U.S. Navy, NGA, GEBCO
27°27'18.66" N 31°15'10.60" W elev -5119 m
©2009 Google
Eye alt 5695.28 km

DSDP Site 137

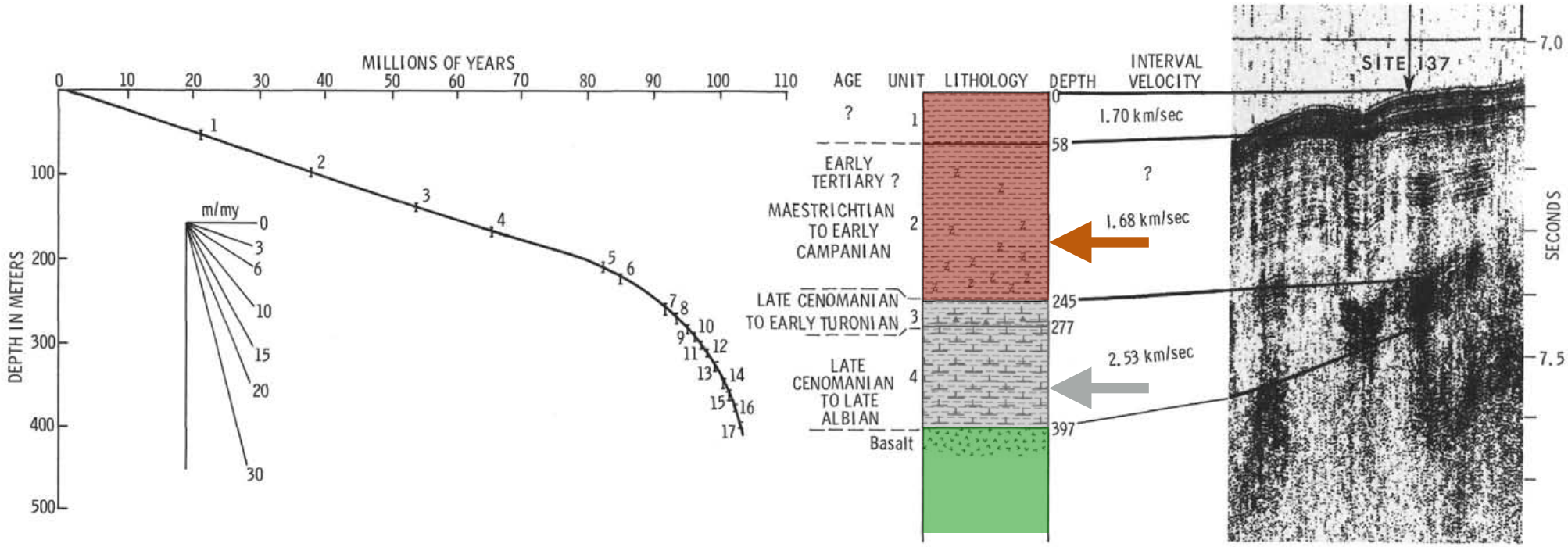

Figure 3. *Geological synthesis at Site 137.*

- Seafloor depth: 5361 m
- 0-245 m below seafloor (mbsf): Deep-sea clay
- 245-397 mbsf: Calcareous ooze, 90-100 Ma
- 397-402 mbsf: Basalt

E. Atlantic abyssal plain (26°N, 27°W)

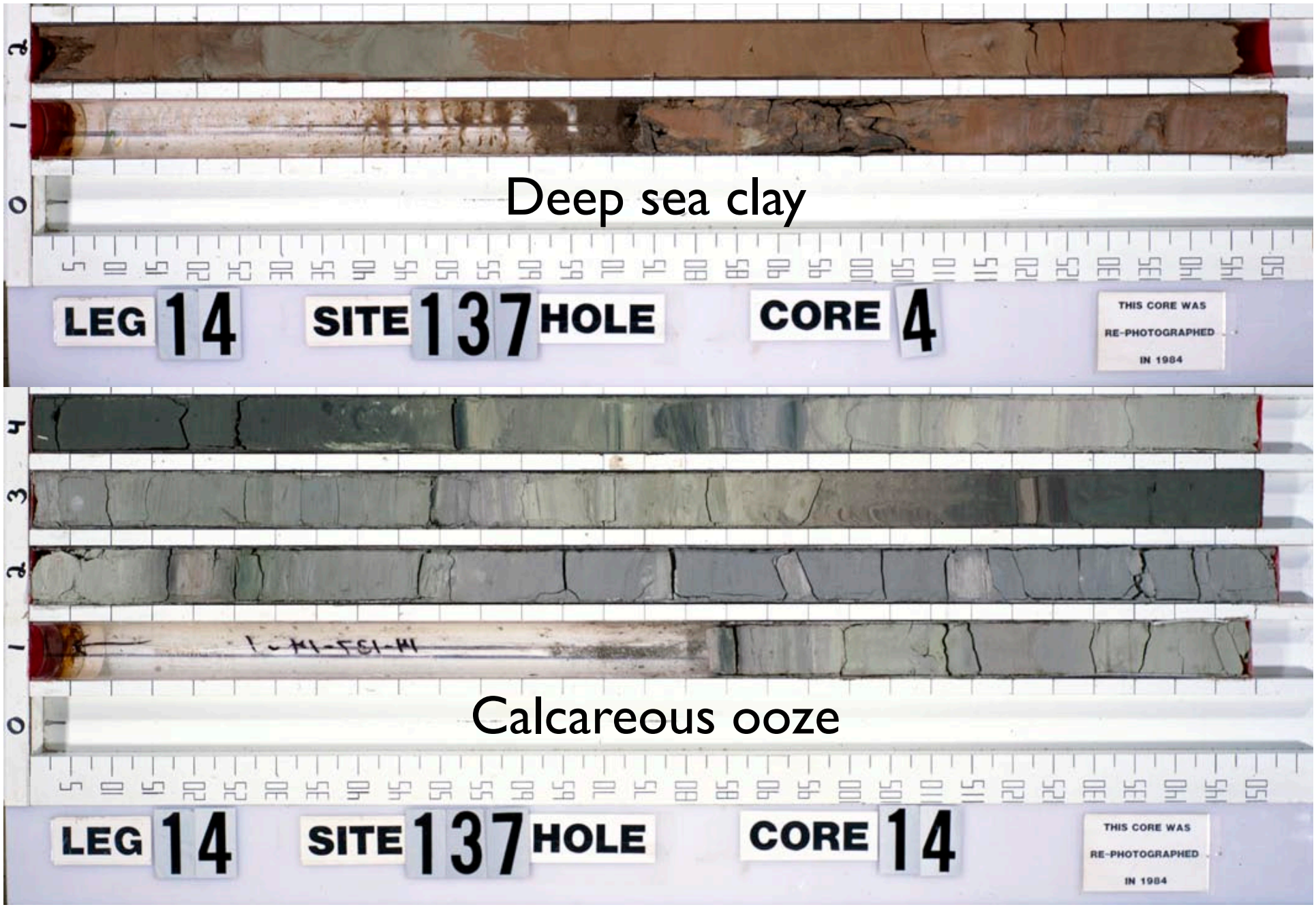

Ocean basement depth-age relationship

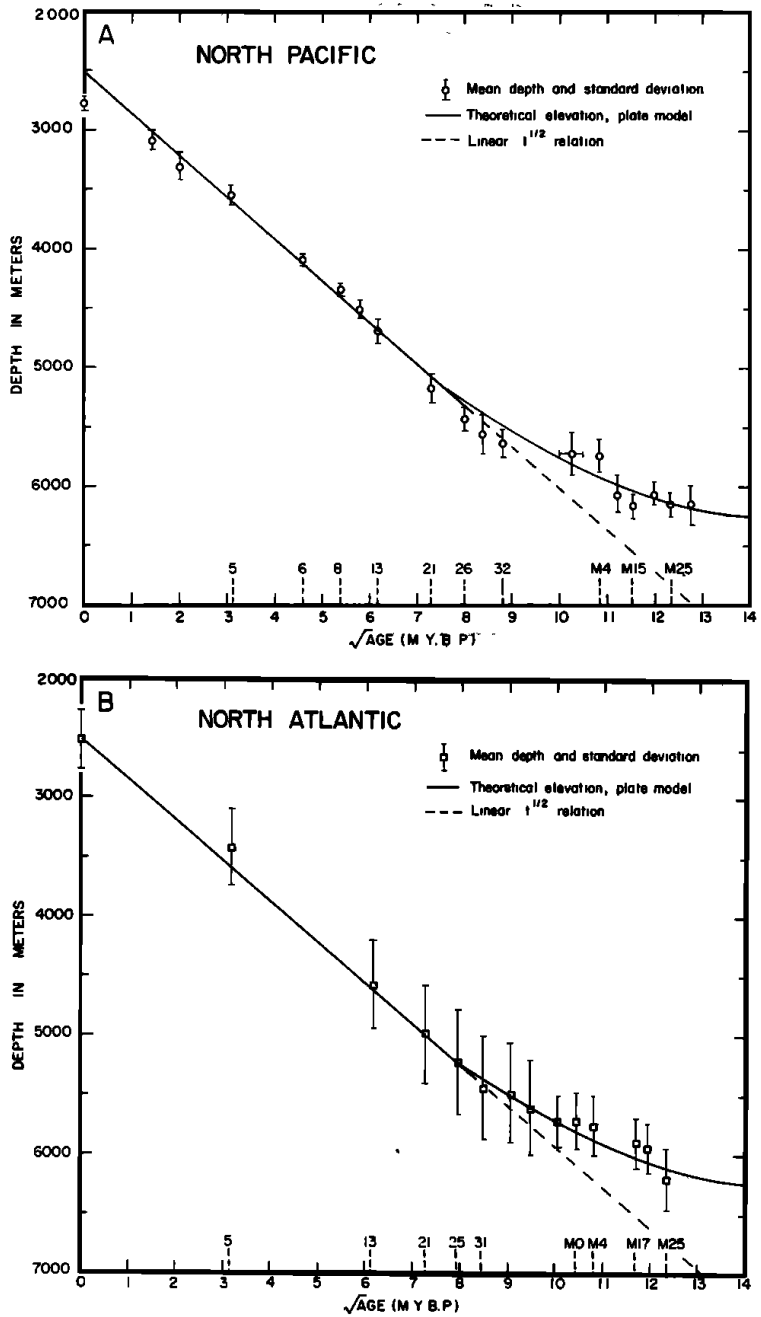

- Age t in million years (Ma), depth z in meters
- $t < 70$ Ma: $z(t) = 2500 + 350\ t^{1/2}$
- $t > 20$ Ma: $z(t) = 6400 - 3200 \exp(-t / 62.8)$

Parsons and Sclater 1977

Paleo-depth of CCD

Deep-sea clay

Calcareous ooze

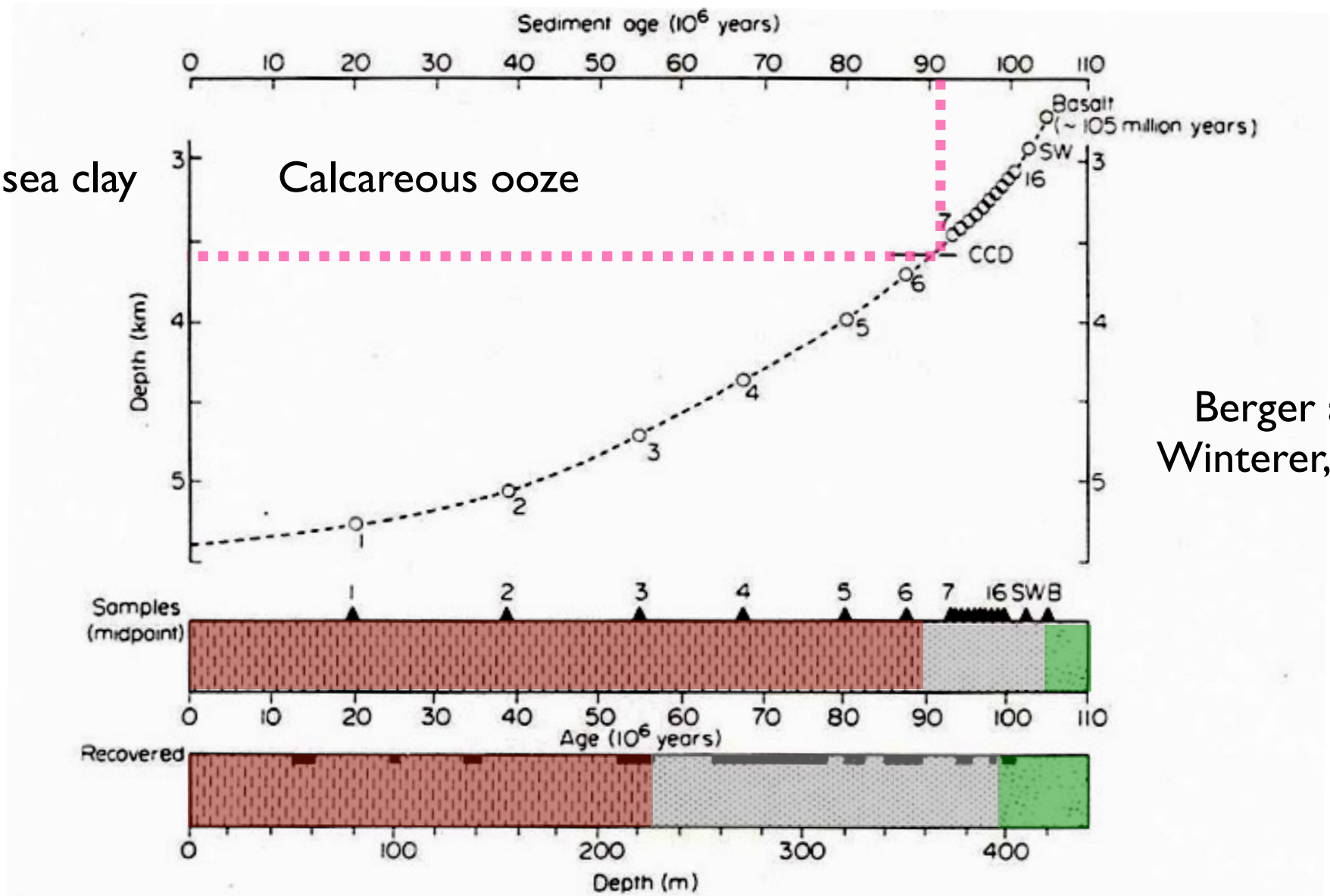

Berger and Winterer, 1974

Fig. 21. Backtracking of Site 137, Leg 14 (Hayes, Pimm *et al.*, 1972). Symbols from left to right: clay, calcareous ooze, basalt. Sample numbers: core number of Site 137.

CCD in the geologic past

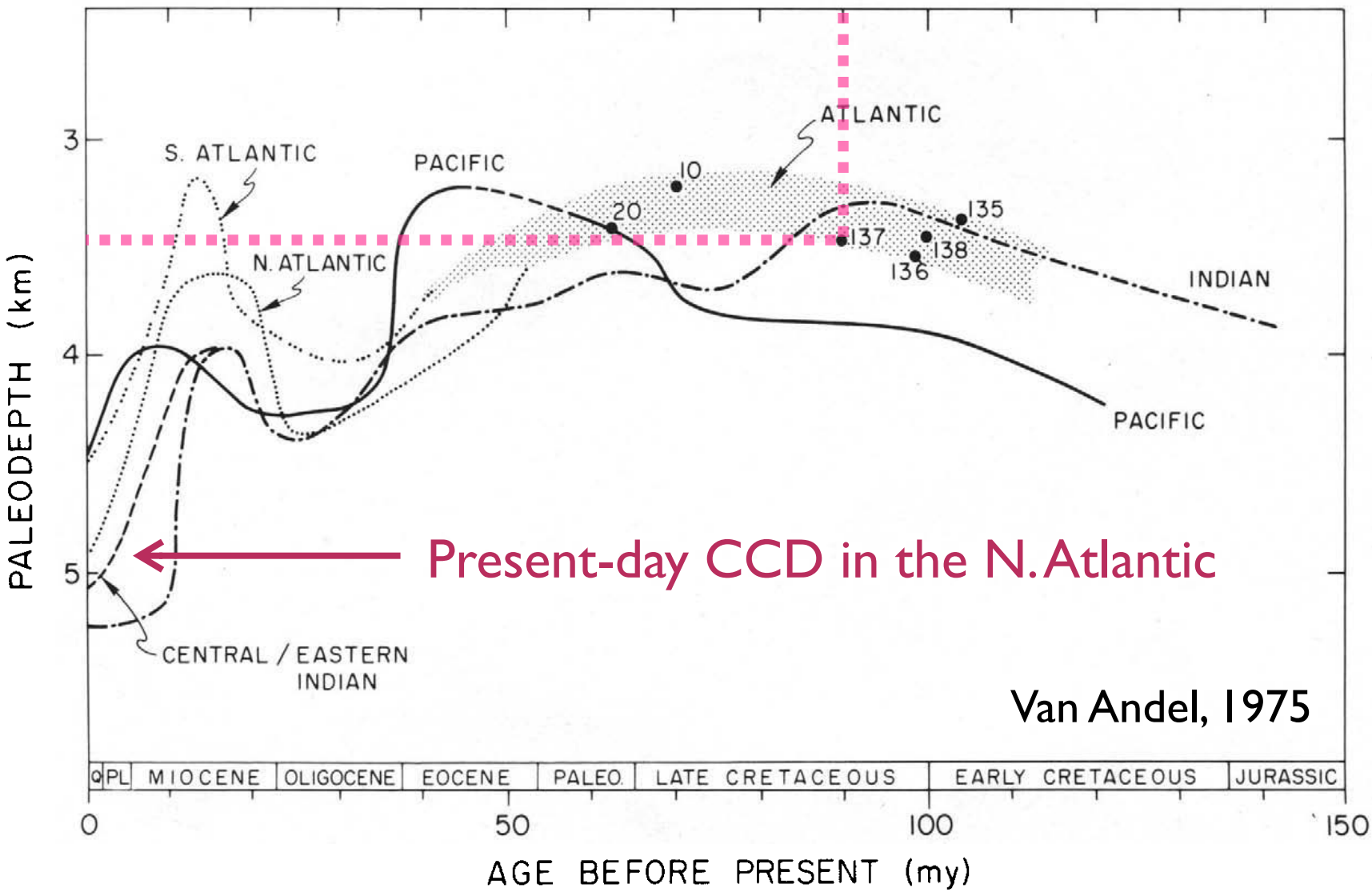

Fig. 4. Composite of CCD curves for Indian, Pacific, and Atlantic Oceans. Atlantic curves for the Cenozoic are from Berger and Von Rad [5]. Cretaceous CCD indicated with a zone of shading based on data points (with drill site numbers) as shown, mainly after [5]. For the Pacific since the Eocene only the CCD_{pac} is shown because it is more typical for the mean level of the CCD in the Pacific.

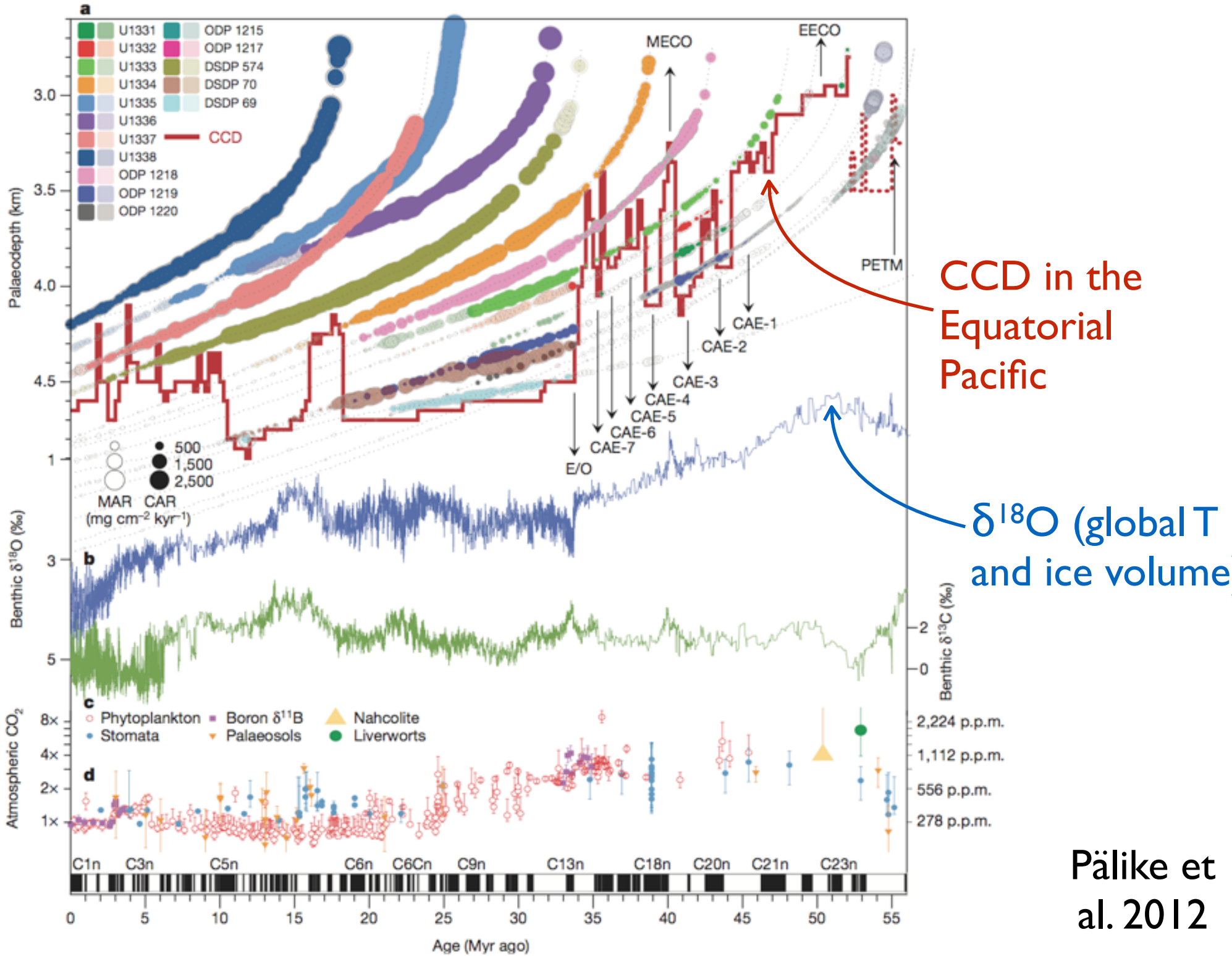

CCD in the Equatorial Pacific

$\delta^{18}O$ (global T and ice volume)

Pälike et al. 2012

Neritic $CaCO_3$

Geol Rundsch (1996) 85:496–504

ORIGINAL PAPER

J. D. Milliman · A. W. Droxler

Neritic and pelagic carbonate sedimentation in the marine environment: ignorance is not bliss

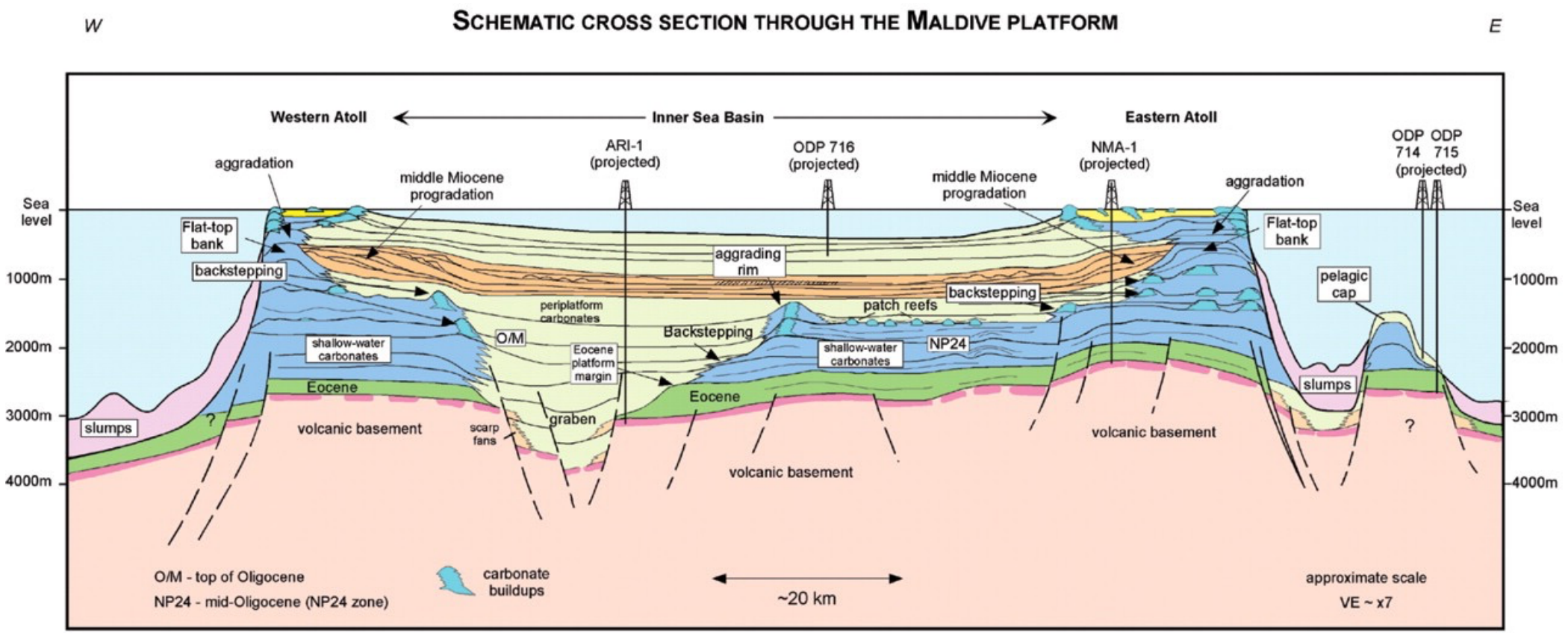

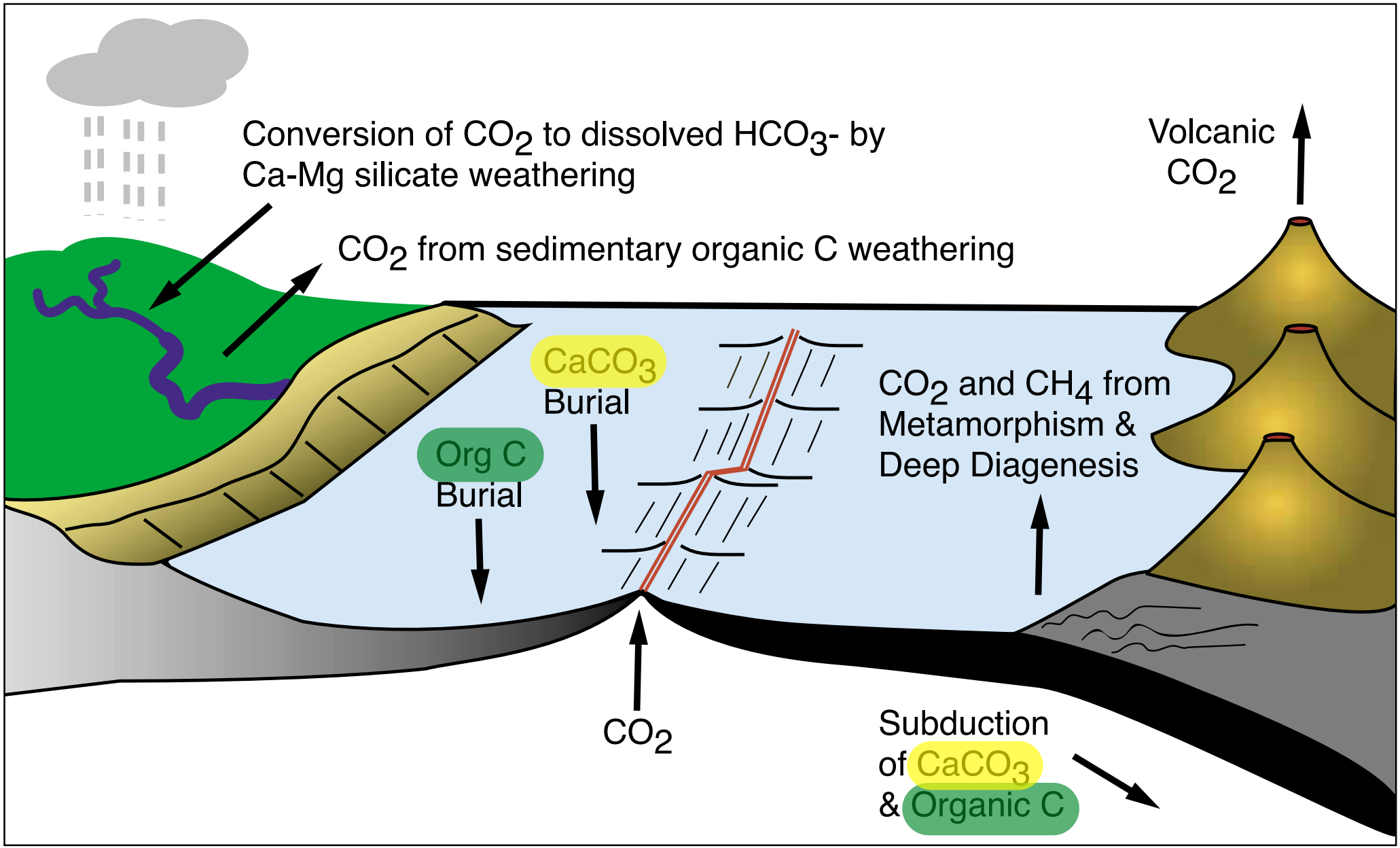

Figure 1. An idealized and simplified representation of the surficial aspects of the long-term carbon cycle. Note the exchange of carbon between rocks, on the one hand, and the oceans and atmosphere, on the other; this is the distinguishing characteristic of the long-term cycle.

Berner, 1999

Particulate organic carbon (POC)

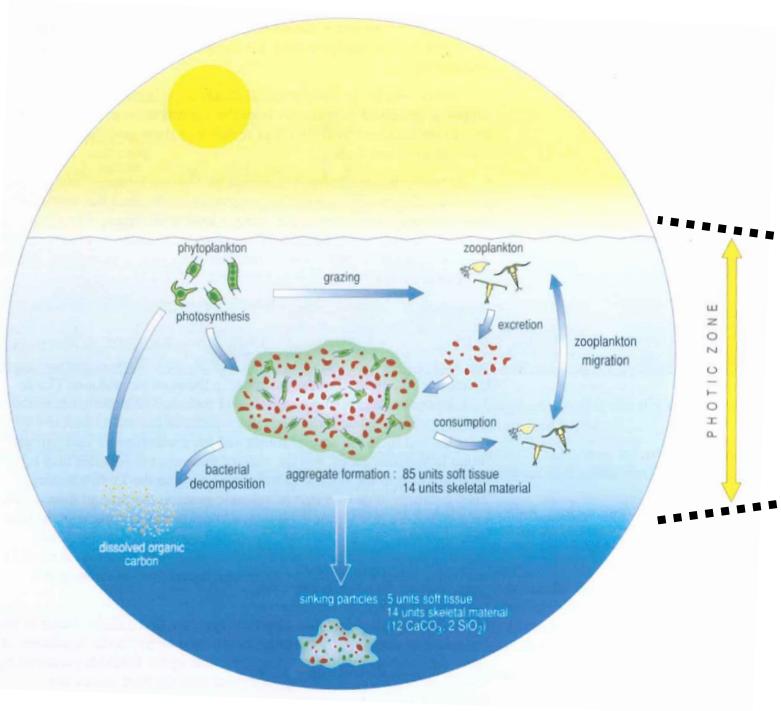

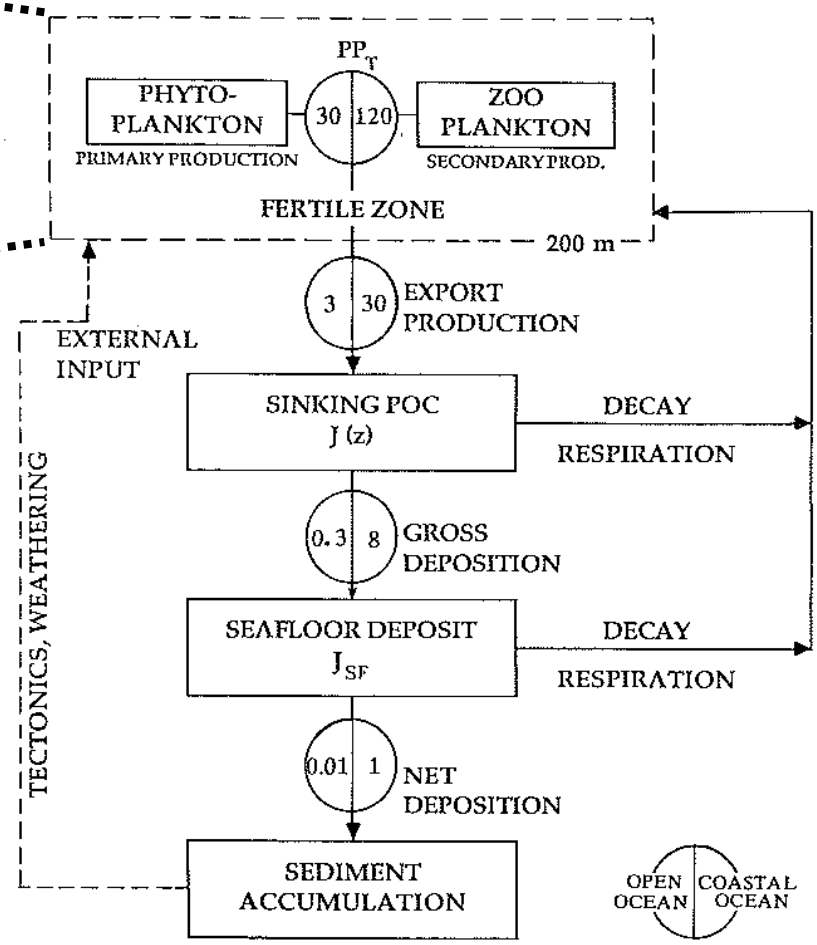

- Photosynthesis

$$CO_2 + H_2O + \textit{energy} \rightarrow CH_2O + O_2$$

- Aerobic respiration

$$CH_2O + O_2 \rightarrow CO_2 + H_2O + \textit{energy}$$

Seibold and Berger 1996

Fig. 6.1. Sketch of transfer of particulate organic carbon in the ocean, from primary production to burial in the sediment. *Numbers* are fluxes in $gC/m^2/yr$; within each circle the value to the *left* refers to typical open ocean conditions, that to the *right* to the coastal ocean environment. [W. H. Berger, G. Wefer, V. S. Smetacek, 1989, in Productivity of the ocean: present and past. Wiley, Chichester]

Depth control

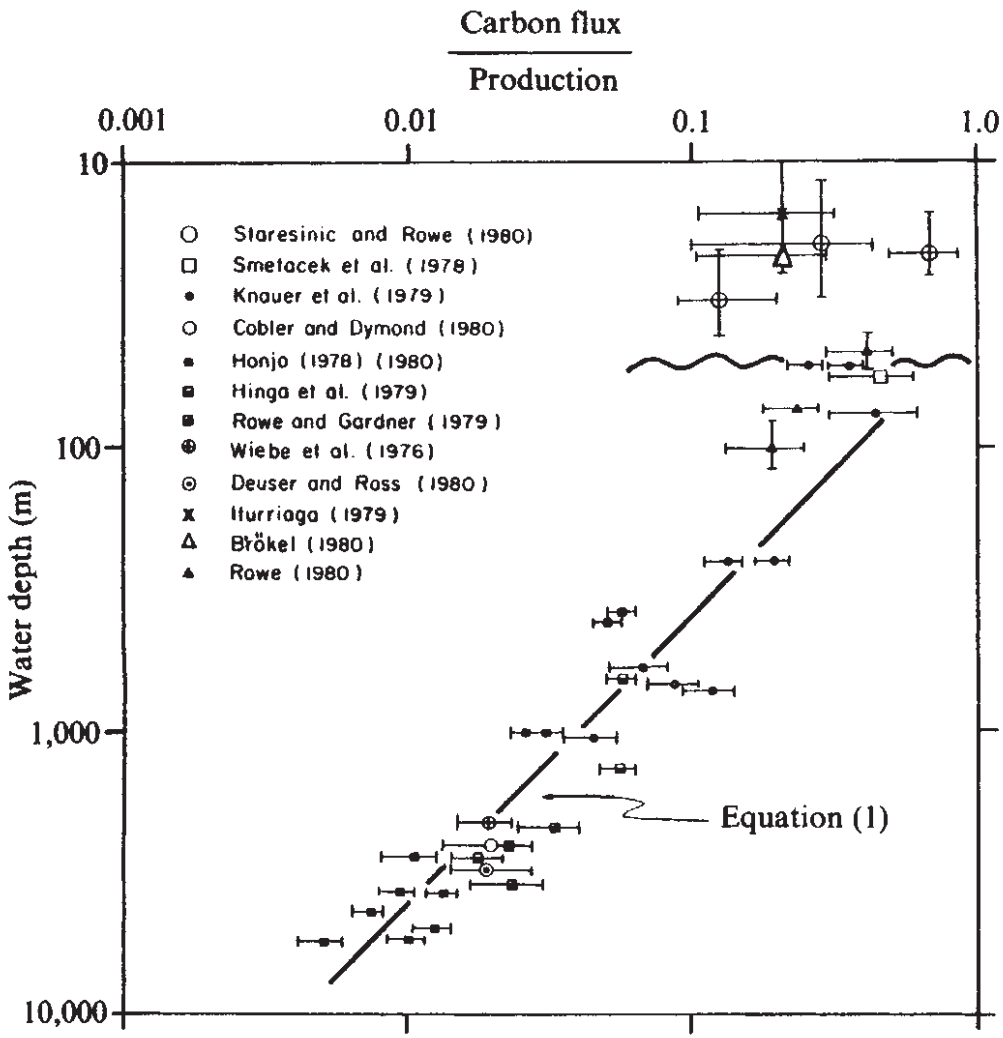

Fig. 1 Organic carbon fluxes with depth in the water column normalized to mean annual primary production rates at the sites of sediment trap deployment. The undulating line indicates the base of the euphotic zone; the horizontal error bars reflect variations in mean annual productivity as well as in replicate flux measurements during the same season or over several seasons; vertical error bars are depth ranges of several sediment trap deployments and uncertainties in the exact depth location. The data points by Rowe (1980) represent selected averages of 2–5 single sites at ~10 m above the bottom, where resuspension was assumed to be minimal.

Suess 1980

Sedimentary control

Accumulation rate

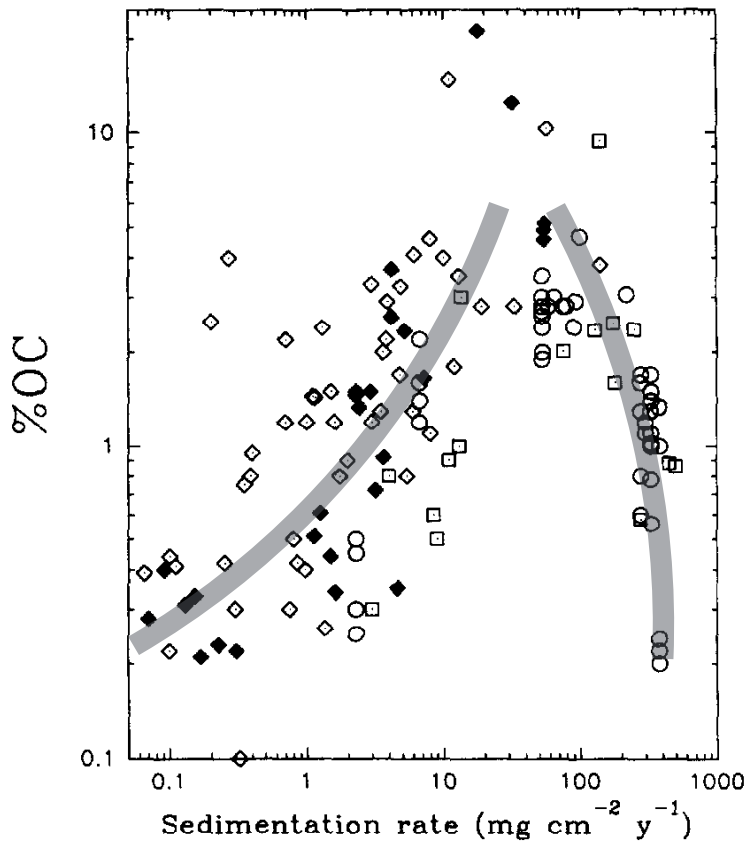

Fig. 4. Plot of weight percent of organic carbon (%OC) vs. accumulation rate for sediments from a variety of depositional environments. ◆ = data from Müller and Suess, 1979; ◇ = data compiled by Henrichs and Reeburgh, 1987; □ = data from Reimers et al. (various papers); ○ = data from the Washington Coast (Carpenter et al., 1981, 1982).

Grain size

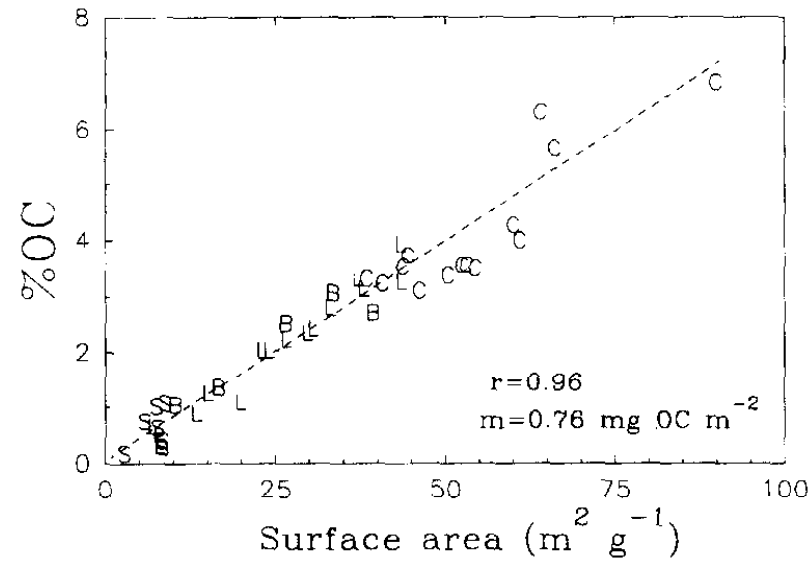

Fig. 7. Weight percent of organic carbon plotted vs. mineral surface area for bulk material (B) as well as sand- (S), silt- (L), and clay-sized (C) fractions from samples of suspended sediments in the Columbia River estuary and surface (0–5 cm) sediments from four sites along the adjacent continental shelf and slope off Washington state. This plot shows data for sediments from which discrete particles of organic matter have been removed by heavy liquid flotation. Corrections of total surface areas for a small measured component of interbasal surfaces in expandable clay minerals have also been applied (data from Keil et al., 1994a).

Hedges and Keil 1995

Marine and terrestrial POC

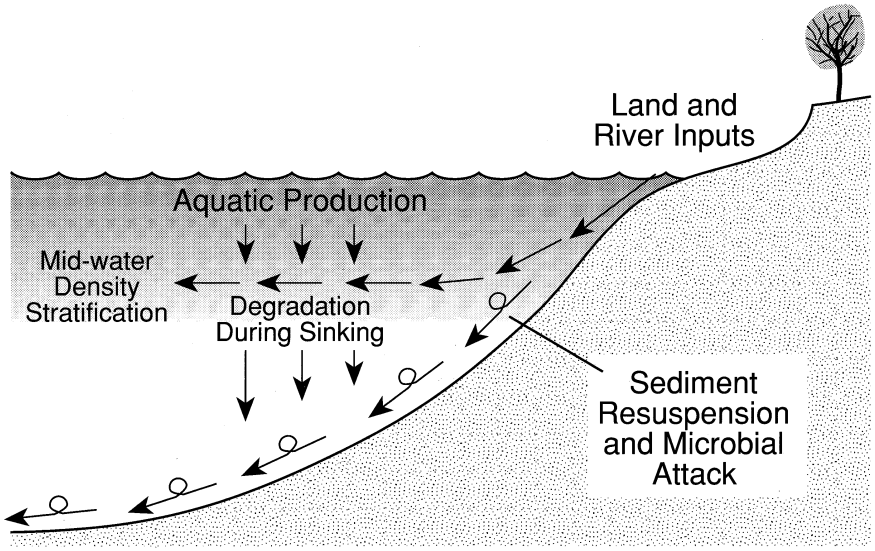

Fig. 1. Summary of the principal sources and alteration processes that affect the sedimentation of organic matter. Organic matter from algal production in the photic zone and from plants on nearby land areas are the major initial sources. Suspended particles congregate at midwater density discontinuities and can be advected laterally. Resuspension and downslope transport moves sediments from coastal locations to basinal depths. Microbial reprocessing of organic matter is intense in the upper water column and in the surface sediments, diminishing the total amount and substituting microbial contributions for original components.

Meyers 1997

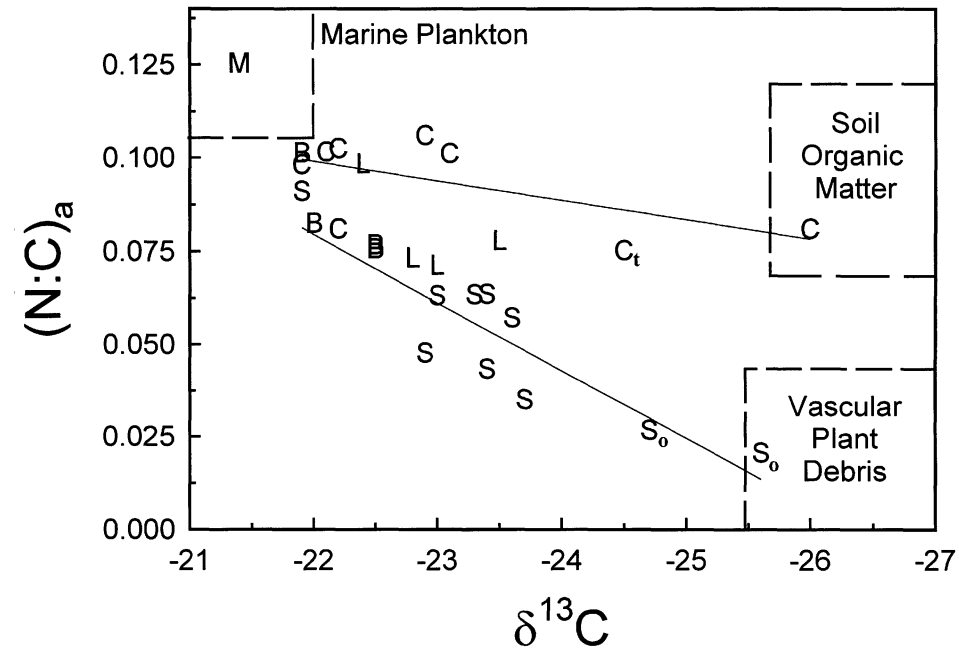

Fig. 5. Atomic N/C ratio versus stable carbon isotopic composition ($\delta^{13}C$, ‰) of organic matter in size and density fractions isolated from Washington coast sediments (Keil *et al.*, 1994). M is marine material, B is bulk sediment, C is clay-, L is silt- and S is sand-sized sediment. Subscript t is high density ($\rho > 2.6$) fraction and subscript o is low density ($\rho < 1.5$) fraction.

Hedges et al. 1997

POC in seafloor sediments

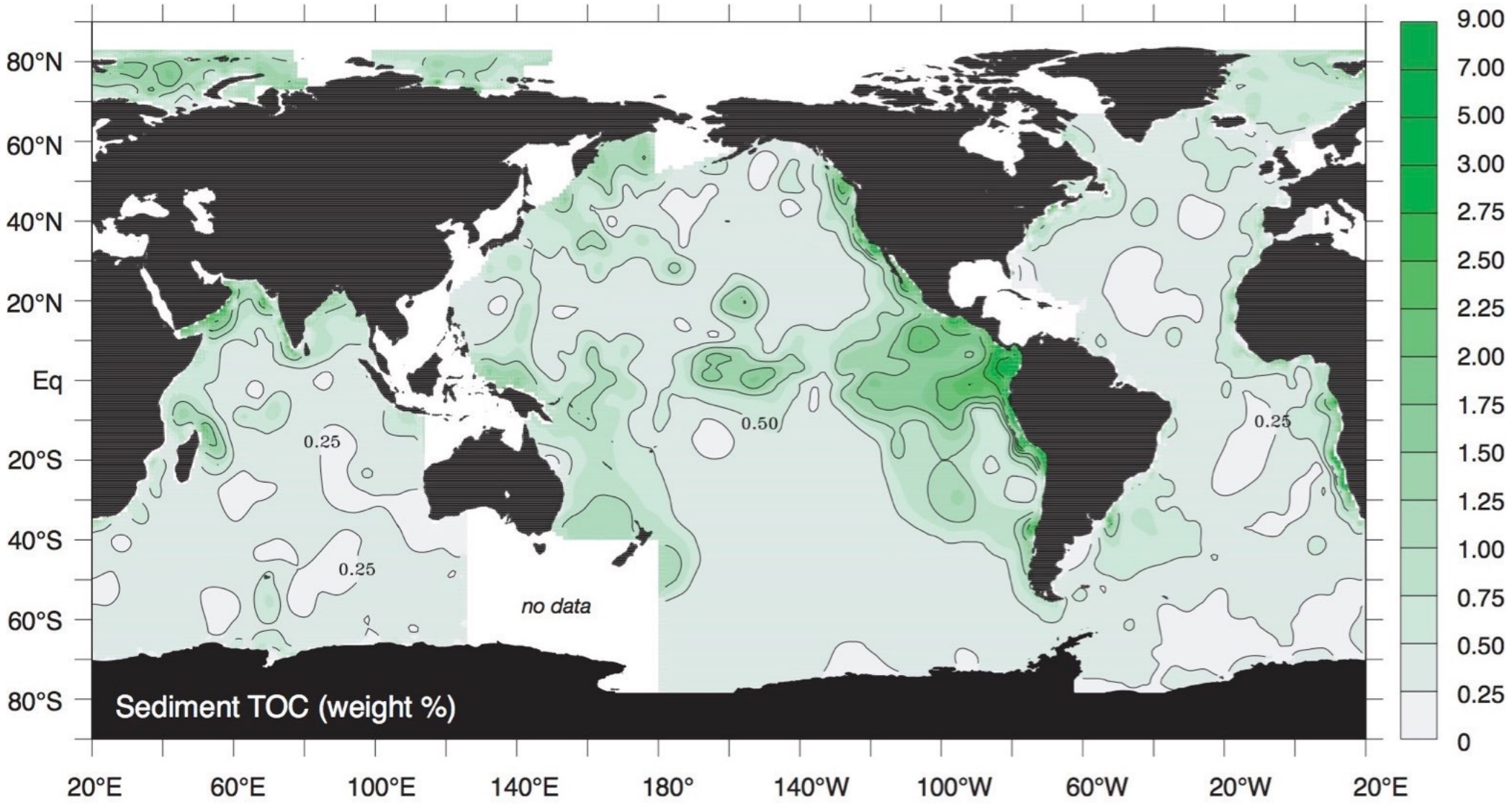

Seiter et al. 2004

Total Sediment Thickness of the World's Oceans & Marginal Seas

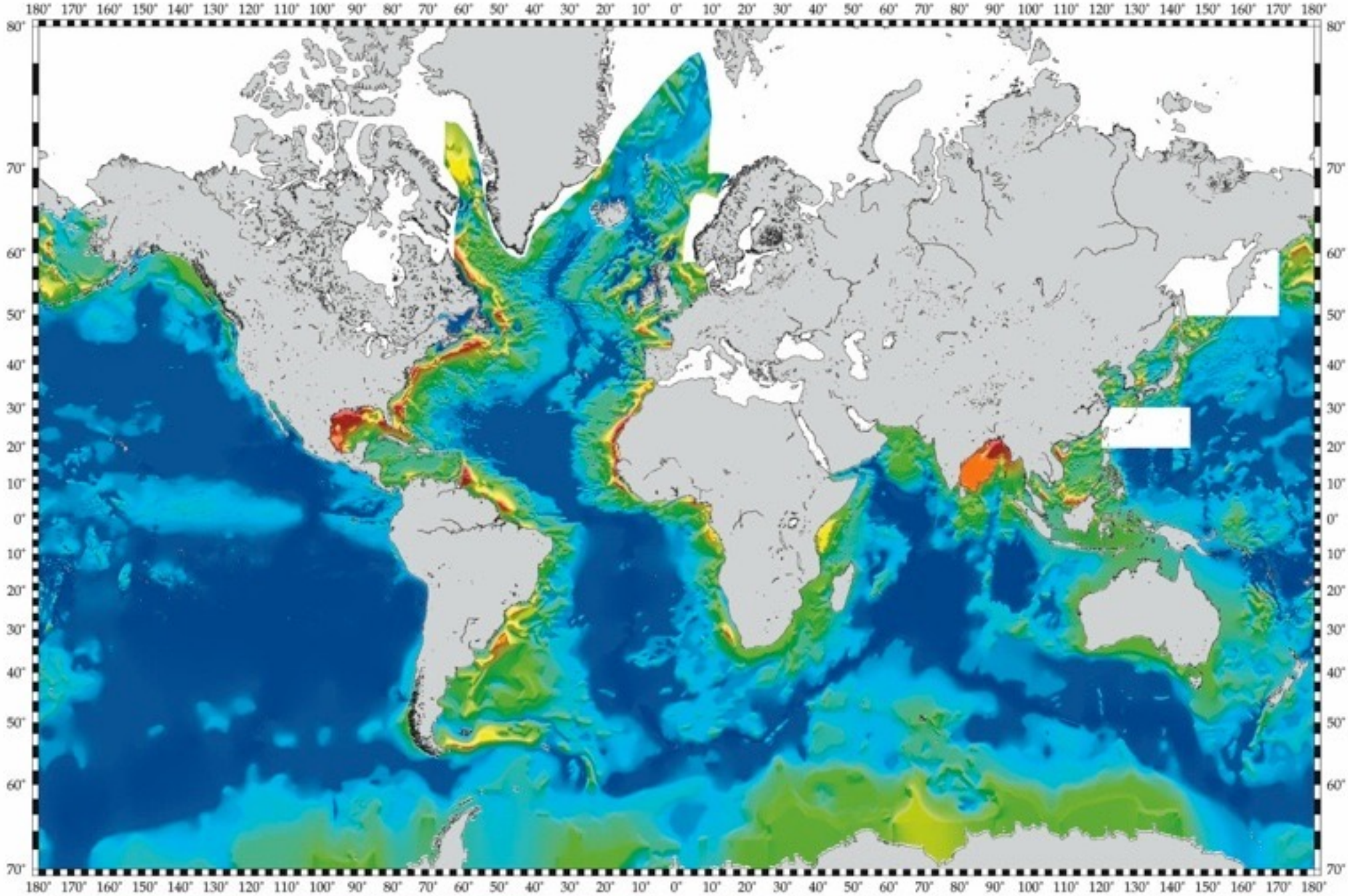

C in ocean sediments

- Inorganic, as $CaCO_3$ in biogenic sediments
  - Carbonate oozes on mid-ocean ridge flanks
  - Relatively thin sediment column
  - High concentrations (up to almost 100% = 12% C)
- Organic, as POC in mostly terrigenous sediments
  - Continental margins
  - Sediment column can be thick
  - Low concentrations (0.1-1% C)

Input to subduction

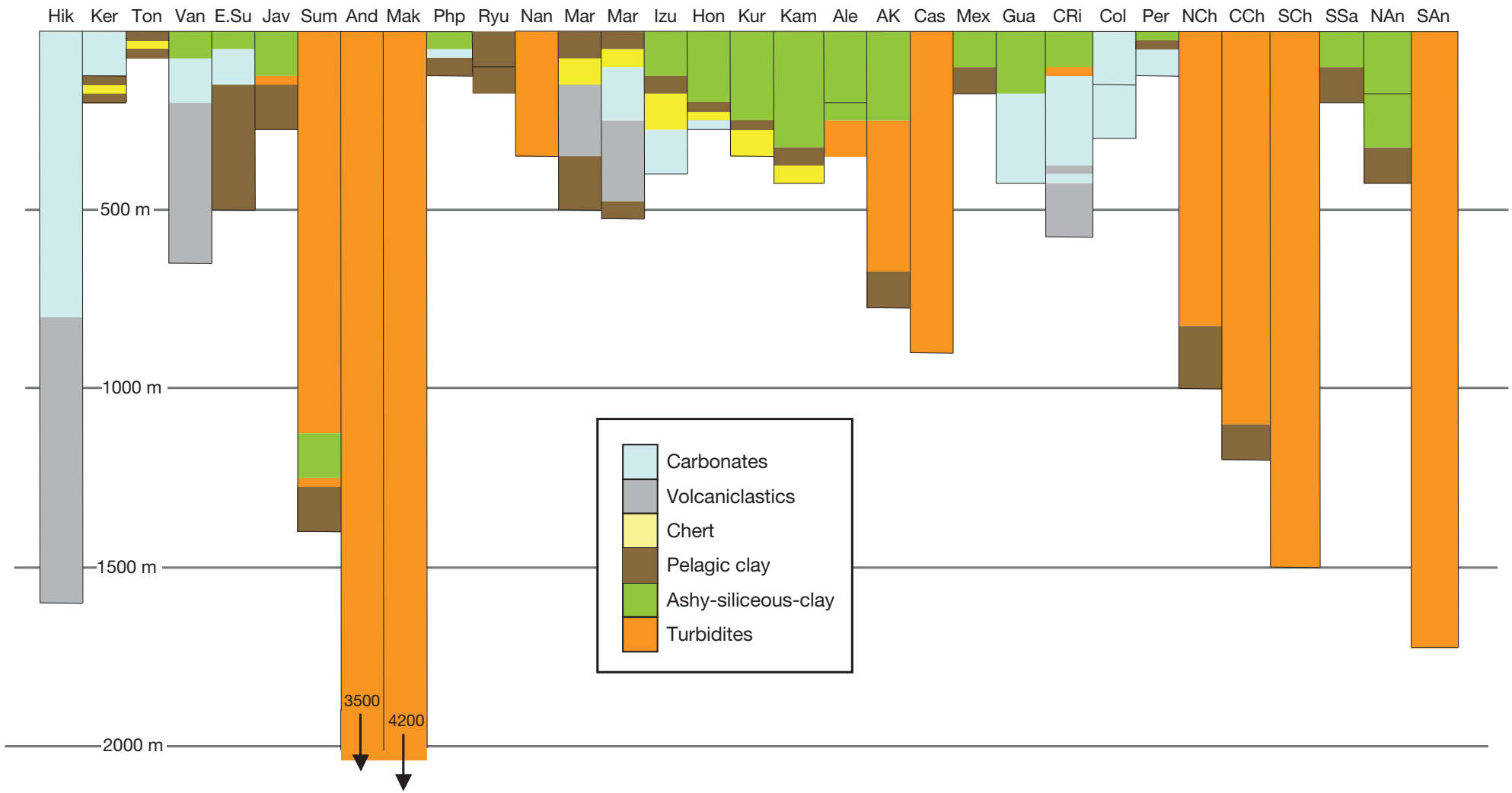

Figure 7 Sedimentary thickness and summary lithology subducting at each trench. See supplementary Table B for a more detailed version of this figure, with site-specific lithological descriptions and reference drill sites.

Plank 2014

C in subducting sediments

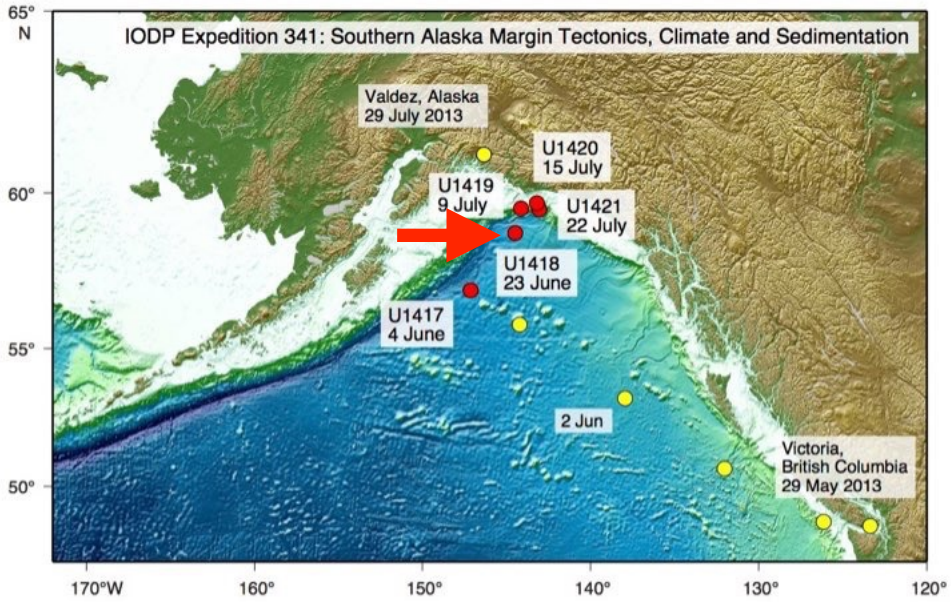

Organic C ≈ 2 x carbonate C

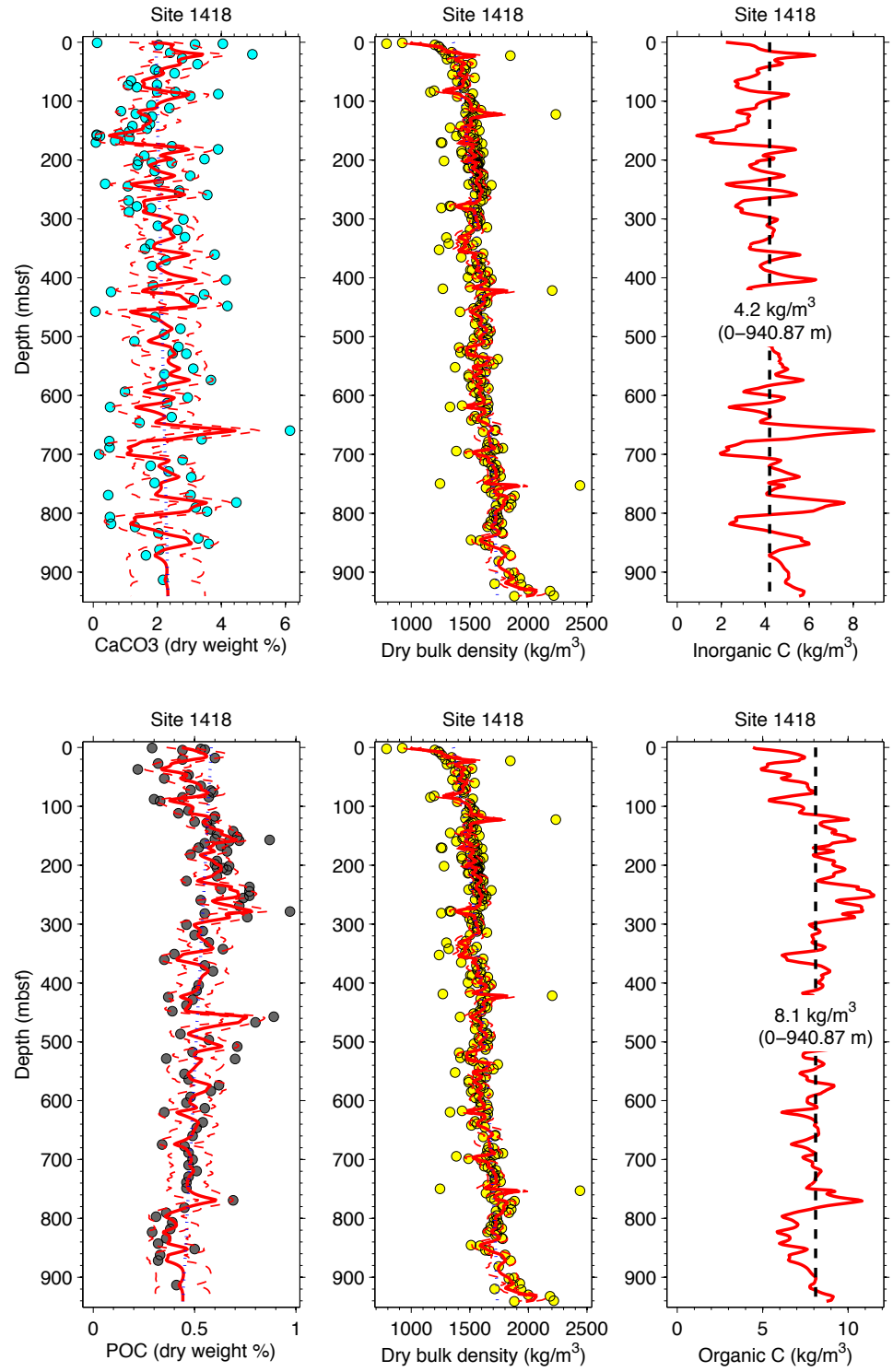

Microbial populations in sediments

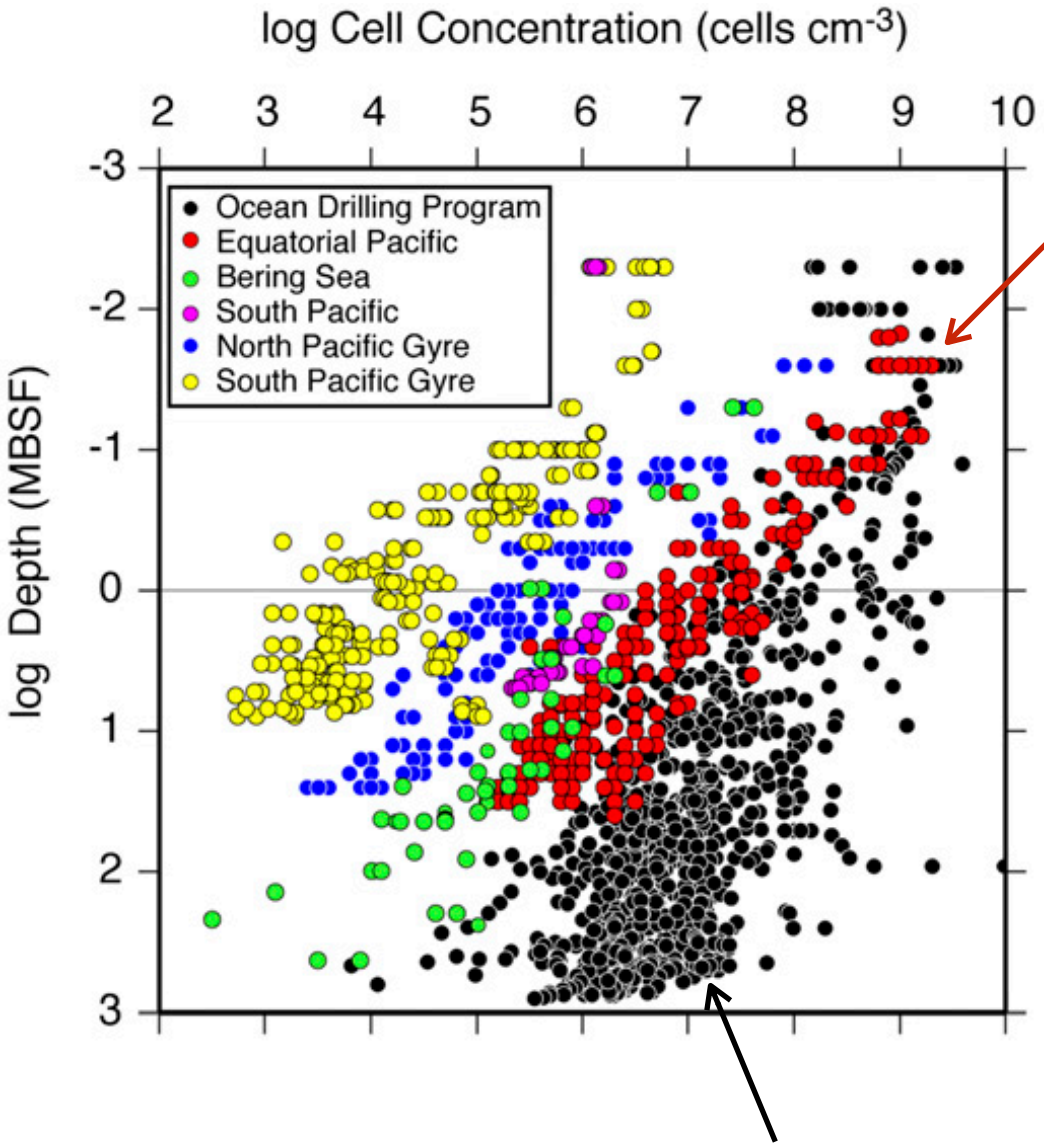

Equatorial upwelling

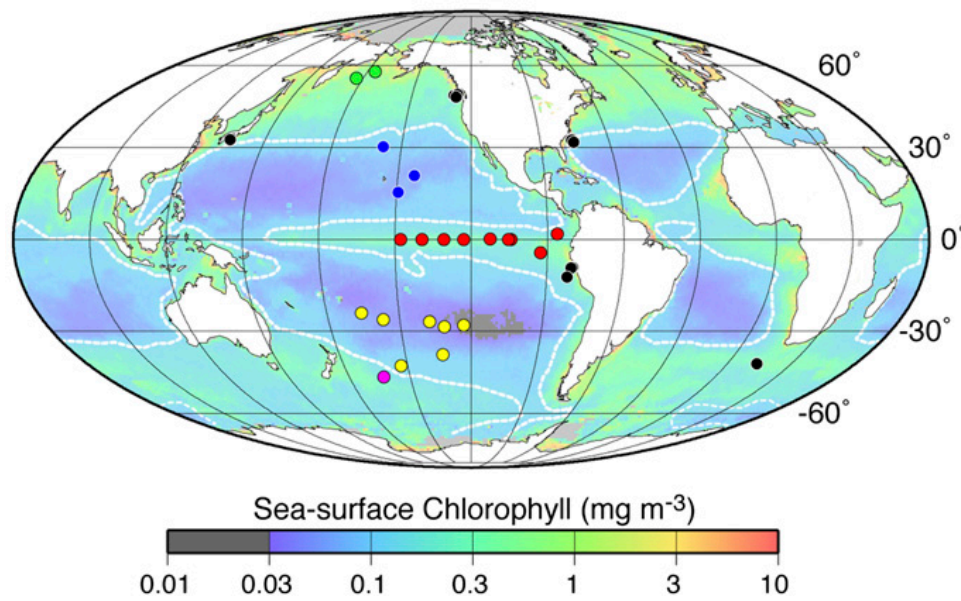

Continental margins

Kallmeyer et al., 2012

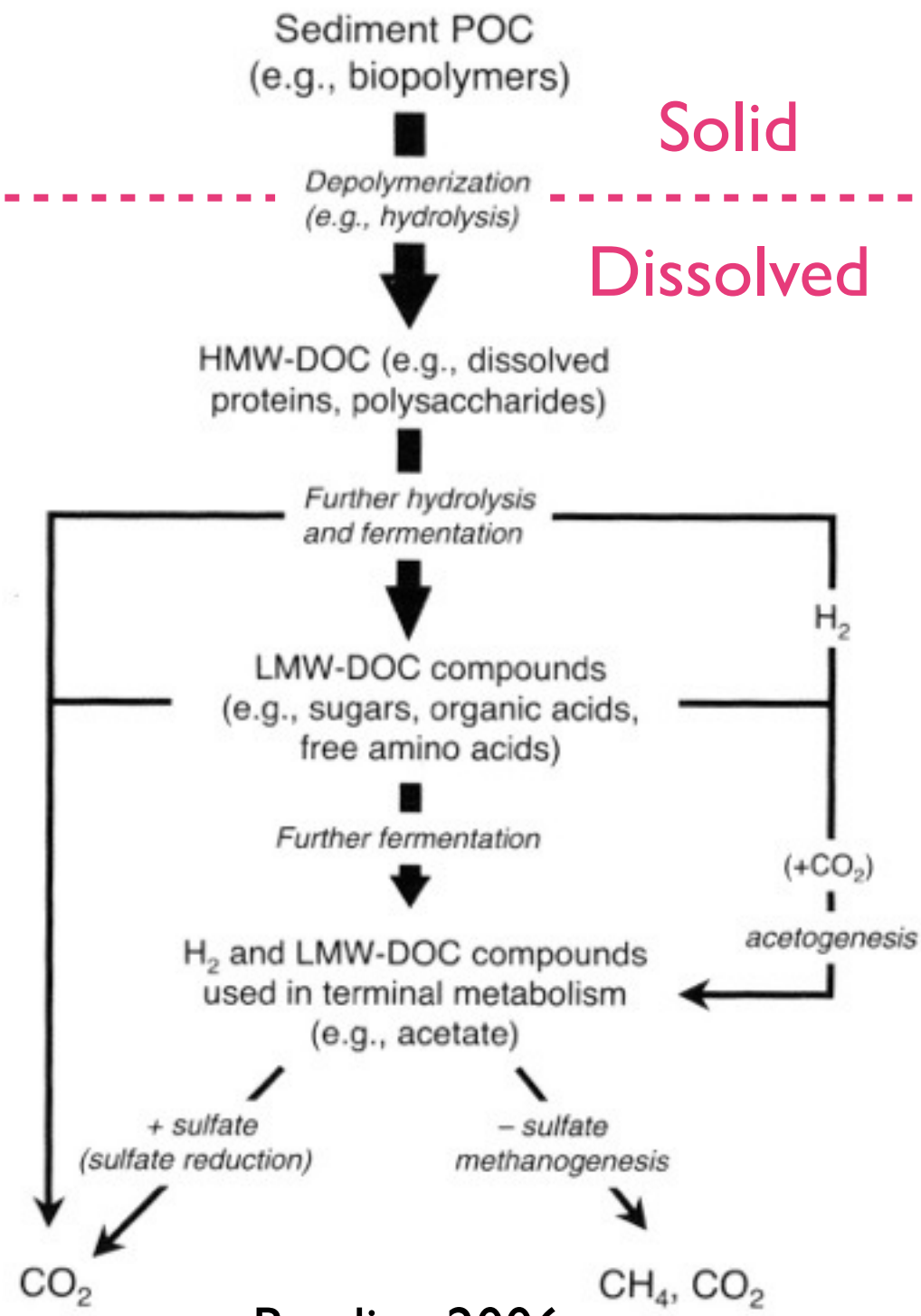

Burdige 2006

- Organic matter degradation or remineralization
- First step: conversion POC to dissolved OC (DOC)
- DOC then becomes available to microorganisms

Diagenetic reactions

Electron acceptors

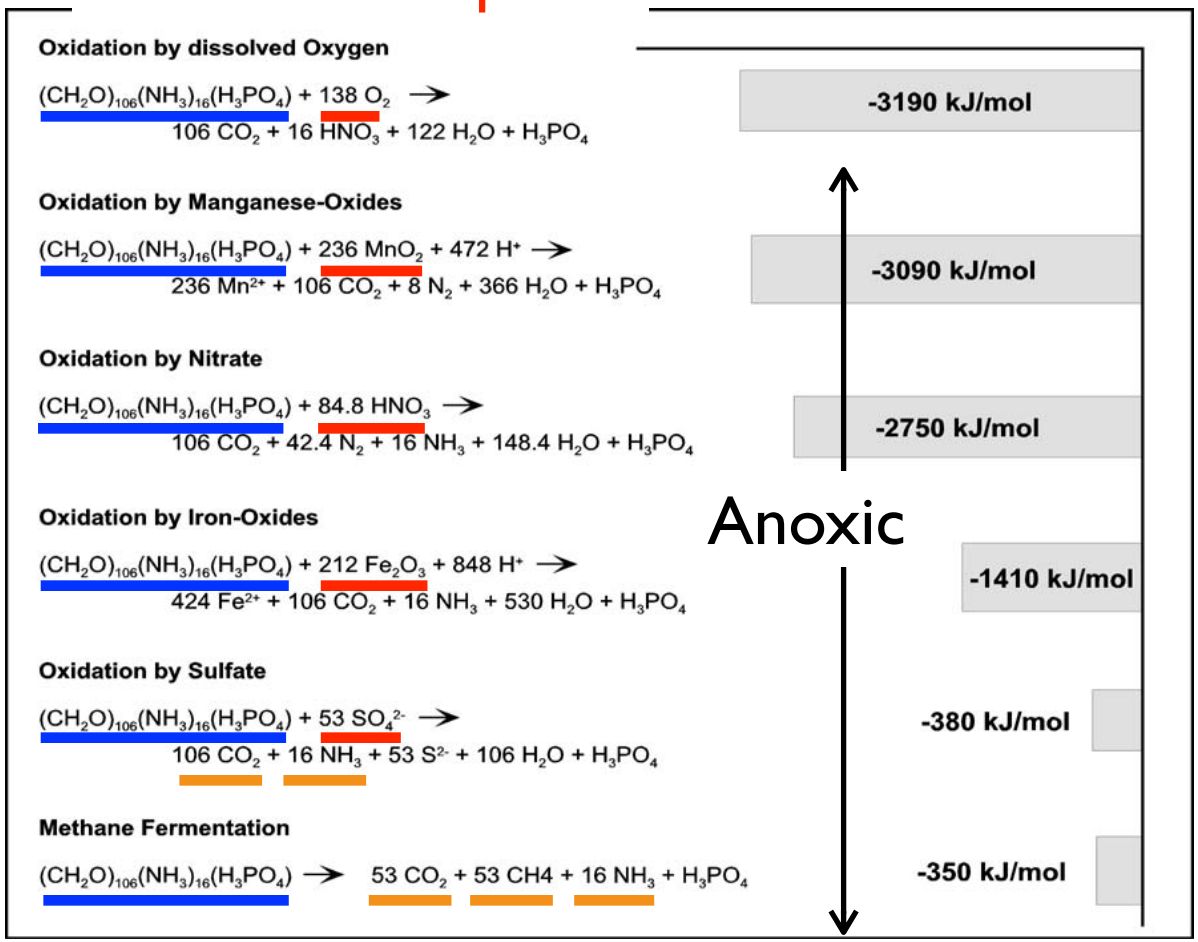

Fig. 3.11 Degradation of organic matter with different electron acceptors (Froelich et al. 1979). The columns represent the different amounts of resulting energy. The oxidation of organig matter by nitrate describes a reaction of the nitrate to elementary nitrogen and leaves the nitrogen of the organic matter as ammonium. Other reactions are possible (cf. section 6.3).

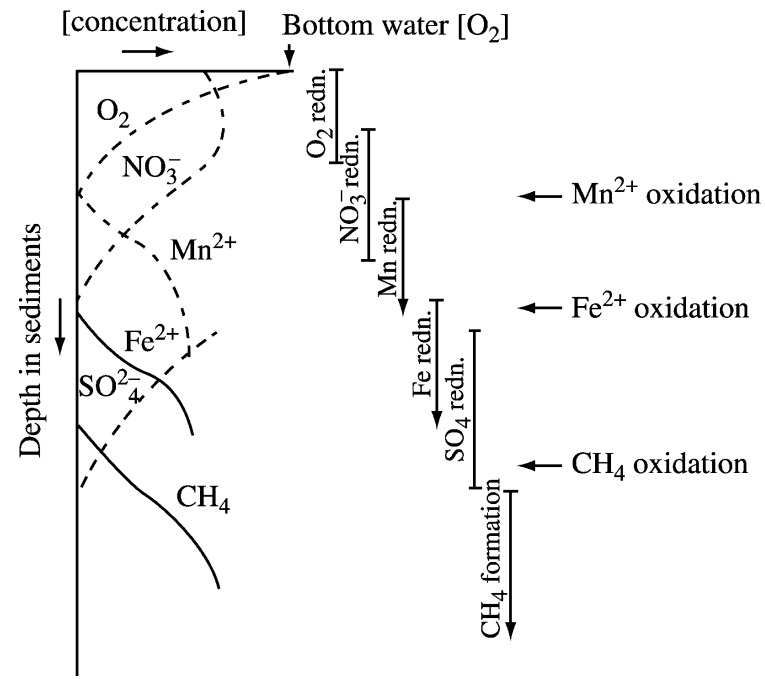

Figure 1 A schematic representation of the pore-water result of organic matter degradation by sequential use of electron acceptors.

Froelich et al., 1979

- Microbes accelerate diagenetic reactions
- Main products of metabolism: CO_2, NH_3, CH_4

Interpreting concentration profiles

Non-reacting substance (▼= seawater concentration)

Substance consumed in a reactive layer

Substance released in a reactive layer

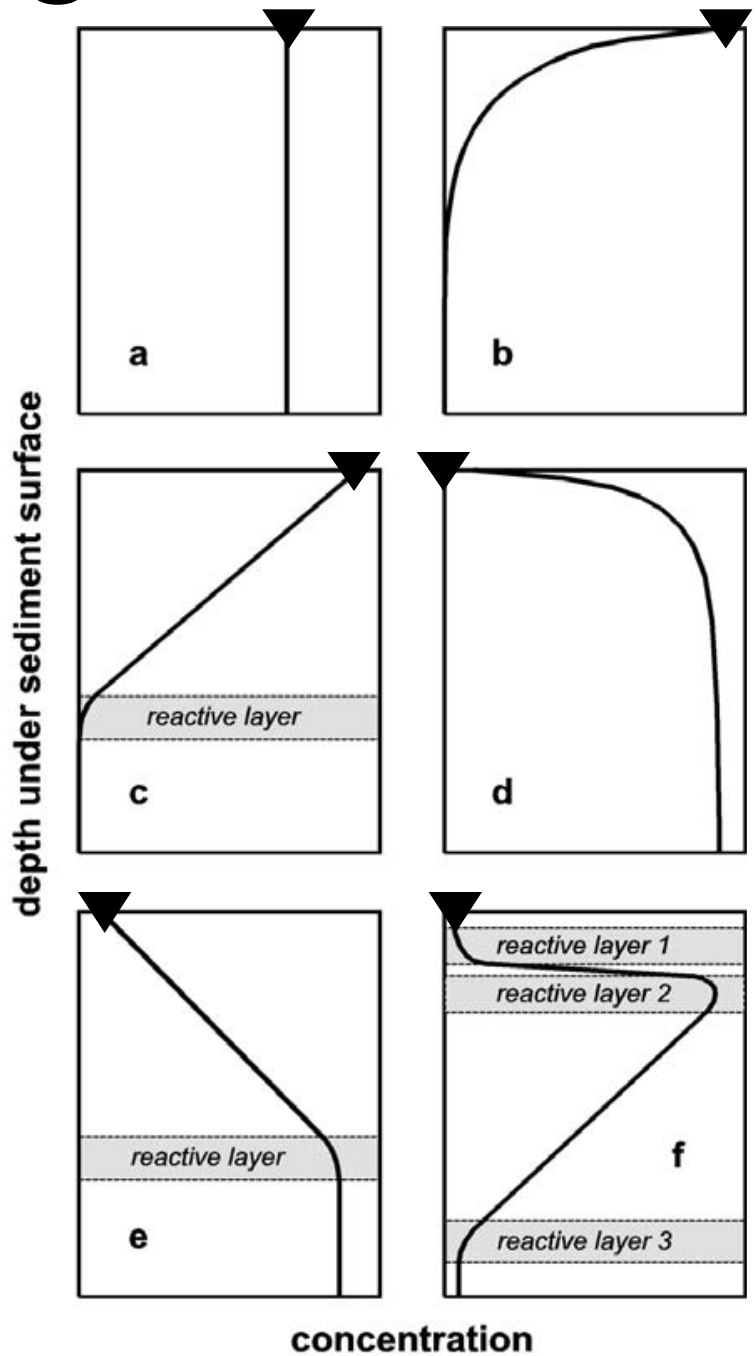

Substance consumed in the upper layers

Substance released in the upper layers

Complicated!

Schulz, 2006

End-member sites

Type A sites:			Type B sites:		
Leg	Site	Location	Leg	Site	Location
199	1218	Paleogene equatorial Transect (Pacific Ocean)	204	1251	Gas Hydrates (Cascadia Margin)
201	1225	Microbial communities, Eastern equatorial Pacific and Peru Margin	201	1230	Microbial communities, Eastern equatorial Pacific and Peru Margin
114	703	Subantarctic South Atlantic	175	1084	Benguela Current (W African margin)
157	954	Gran Canaria and Madeira Abyssal Plain	150	905	New Jersey Sea-Level Transect
130	803	Ontong Java Plateau	170	1041	Costa Rica Accretionary Wedge
145	884	North Pacific Transect	131	808	Nankai Trough
115	709	Mascarene Plateau	117	723	Oman Margin
208	1263	Walvis Ridge (Southern Atlantic)	155	935	Amazon Deep-Sea Fan
181	1120	Southwest Pacific Gateways	133	819	Northeast Australian Margin
126	791	Izu-Bonin Arc-Trench System	128	798	Japan Sea

POC and metabolites (A)

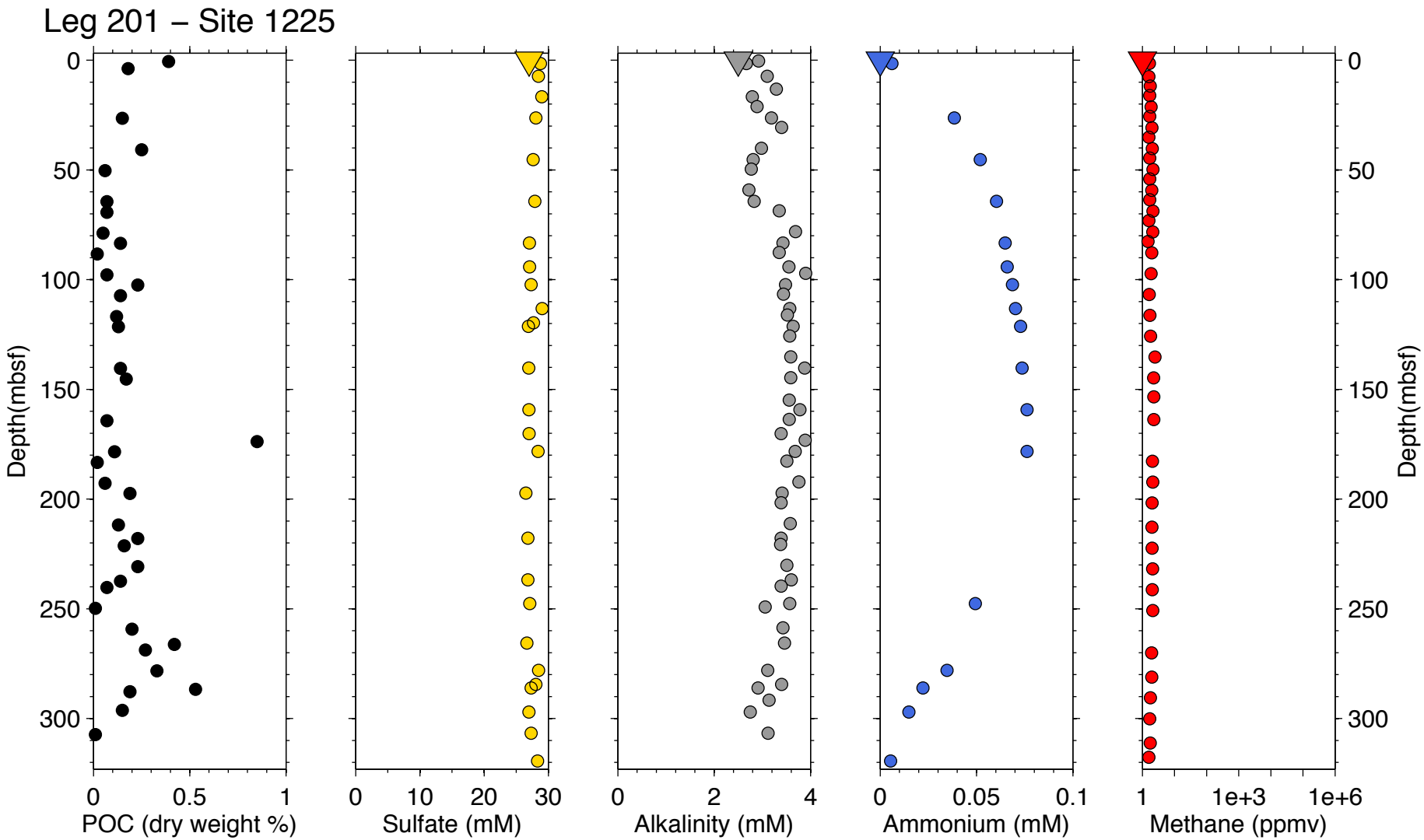

▽ = seawater concentration

Alkalinity ≈ total DIC

Methane in bubbles within sediment or from sediment degassing (headspace gas)

POC and metabolites (B)

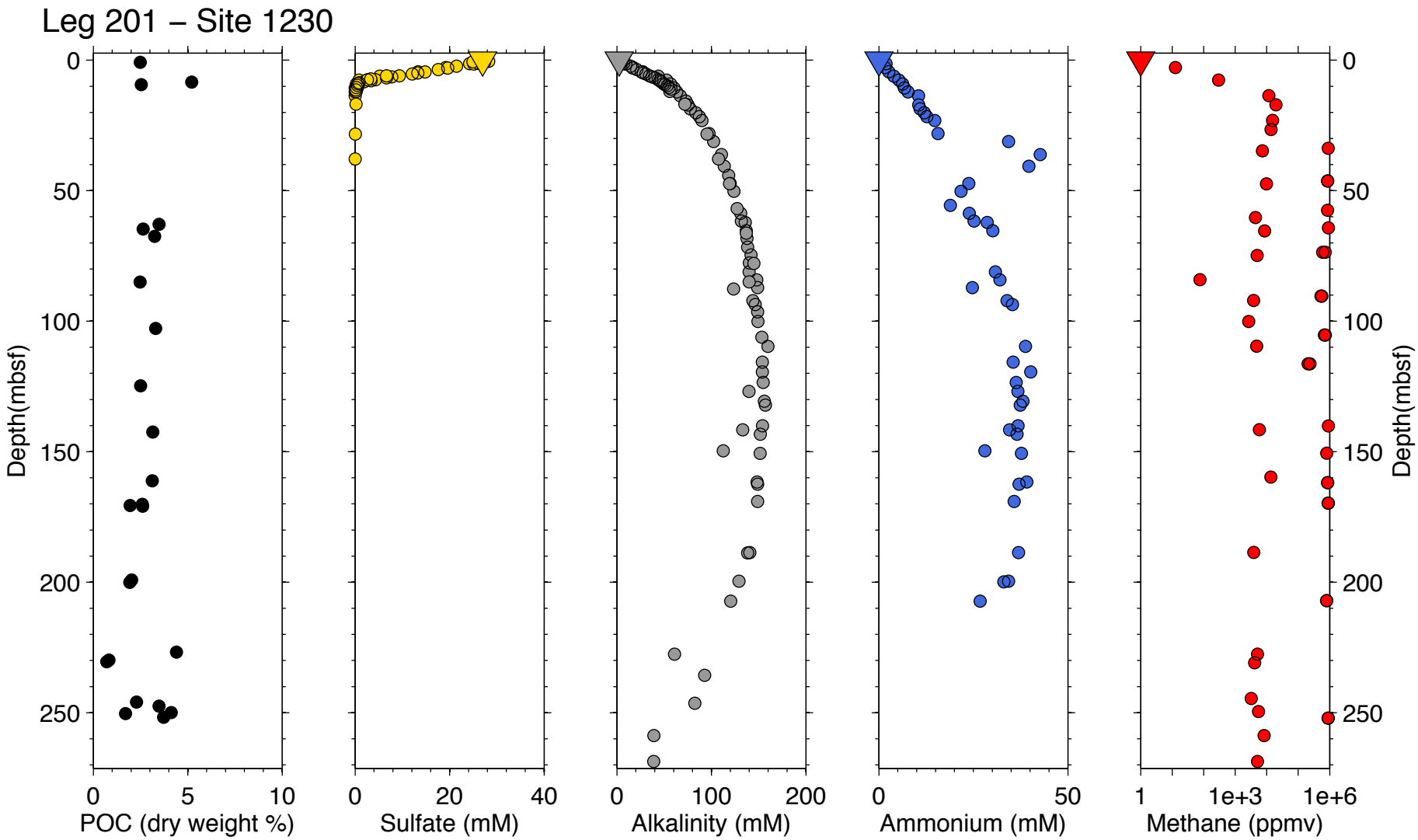

= Constant sulfate concentration > 0 (circle size) at depth indicated by color

= Zero sulfate at depth indicated by color

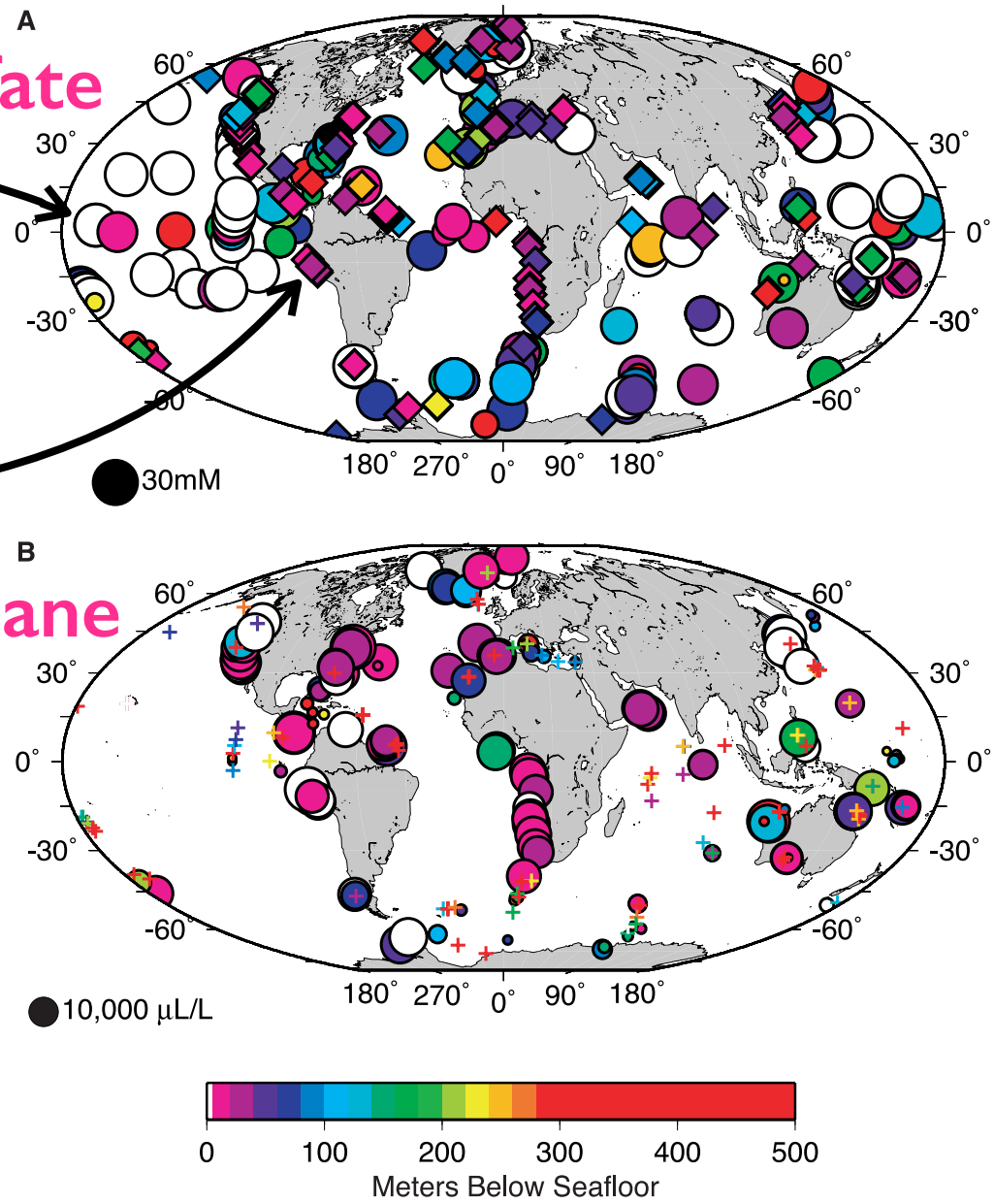

Science, 2002

Metabolic Activity of Subsurface Life in Deep-Sea Sediments

Steven D'Hondt,* Scott Rutherford, Arthur J. Spivack

Global maps of sulfate and methane in marine sediments reveal two provinces of subsurface metabolic activity: a sulfate-rich open-ocean province, and an ocean-margin province where sulfate is limited to shallow sediments. Methane is produced in both regions but is abundant only in sulfate-depleted sediments. Metabolic activity is greatest in narrow zones of sulfate-reducing methane oxidation along ocean margins. The metabolic rates of subseafloor life are orders of magnitude lower than those of life on Earth's surface. Most microorganisms in subseafloor sediments are either inactive or adapted for extraordinarily low metabolic activity.

Fig. 2. (**A**) Global SO_4^{2-} map. Symbol color indicates the depth of the shallowest sample where subsurface SO_4^{2-} concentrations either stabilize at a nonzero value (circles) or reach zero (diamonds) (white, ≤5 mbsf). Circle size indicates the SO_4^{2-} concentration at which each subsurface SO_4^{2-} profile stabilizes. (**B**) Global CH_4 map. Circle color indicates the depth of the shallowest sample that exhibits a CH_4 concentration above the laboratory background level (white, ≤5 mbsf). Circle size indicates the peak subsurface concentration. Crosses mark sites where CH_4 never rises above laboratory background. Cross color marks the depth of the deepest sample analyzed (*36*).

Claypool & Kaplan, 1974

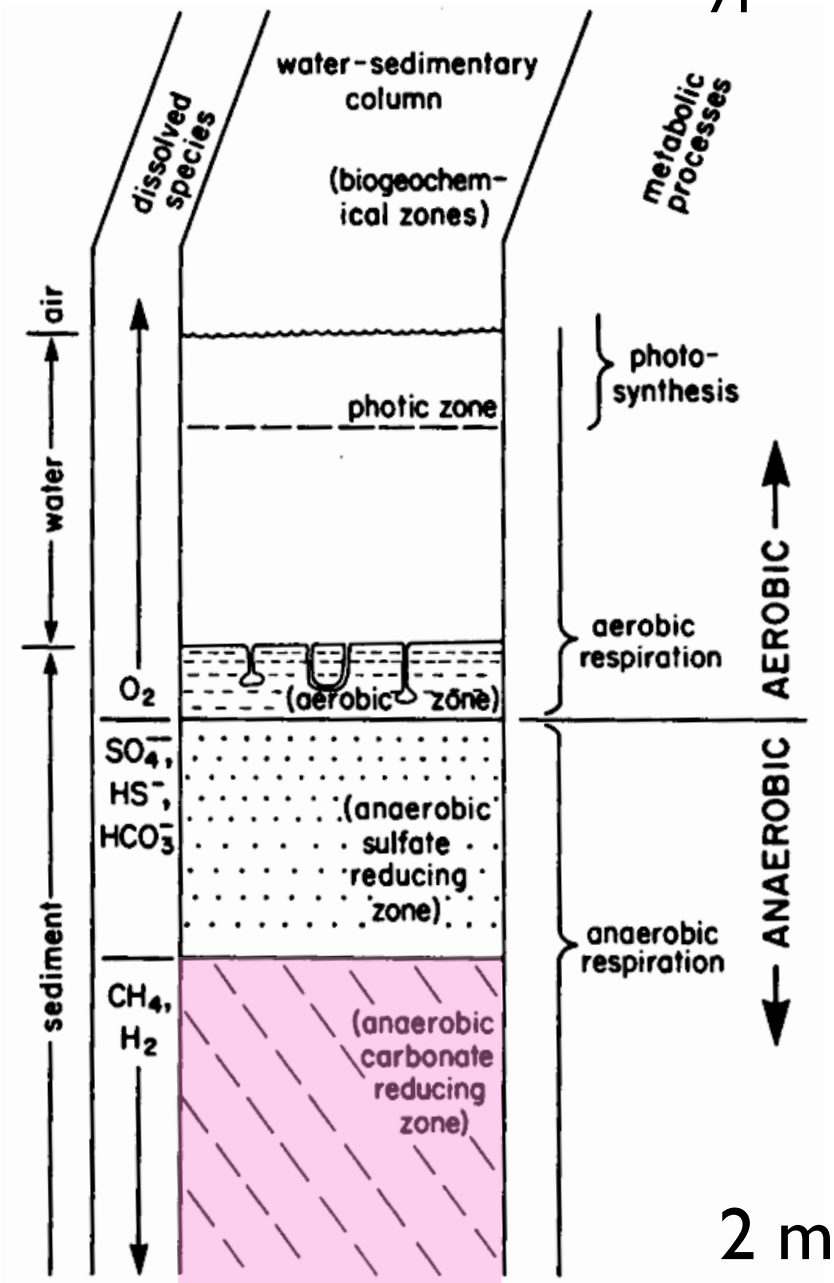

		$\Delta G^{\circ\prime}$ (kcal per mole of glucose equivalent oxidized)
a.	Aerobic respiration	
	$CH_2O + H_2O \rightarrow CO_2 + 2H_2$	
	$2H_2 + O_2 \rightarrow 2H_2O$	
	$CH_2O + O_2 \rightarrow CO_2 + H_2O$	-686
b.	Nitrate reduction	
	$5CH_2O + 5H_2O \rightarrow 5CO_2 + 10H_2$	
	$10H_2 + 4NO_3^- + 4H^+ \rightarrow 2N_2 + 12H_2O$	
	$5CH_2O + 4NO_3^- + 4H^+ \rightarrow 2N_2 + 5CO_2 + 7H_2O$	-579
c.	Sulfate reduction	
	$2CH_2O + 2H_2O \rightarrow 2CO_2 + 4H_2$	
	$4H_2 + SO_4^= \rightarrow S^= + 4H_2O$	
	$2CH_2O + SO_4^= \rightarrow S^= + 2CO_2 + 2H_2O$	-220
d.	Carbonate reduction	
	$2CH_2O + 2H_2O \rightarrow 2CO_2 + 4H_2$	
	$4H_2 + HCO_3^- + H^+ \rightarrow CH_4 + 3H_2O$	
	$CO_2 + H_2O \rightarrow HCO_3^- + H^+$	
	$2CH_2O \rightarrow CH_4 + CO_2$	- 99

2 moles of C in organic matter → 1 mole of CH_4 + 1 mole of CO_2

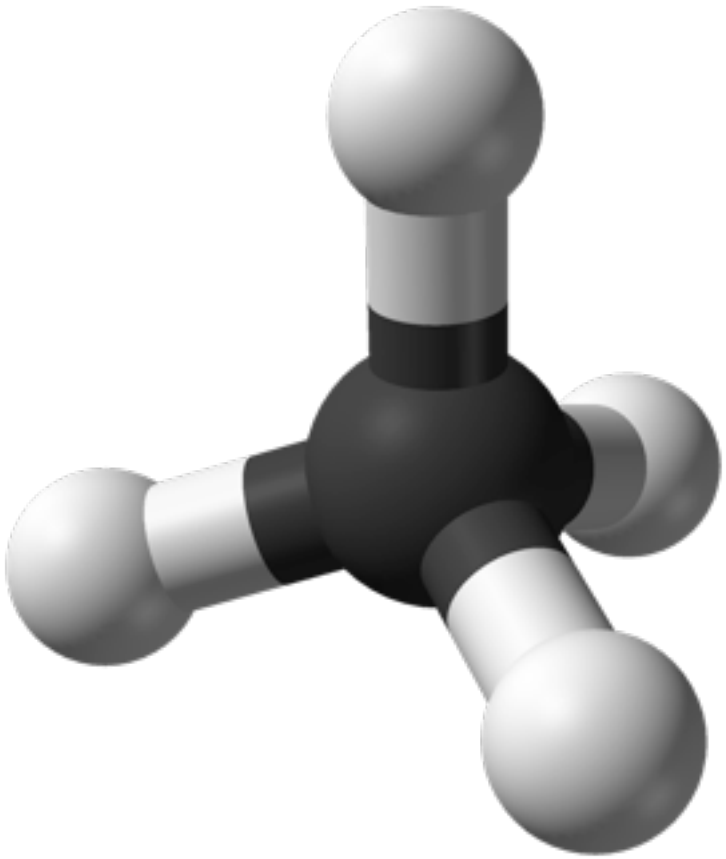

Most reduced C

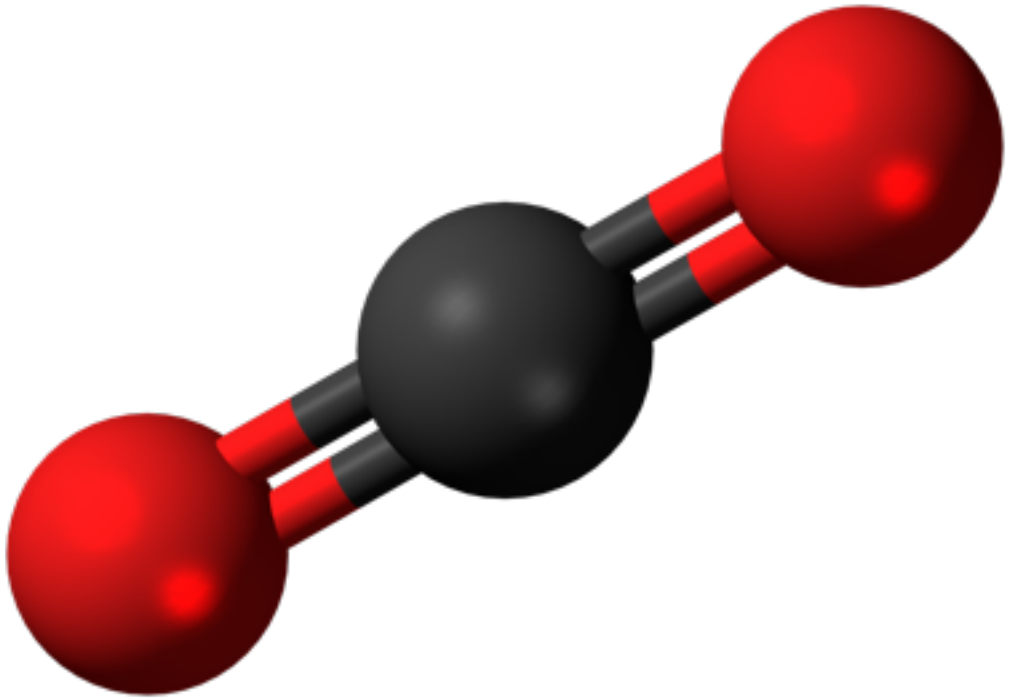

Most oxidized C

Methane hydrates

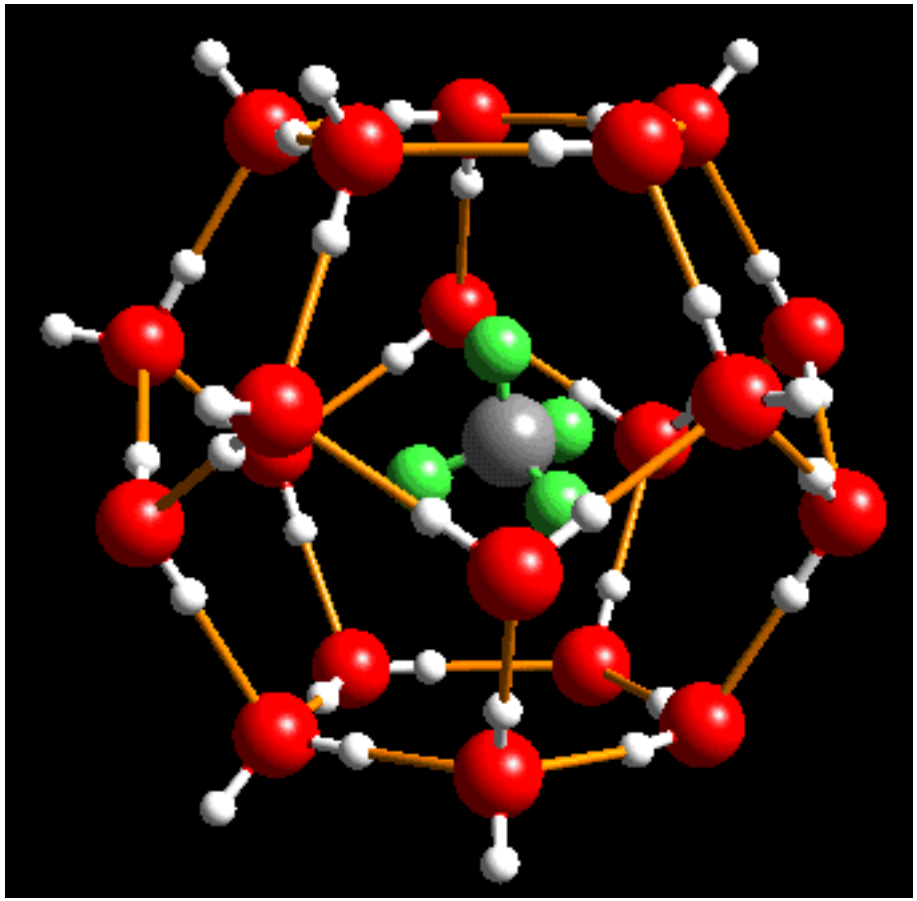

clathrate
(Chemistry) a compound in which molecules of one component are physically trapped within the crystal structure of another.
ORIGIN 1940s: from L. clathratus, from clathri 'lattice-bars'.

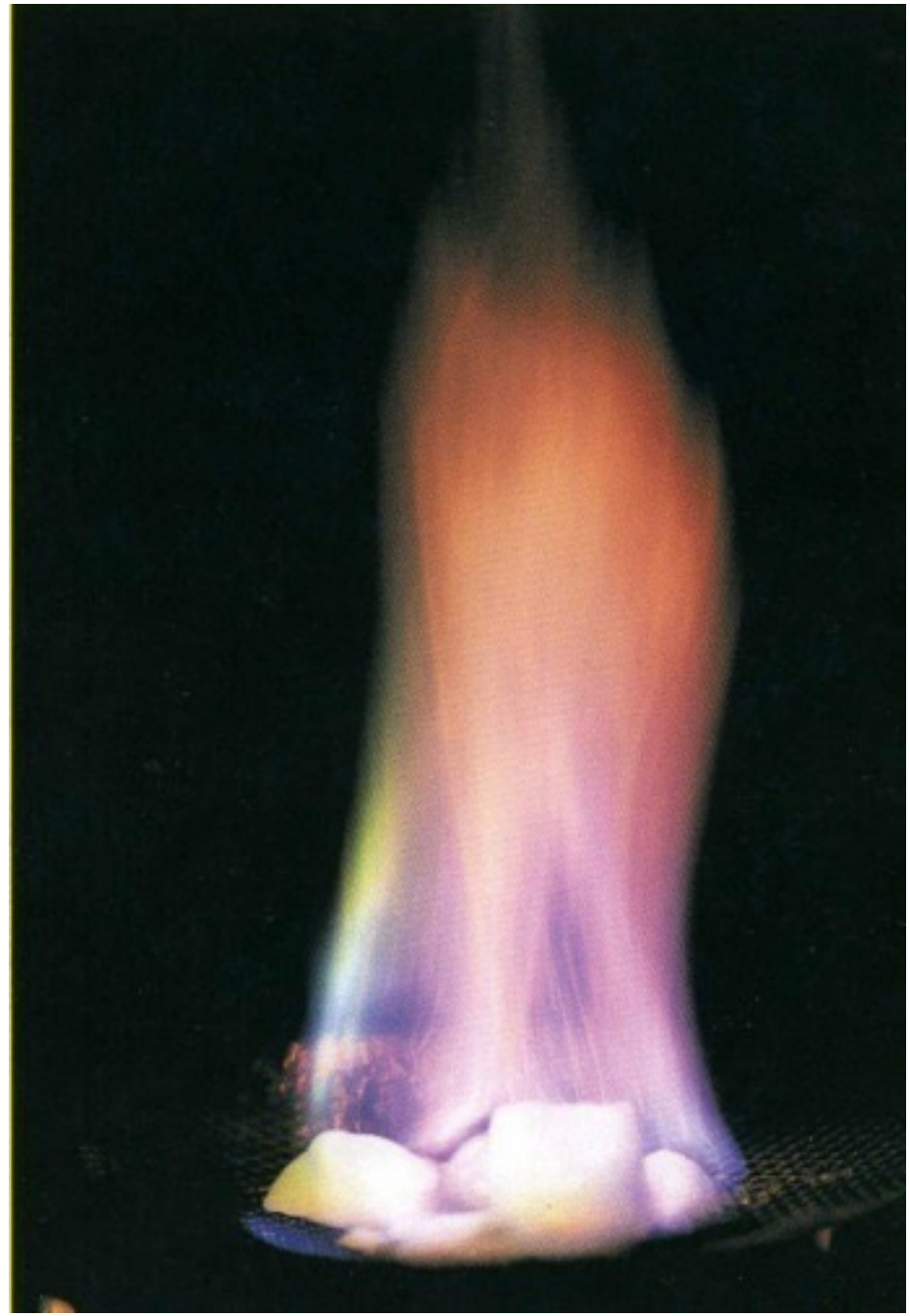

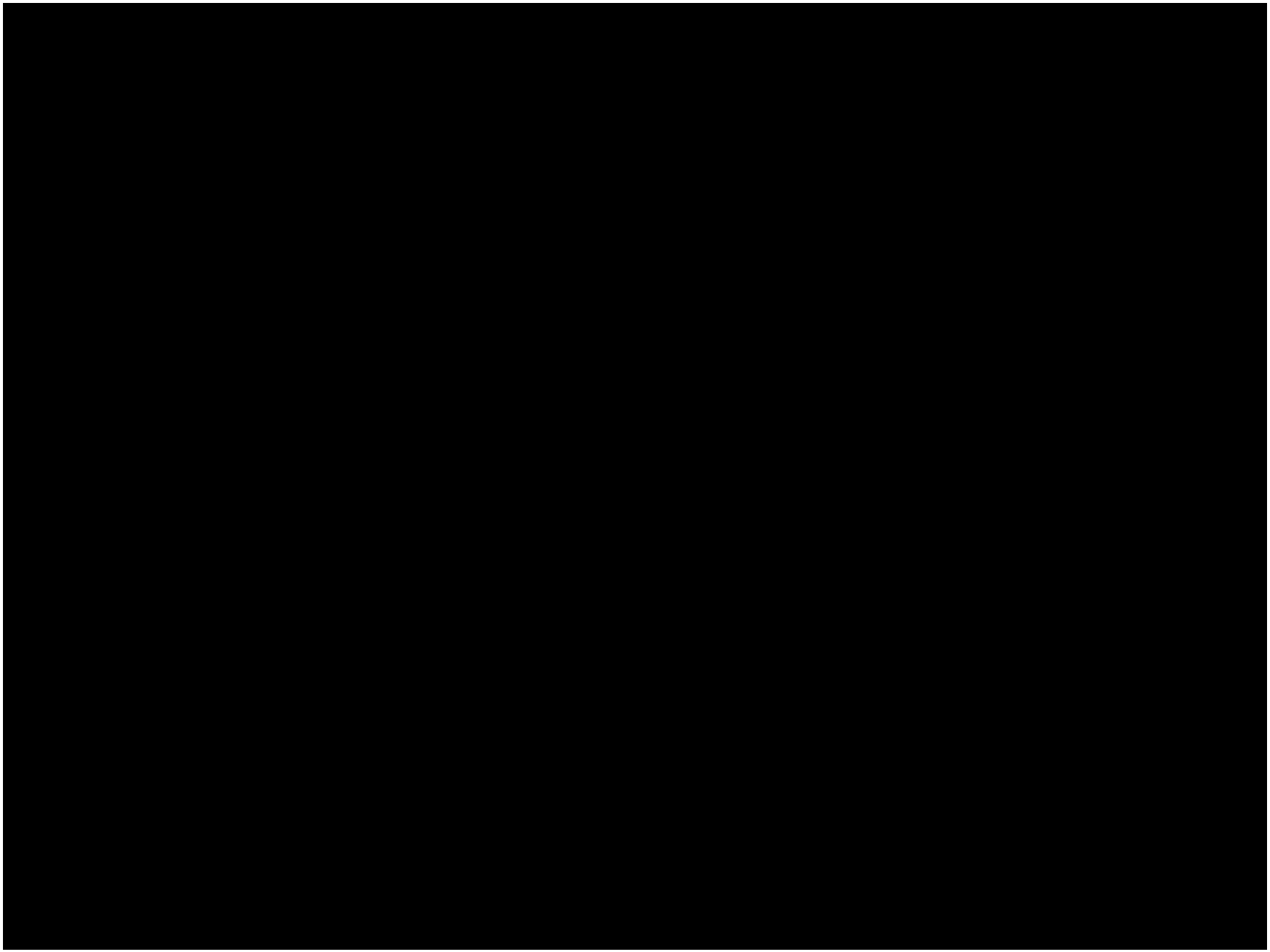

Permafrost

Ocean

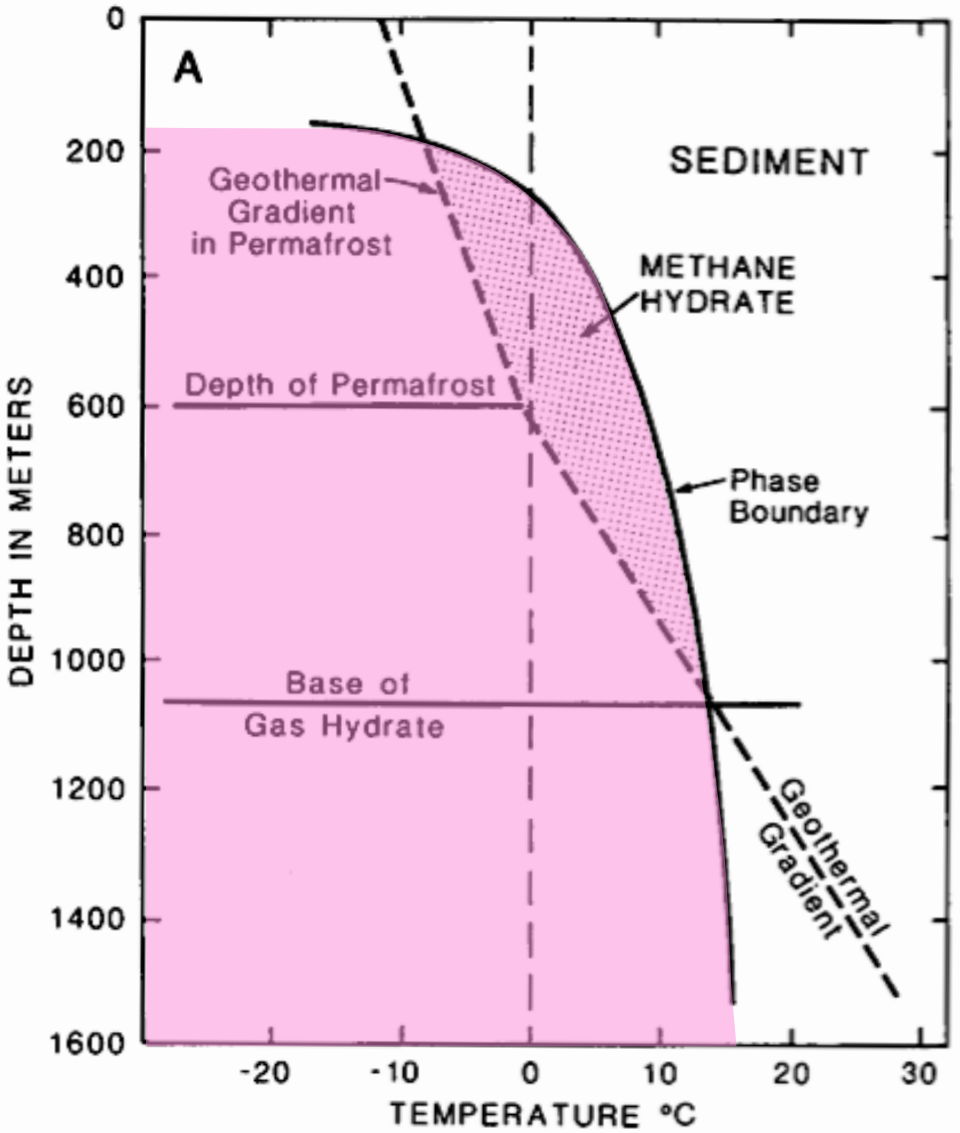

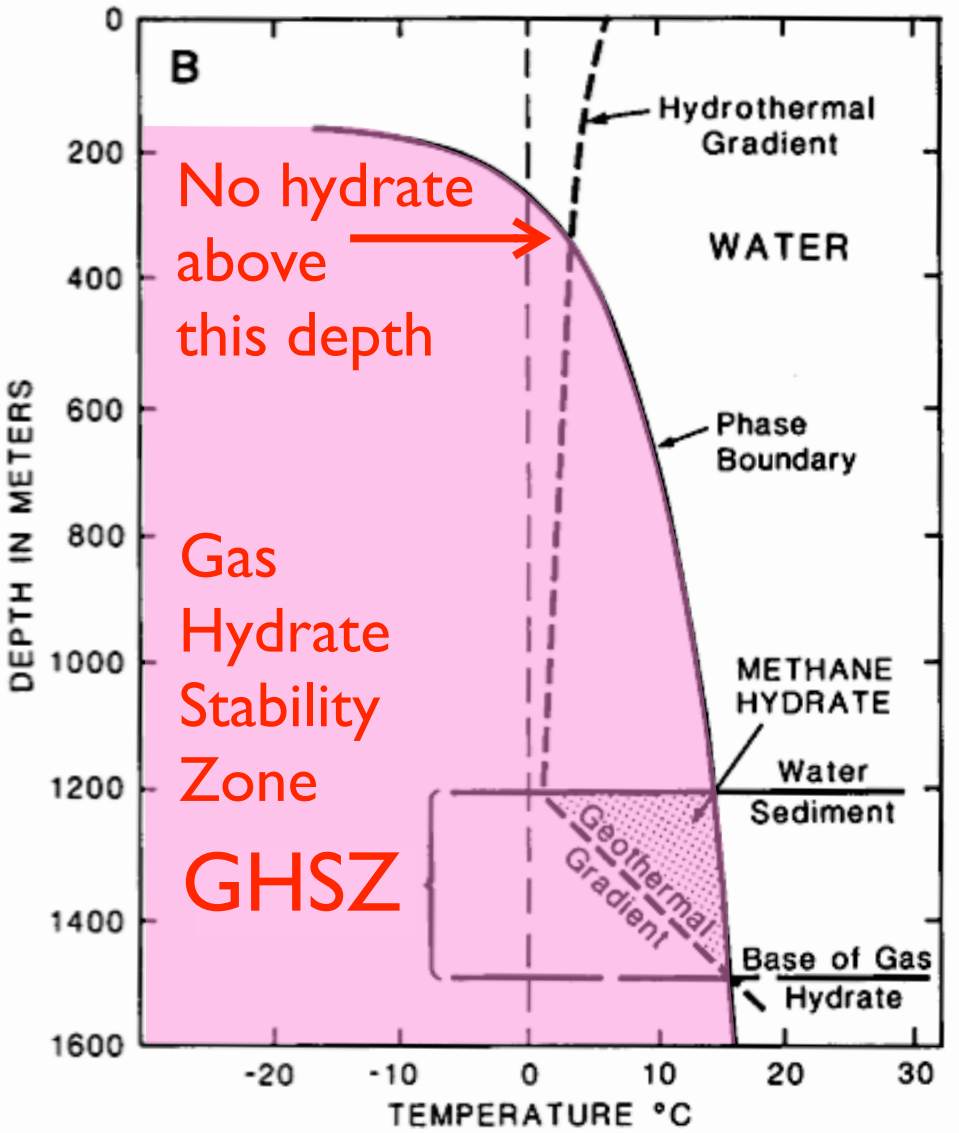

Figure 2. Examples of different depth-temperature zones for gas-hydrate occurrence. (A) conditions that are favorable for gas-hydrate formation where permafrost is present (after Bily and Dick, 1974; Collett, 1983). (B) conditions in which gas hydrates are stable in outer continental margin sediments (modified from Kvenvolden and McMenamin, 1980).

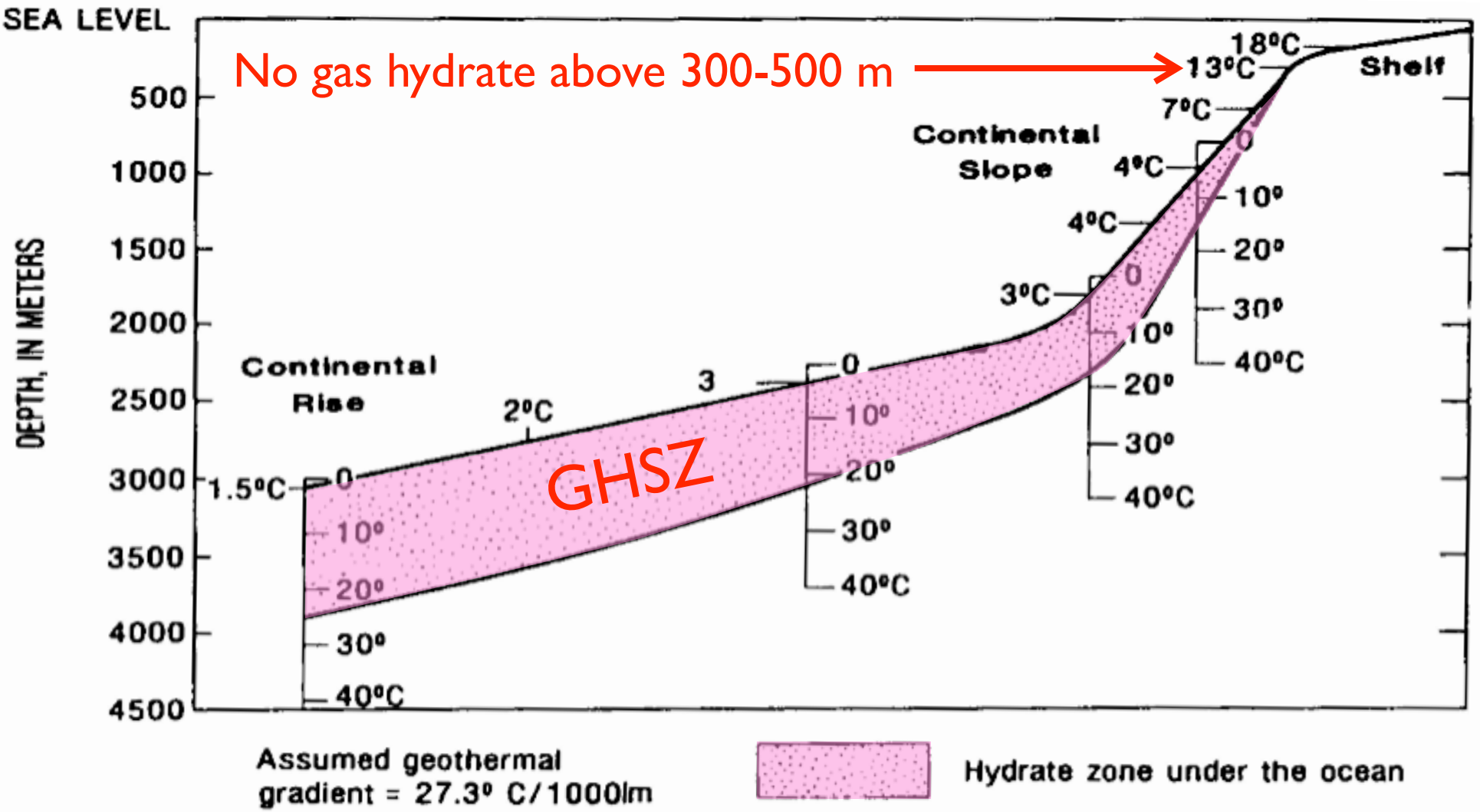

Figure 3: Inferred thickness of the GHSZ (dot pattern) in sediments of a continental margin assuming a typical geothermal gradient (from Kvenvolden and Barnard, 1982)

Gas hydrates are widespread

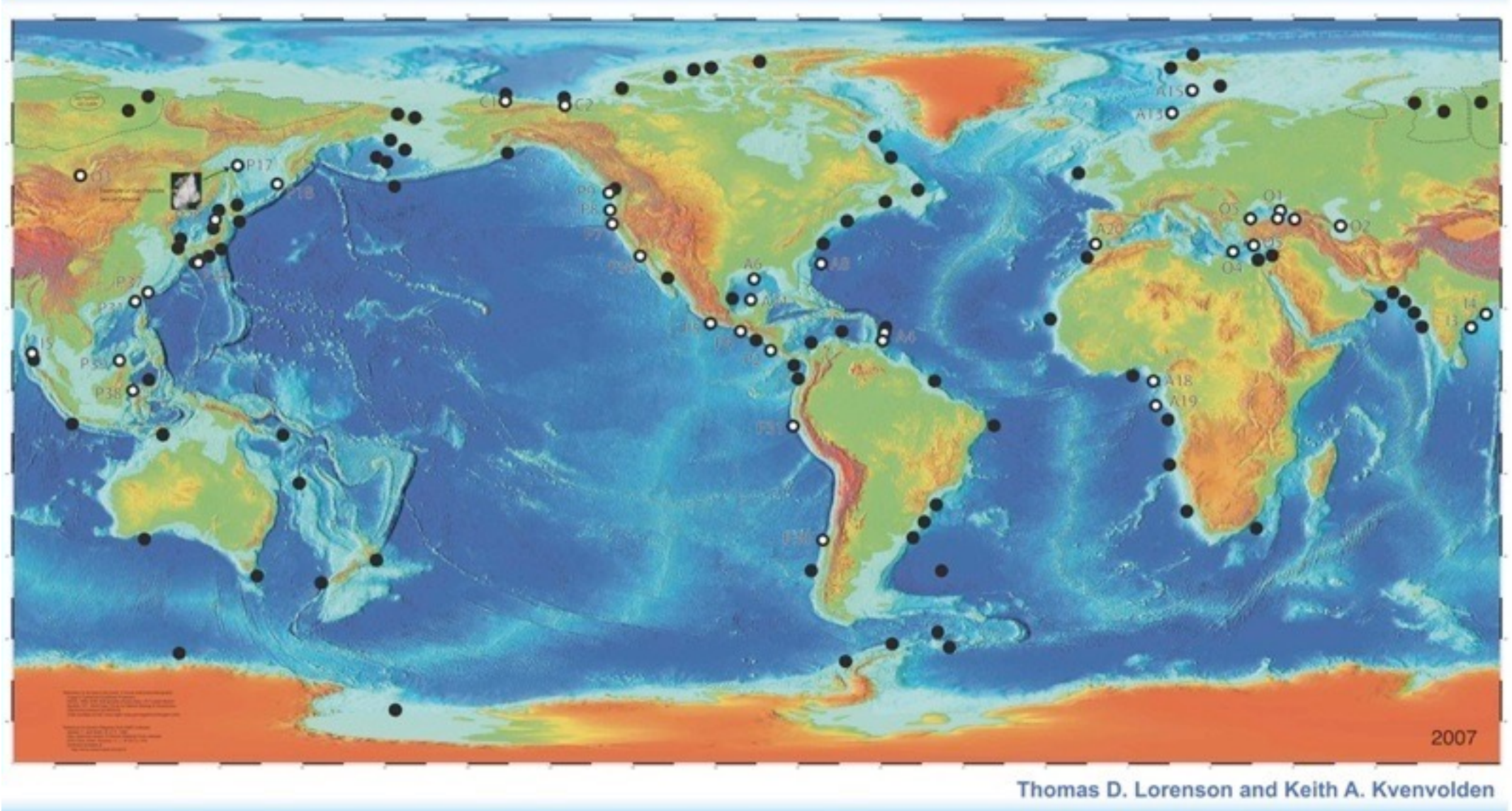

- ° Gas hydrate samples recovered
- • Gas hydrates inferred


IODP Exp. 311
00 101 102 103 104 105

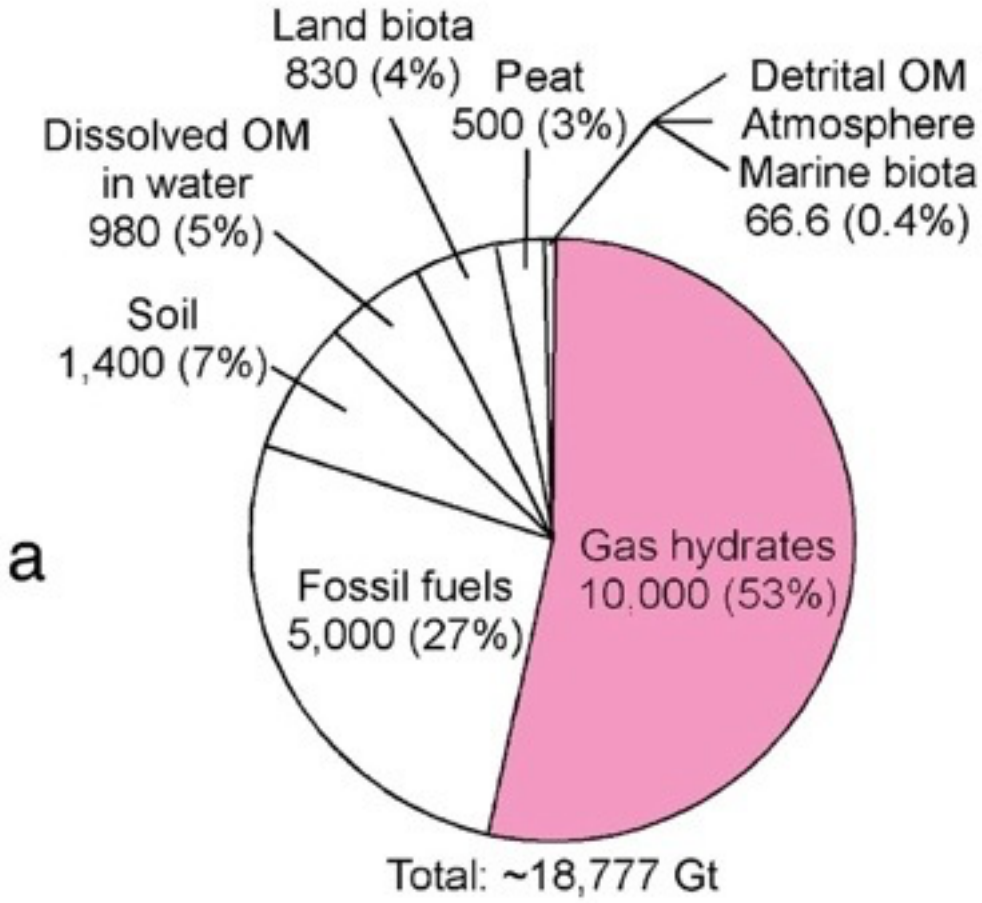

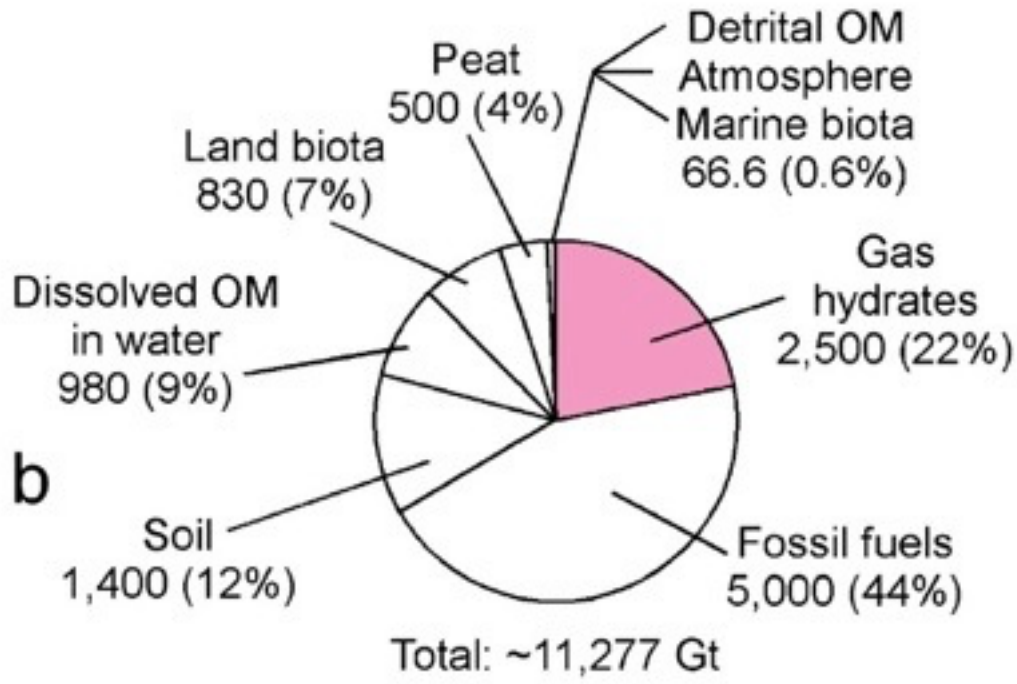

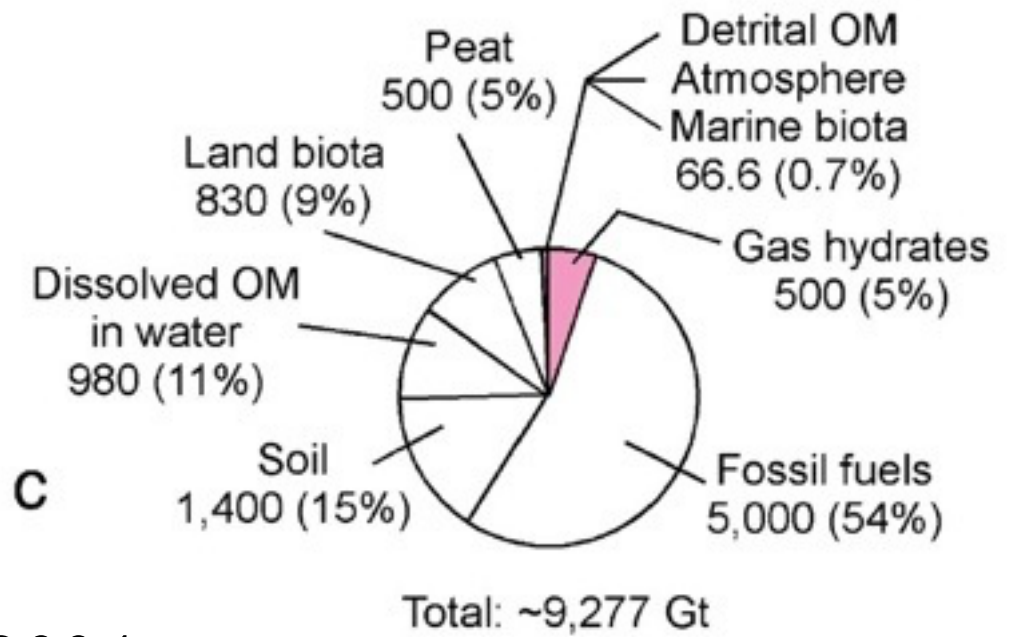

Fig. 4. Distribution of organic carbon in the Earth (excluding dispersed organic carbon such as kerogen and bitumen) with varying estimates of the global hydrate inventory. Values are given in Gt of carbon. (a) The distribution based on the estimate of 10 000 Gt of methane carbon in gas hydrates (Kvenvolden, 1993). (b) The distribution based on the revised estimate of the global gas hydrate inventory assuming the global volume of hydrate-bound gas at upper bound. (c) The distribution based on the revised estimate of the global gas hydrate inventory assuming the global volume of hydrate-bound gas at lower bound.

Milkov 2004

The carbon cycle with gas hydrates

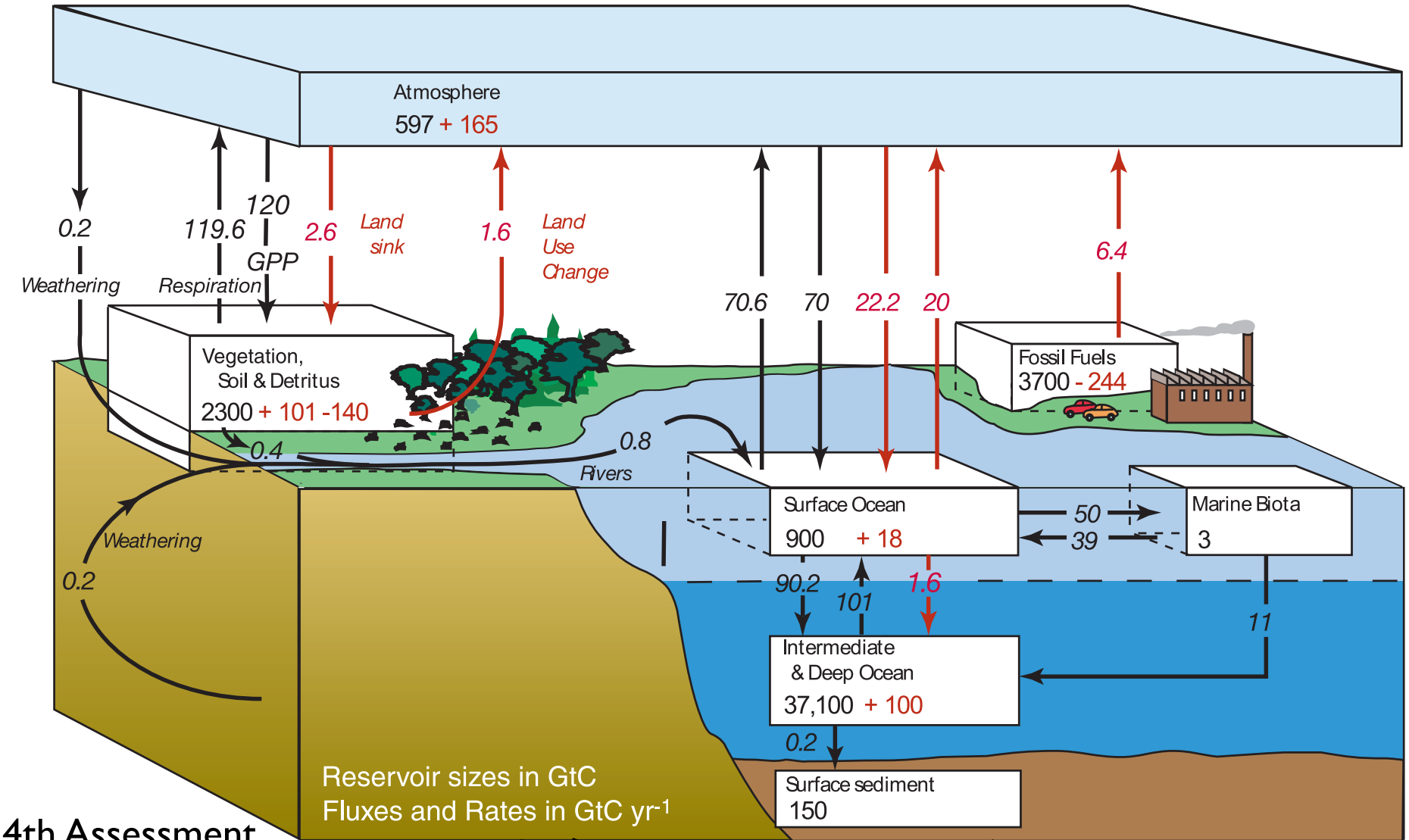

IPCC 4th Assessment Report, Climate Change 2007: The Physical Science Basis, Chapter 7

Methane hydrates
1,000s(?) GtC

Table 1. Short-Term (<10^4 years) Exchangeable Carbon Reservoirs (Present-Day)

Reservoir	Mass C, 10^{15}g		$\delta^{13}C_{PDB}$, ‰
	BP93 / K88	S93 / GF94	
Inorganic			
Atmosphere	500	750	
Ocean	30,000	38,000	
Combined inorganic	30,500	38,750	0
Organic			
Land biota	500	550	
Soil and humus	1500	1500	
Dissolved marine	1500	1600	
Combined organic	3500	3650	-25
Total exchangeable (excluding hydrate)	34,000	42,400	-2.1 to -2.6
Oceanic methane hydrate	8250	>10,500	-60

Estimates for the mass of various inorganic and organic C reservoirs are from *Broecker and Peng* [1993] and *Siegenthaler* [1993]; estimates for the mass of the oceanic methane hydrate reservoir are from *Kvenvolden* [1988] and *Gornitz and Fung* [1994]. A suggested range for the latter mass, however, is 7,500 to 15,000 x 10^{15} g (see *Kvenvolden* , 1993; *Gornitz and Fung* , 1994). The organic and inorganic reservoirs do not include conventional fossil fuels (coal deposits and oil reserves) and carbonate rocks.

Dickens et al. 1995

$\delta^{13}C$ at the Paleocene-Eocene

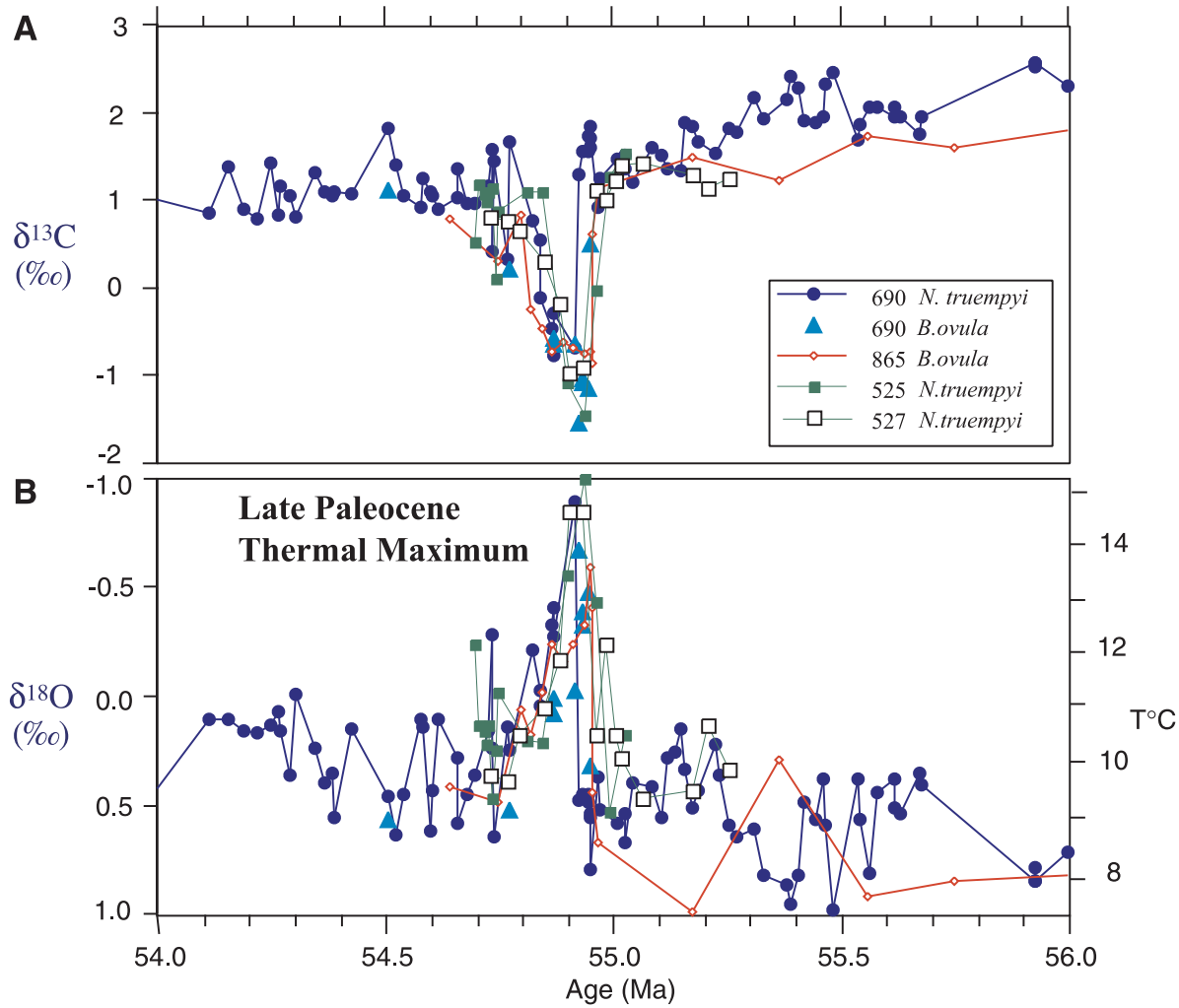

Zachos et al. 2001

Fig. 5. The LPTM as recorded in benthic $\delta^{13}C$ and $\delta^{18}O$ records (**A** and **B**, respectively) from Sites 527 and 690 in the south Atlantic (*73*), and Site 865 in the western Pacific (*26*). The time scale is based on the cycle stratigraphy of Site 690 (*30*) with the base of the excursion placed at 54.95 Ma. The other records have been correlated to Site 690 using the carbon isotope stratigraphy. Apparent leads and lags are artifacts of differences in sample spacing. The oxygen isotope values have been adjusted for species-specific vital effects (*118*), and the temperature scale on the right is for an ice-free ocean. The negative carbon isotope excursion is thought to represent the influx of up to 2600 Gt of methane from dissociation of seafloor clathrate (*111*).

$\delta^{13}C$ and gas hydrate dissociation at Paleocene-Eocene Thermal Maximum

- Exchangeable organic and inorganic C reservoir: mass M_T = 40,000 Gt of C, $\delta^{13}C_T$ = –2.4‰
- Hypothetical amount of dissociating gas hydrate at the PETM: M_H = 2,000 Gt of C, $\delta^{13}C_H$ = –60‰
- Equation for combined reservoir after gas hydrate dissociation:

$$(M_T + M_H)(\delta^{13}C_{T+H}) = M_T(\delta^{13}C_T) + M_H(\delta^{13}C_H)$$

- $\delta^{13}C_{T+H}$ is consistent with a shift of –2 to –3‰ at the PETM

Dickens et al. 1995

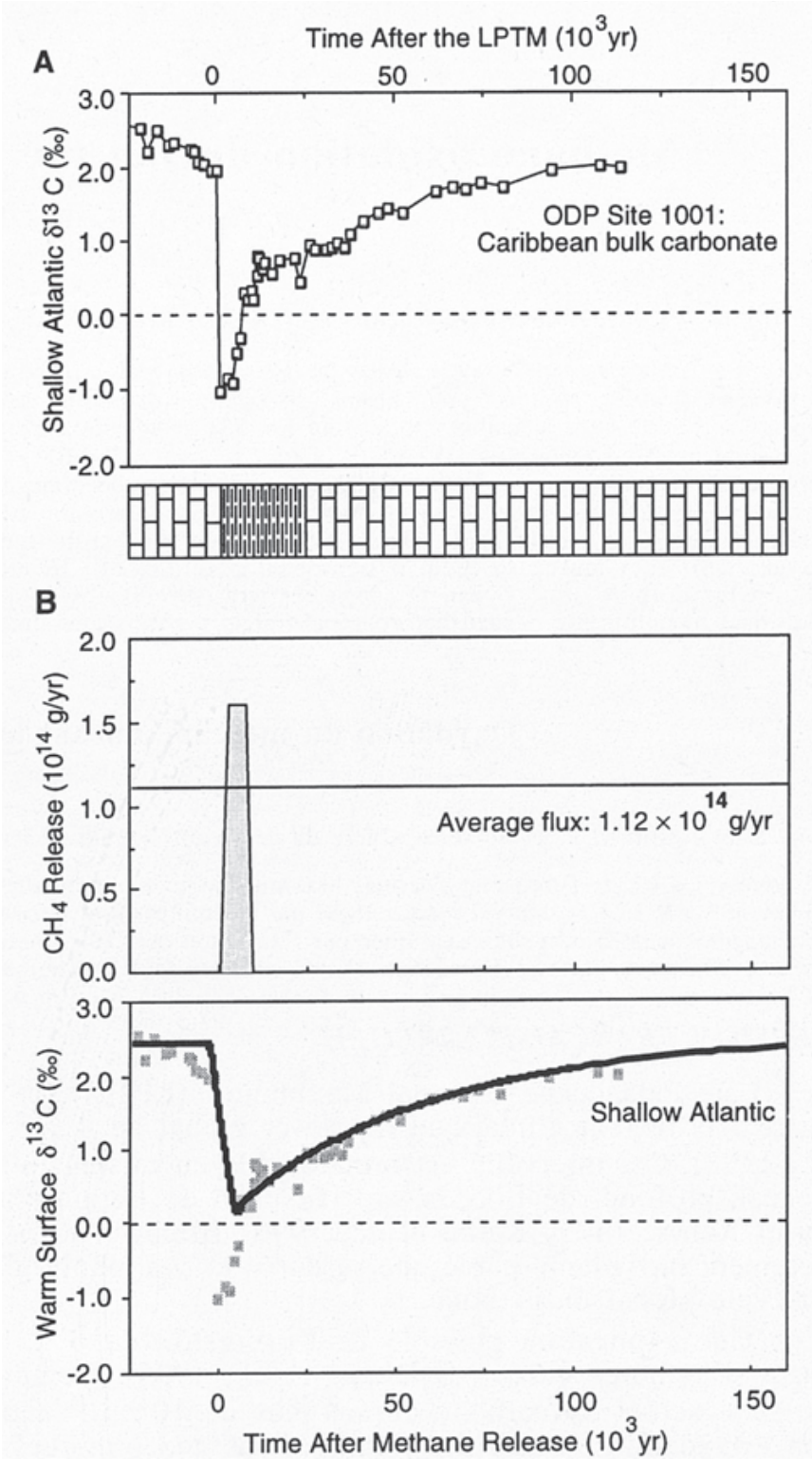

FIG. 1. – An example of the LPTM $\delta^{13}C$ excursion compared to a simulated $\delta^{13}C$ excursion caused by massive release and oxidation of CH_4 in the present-day carbon cycle. (A) High-resolution carbon isotope record for bulk carbonate (mostly nannofossils) at Ocean Drilling Program (ODP) Site 1001 in the Caribbean Sea with described lithology and estimated age by biostratigraphy [Bralower *et al.*, 1997]. An apparently rapid – 3.0 ‰ excursion in bulk carbonate $\delta^{13}C$ occurs across the LPTM coincident with pronounced carbonate dissolution. (B) The modeled response of the $\delta^{13}C$ of ΣCO_2 in warm surface ocean after a stepwise release of CH_4 at an average rate of 1.12×10^{14} g of CH_4/y over 10^4 yr [Dickens *et al.*, 1997a]. Superimposed on the curve are data points from the Caribbean carbon isotope curve. It is noteworthy that the modeled response was offered prior to and independent of isotope analyses and biostratigraphic age estimates for Site 1001.

Time constant ~100 kyr
(residence time in the
short-term C cycle)

Dickens, 2000

Modeling gas hydrate content

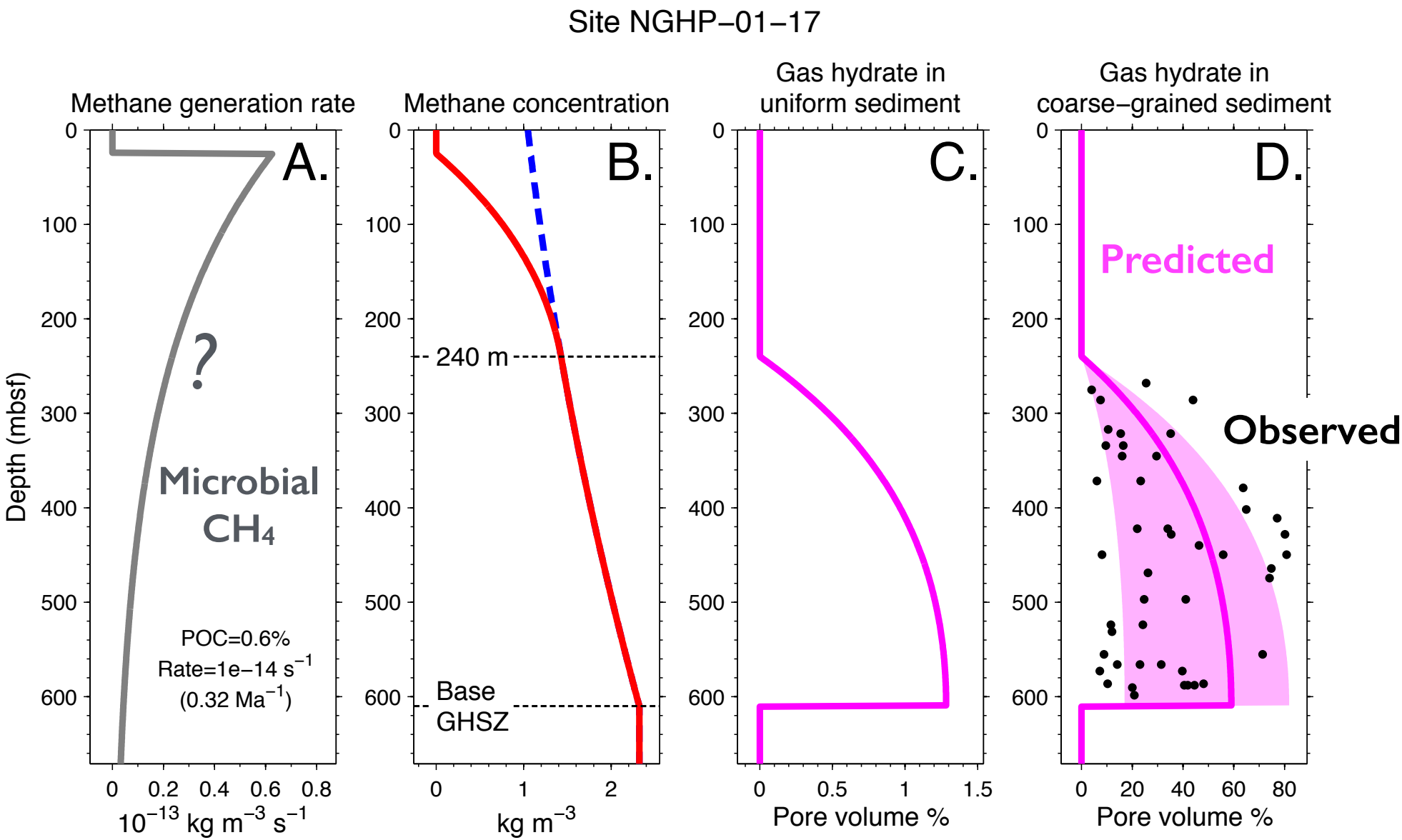

Malinverno and Goldberg, 2015